IMPERIAL COLLEGE

Assessment of the Value of Flexibility by Using Stochastic Scheduling Tool

A thesis submitted to Imperial College, London for the degree of Doctor of Philosophy

By Fei Teng

May 2015

Department of Electrical and Electronic Engineering,
Imperial College

Declaration

The material contained within this thesis is my own work, except where other work is appropriately referenced. Any use of the first person plural is for reasons of clarity.

Abstract

This thesis proposes novel analytical models for assessing the role and the value of various flexibility resources in the future low-carbon systems with high penetration of renewable energy resources. A novel stochastic scheduling model is developed, which optimises system operation by simultaneously scheduling energy production, standing/spinning reserves and inertia-dependent frequency regulation in light of uncertainties associated with wind energy production and thermal generation outages. The proposed model is shown to be particularly suitable for analysing the value of flexibility.

Following this, the thesis presents an assessment of the value that energy storage may deliver to the owner in the application to energy and ancillary service markets. The results suggest that the value of energy storage is mainly driven by the temporal arbitrage opportunities created by volatility in energy prices. The value of energy storage is shown to be site-specific when there are active network constraints.

A novel methodology is then proposed and applied to assess the role and the value of frequency regulation support (synthetic inertia (SI) and primary frequency response (PRF)) from wind plants (WPs). The results suggest the SI could effectively reduce the system operation cost in the system, especially with high penetration of wind generation. The analysis also demonstrates the value for WPs in providing PFR is system-specified. Combined provision of SI and PFR is required, in the case that there exists severe recovery effect associated with SI provision.

This thesis also proposes a novel demand side response model (DSRM), which models and controls the recovery period during and after frequency regulation provision and thus optimally allocates multiple frequency services. The results attest the value of the DSRM compared with alternative approaches for demand response schemes. Moreover, this thesis quantifies the implications of electric vehicle deployment, heat pumps, industrial and commercial and dynamic time-of-use tariffs for the carbon emissions and renewable integration cost of the broader GB electricity system.

Finally, this thesis investigates the value of enhanced flexibility from conventional plants. It has been shown that the value increases with penetration of RES; however,

different systems may require different types of enhanced flexibility features. Moreover, different system scheduling methods, risk attitudes, frequency response requirements and carbon prices could significantly change the value of flexibility.

Table of Contents

Acknowledgements

I would like to thank Prof. Goran Strbac. He has been an excellent supervisor, constantly pushing me when needed and always available to help out, in spite of his already extreme busy schedule. His lucid and thought provoking insights into the intermittency and system flexibility problems inspired me to study the subject in depth and have resulted in this thesis.

Thanks also to past and present colleagues in the Control and Power Group at Imperial College, especially Alexander Sturt, Marko Aunedi, Danny Pudjianto and Rodrigo Moreno, for all their help in the field of power system scheduling simulation, and for the friendly and international atmosphere in which we worked. In particular, the work of Alexander Sturt with regard to stochastic scheduling are gratefully acknowledged.

I would also like to thank the colleagues from Alstom Power, National Grid, Arup, Carbon Trust and UKPN. Their inputs over the years are much appreciated.

The comments of Professor Richard Vinter and Dr Jianzhong Wu, two examiners of this thesis, are very much welcome.

Finally, I would like to thank my parents, for their unconditional patience and love over the past few years. Completing this thesis would have simply not been possible without them.

List of Publications

Journal Papers

F. Teng, V. Trovato and G. Strbac, "Stochastic Scheduling with Inertia-dependent Fast Frequency Response Requirements," IEEE Trans. Power Syst, accepted.

F. Teng, D. Pudjianto, G. Strbac, N. Brandon, A. Thomson and J. Miles, "Potential Value of Energy Storage in the UK Electricity System" Proceedings of the ICE - Energy, accepted.

F. Teng and G. Strbac, "Assessment of the Role and Value of Frequency Response Support from Wind Plants," *IEEE Trans on Sustain Energy,* Submitted.

V. Trovato, F. Teng and G. Strbac, "Stochastic Scheduling with Flexible Demand Response from Thermostatic Loads," *IEEE Trans. Smart Grids,* Submitted.

Conference Papers

F. Teng, D. Pudjianto, G. Strbac, F. Ferretti and R. Bove, "Assessment of the Value of Plant Flexibility," in *Renewable Power Generation Conference (RPG 2014), 3rd*, Naples, 2014.

R. Bove, F. Ferretti, P. Paelinck, G. Strbac and F. Teng, "Installed Base and Flexibility: New Realities for the European Power Sector," in *PowerGen Europe*, 2013.

F. Teng, M. Aunedi and G. Strbac, "Value of Demand Side Participation in Frequency Regulation," in *23rd International Conference on Electricity Distribution*, 2015.

F. Teng and G. Strbac, "Evaluation of Synthetic Inertia Provision from Wind Plants," in *IEEE PES General Meeting* , 2015.

Technical Report

M. Aunedi, F. Teng and G. Strbac, "Carbon impact of smart distribution networks," Report D6 for the "Low Carbon London" LCNF project: Imperial College London, 2014.

G. Strbac, M. Aunedi, D. Pudjianto, P. Djapic, F. Teng, A. Sturt, D. Jackravut, R. Sansom, V. Yufit and N. Brandon, "Strategic Assessment of the Role and Value of Energy Storage Systems in the UK Low Carbon Energy Future," Carbon Trust, London, 2012.

List of Symbols

Indices

g	Thermal generator group
s	Number of timesteps ahead
j	All-purpose index variable
k	Current timestep
n	Node number
s	Storage unit

Sets

$A(n)$	Set of nodes that are ancestors of node n.s
$\mathcal{G}$	Set of thermal generators.
$I(n)$	Set of timesteps ahead spanned by node *n*
S	Set of storage units.
$\mathcal{N}$	Set of nodes on the scenarios tree.
P	Set of nodes corresponding to system states in the past

Constants

$\Delta\tau(n)$	Time interval corresponding to node n (h).
$\mu(j)$	Diurnal adjustment constant corresponding to the j^{th} time step of the day.
$\pi(n)$	Probability of reaching node *n*
σ	Standard deviation of random Gaussian increments in autoregressive time series.
$\sigma_z(i)$	Standard deviation of forecast error in normalized wind level, *i* time steps ahead.
φ_1, φ_2	Autoregressive parameters.

c^{LS}	Value of lost load (£/MWh).
c_g^m	Marginal cost of thermal unit g (£/MWh).
c_g^{nl}	No-load cost of thermal unit g (£/h).
c_g^{st}	Startup cost of thermal unit g (£).
P_g^{max}	Maximum generation of thermal unit g (MW).
P_g^{msg}	Minimum stable generation of thermal unit g (MW).
T_g^{mo}	Minimum off time of thermal unit g (h).
T_g^{mu}	Minimum up time of thermal unit g (h).
T_g^{st}	Startup time of thermal unit g (h).
P_s^{cmax}	Maximum charge rate of storage unit s (MW)
P_s^{dmax}	Maximum discharge rate of storage unit s (MW)
R_g^{max}	Maximum frequency response capability of thermal unit g (MW).
R_s^{max}	Maximum frequency response capability of storage unit s (MW).
R_g^{Pmax}	Maximum primary response capability of thermal unit g (MW).
R_s^{Pmax}	Maximum primary response capability of storage unit s (MW).
R_g^{Smax}	Maximum secondary response capability of thermal unit g (MW).
R_s^{Smax}	Maximum secondary response capability of storage unit s (MW).
f_g^F	The proportion of the spinning headroom for frequency response provision.
H_g	Inertia constant of thermal unit g (s).
D	Load damping rate (%/Hz)
T_d	Delivery time of frequency response (s)
$RoCoF_{max}$	Maximum rate of change of frequency (Hz/s).
Δf_{max}	Maximum frequency deviation requirement in Nadir (Hz).
Δf_{max}^{ss}	Maximum frequency deviation requirement at quasi steady state (Hz).

Δf_{DB}	Frequency deadband of governor (Hz)
$q(n)$	Forecast error quantile of branch leading to node *n*.
$W(\cdot)$	Sigmoid-shaped function which transforms the wind level to an aggregated wind output.
$W^{-1}(\cdot)$	Inverse function of W
$X(k)$	k^{th} element in an autoregressive time series which represents normalized wind level.
E_s^{min}	Minimum stored energy of storage unit s (MWh)
E_s^{max}	Maximum stored energy of storage unit s (MWh)
P_s^{cmin}	Minimum charge power rate of storage unit s (MW)
P_s^{cmax}	Maximum charge power rate of storage unit s (MW)
P_s^{dmin}	Minimum discharge power rate of storage unit s (MW)
P_s^{dmax}	Maximum discharge power rate of storage unit s (MW)
P_s^{ResMAX}	Maximum response capability of storage unit s (MW)
P_s^{STOMAX}	Maximum STOR service capability of storage unit s (MW)
P_{DN}^{Max}	Maximum capacity of distribution network DN (MW)
η_s^c/η_s^d	Charge/discharge efficiency of storage unit s
H_{gSI}	Synthetic Inertia constant of wind plants (s).
$R_g^{P,max}$	Maximum primary response capability of thermal unit *g* (MW).
$R_g^{s,max}$	Maximum secondary response capability of thermal unit *g* (MW).
f_g^P/f_g^S	The proportion of the spinning headroom for primary/secondary response.
r_g^{max}	Maximum generator ramp rate (MW/min)
t_P/t_R	Primary response/ reserve delivery time (s)
Δf_{DB}	Frequency deadband (Hz)
$\hat{\tau}$	Thermal time constant [h]

$b(n)$	The progenitor of node n
$F(k, i)$	Median of the forecast distribution of normalised wind level at i timesteps ahead, as predicted at timestep k
$Z(k, i)$	Error in forecast normalised wind level, as forecast at timestep k for i timesteps ahead (i.e. the overprediction error in the forecast median normalised wind level
$z(n)$	Forecast error in normalised wind level assumed at node n

Semi-constants

$P^D(n)$	Total demand at node n (MW).
$P^{WN}(n)$	Total available wind generation at node n. (MW).
$P_s^{Res}(n)$	Scheduled response regulation of storage unit s at node n (MW)
$P_s^{STO}(n)$	Scheduled STOR service of storage unit s at node n (MW)
t	Time after contingency (s).
$Pr_{RT}(n)$	Real time price at node n (£/MWh)
Pr_{Res}	Frequency response service price (£/MW/h])
Pr_{STOR}	STOR service price (£/MW/h)
Pr_{GEN}	Generation tariff (£/MWh)
Pr_{Retail}	Retail electricity price (£/MWh)
Pr_{EXP}	Exporting electricity price (£/MWh)
$E_{co2}(t)$	Average grid emission rate at hour t (g/kWh)
$P_{online}^{WN}(n)$	Total capacity of online wind plants at node n (MW).
t_{DB}	The time when frequency deviation reaches the dead-band.

Decision Variables

$N_g^{sd}(n)$	Number of thermal unit g that are shut down at node n.
$N_g^{st}(n)$	Number of thermal unit g that are started up at node n.

$P^{LS}(n)$ Load shed at node *n* (MW).

$P^{WC}(n)$ Wind curtailment at node *n* (MW).

$R_g(n)$ Frequency response provision from thermal unit *g* at node *n* (MW).

$R_s(n)$ Frequency response provision from storage unit s at node *n* (MW).

$R_g^P(n)$ Primary response provision from thermal unit *g* at node *n* (MW).

$R_s^P(n)$ Primary response provision from storage unit s at node *n* (MW).

$R_g^S(n)$ Secondary response provision from thermal unit *g* at node *n* (MW).

$R_s^S(n)$ Secondary response provision from storage unit s at node *n* (MW).

$R_g^R(n)$ Fast reserve provision from storage unit s at node *n* (MW).

$R_s^R(n)$ Fast reserve provision from storage unit s at node *n* (MW).

$R_w(n)$ Frequency response provision from wind plants at node *n* (MW).

$N_s^{Gen}(n)$ Operation status (0/1 for Pump/Generation) of storage unit *g* at node *n*.

$P_s^c/P_s^d(n)$ Charge/discharge power rate of storage unit s at node n (MW/h)

$P_{grid}(t)$ Power injection from grid at hour t (MW)

P_{PV}^{Gen} Power generation of distributed generation at hour t (MW)

$P_{PV}^{EXP}(t)$ Power exported of distributed generation at hour t (MW)

$P_s^c/P_s^d(t)$ Charge/discharge rate of storage unit s at hour t (MW)

$P_T(n)$ TCLs power consumption at node *n* (MW).

$P_T^P(n)$ Primary response from TCLs at node *n* (MW).

$P_T^S(n)$ Secondary response from TCLs at node *n* (MW).

$S_T(n)$ TCLs energy level at node *n* (MW).

Dependent Variables

$P_g(n)$ Power output of thermal unit *g* at node *n* (MW).

$N_g^{up}(n)$ Operation status (0/1 for Offline/Online) of thermal unit *g* at node *n*.

$C_g(n)$ Operating cost of thermal unit g at node n *(£)*

$H(n)$ System inertia at node n (MWs^2).

$R(n)$ Frequency response target (MW) at node n.

$E_s(n)$ Stored energy of storage unit s at node n (MWh)

$P_T^{ar}(n)$ Additional reserve requirement due to TCLs recovery at node n (MW).

Abbreviations

SI	Synthetic inertia
PRF	Primary frequency response
WPs	Wind plants
EVs	Electric vehicles
HPs	Heat pumps
DSR	Demand side response
CCGT	Combined-cycle gas turbine
OCGT	Open-cycle gas turbine
MSG	Minimum Stable Generation
MILP	Mixed integer linear programming
TCLs	Thermostatically Controlled Loads
DSRM	Demand side response model
LCTs	Low carbon technologies
LCL	Low Carbon London
I&C	Industrial and commercial
dToU	Dynamic time-of-use
UC	Unit commitment
SUC	Stochastic unit commitment

AGC	Automatic generation control
ED	Economic dispatch
CDF	Cumulative distribution function
CHP	Combined heat and power
CVaR	Conditional value-at-risk
SQSS	Security and Quality of Supply Standard
RoCoF	Rate of change of frequency
ES	Energy Storage
STOR	Short-term operating reserve
FR	Frequency response
VSWT	Variable speed wind turbines

1. Introduction

1.1 Background

In recent years, climate change and fossil fuel limitation have focused significant public attention on the utilisation of the renewable energy resources (RES). 20% of the EU energy consumption is expected to be supplied by RES by 2020. In order to achieve very significant greenhouse gas emission reductions of 80% in 2050, it is expected that the EU electricity sector would be largely decarbonised by 2030 with significantly increased levels of RES and increased electricity demand driven by the incorporation of heat and transport sectors (e.g. electric vehicles (EVs) and heat pumps (HPs)) into the electricity system.

The traditional power system is dominated by relative flexible and controllable plants that follow a low uncertain and fluctuating demand. However, low carbon electricity system would be characterised by generation mix including significant amounts of low capacity value, variable and difficult to predict intermittent RES (e.g. wind and solar) in combination with less flexible nuclear and thermal plant, which requires a fundamental review of the current methodologies for the system control, operation and planning.

This thesis is primarily concerned with the system operation. In order to accurately analyse the low carbon power system with significant uncertainties driven by RES, it becomes necessary to extend the existing deterministic model to incorporate the stochastic properties of the random components. It is also important to investigate how to properly model the emerging components (e.g. DSR and energy storage) of the system in order to understand their role and value in supporting the integration of RES. Time-domain simulation methods are adopted in this thesis to model how each element can be optimally combined to match demand and supply by estimating the long-term properties of the system, such as operating cost and load shedding frequency. At the same time, time-domain simulation allows us to study the flexibility of the power system by taking account of the inter-temporal constraints (e.g. start-up time for thermal generators, and limitations to the amount of storable energy).

1.2 Need for Enhanced Flexibility

Integration of significant amount of RES in the electricity system will impose a considerable demand for additional flexibility, particularly for services associated with system balancing. Increased requirements for real-time ancillary services, if provided by conventional generation running part-loaded, will not only reduce efficiency of system operation but will significantly undermine the ability of the system to absorb intermittent renewable output, increase emissions and drive up cost.

The key barrier to the cost-effective integration of intermittent RES is the necessity to deliver increased levels of ancillary services, mainly from synchronised conventional generation units. Conventional generation technologies such as large coal, gas or nuclear plants, given their typical dynamic constraints, can only provide the ancillary services for real-time balancing when operating part loaded and also generating a significant amount of electricity that may be unwanted. This becomes a major problem during off-peak i.e. night hours, particularly if combined with high renewable output, as there can be a surplus of available electricity, and the only means to balance the system is to curtail RES.

In addition to RES, meeting the future electricity demand is likely to require the use of non-renewable low-carbon generation technologies such as nuclear or CCS plants. It is expected that both of these technologies will have lower operation flexibility compared to the existing coal and combined-cycle gas turbine (CCGT) units, i.e. that they will strongly favour operating with a flat output close to their maximum capacity.

As it is becoming clear that meeting the future needs for flexibility solely with conventional generators might become very expensive while also potentially worsening the environmental performance of the system, ever more research efforts are focused on the alternative sources of flexibility (as shown in

Figure 1-1), such as:

1. Flexible generation technologies. Key flexibility parameters of conventional generators include: (a) Minimum Stable Generation (MSG), (b) Maximum response capability, (c) ramp rate, (d) commitment time, and (e) idle state. MSG determines the maximum operating ranges in which the plants can change their output. For instance, plant with the capability to change its output from 20%

to 100% contributes more towards system flexibility than a plant with the capability to change its output from 50% to 100%. The maximum response capability defines the maximum proportion of the plant capacity which can contribute to the frequency response service. Higher ramp rate means the plant can adjust its output faster to compensate the changes in the system. Commitment time describes how long thermal plants take from offline status to online status. Shorter commitment time means less uncertainty to face when making start up decision. Idle state is the capability to keep the plant online but without energy production. In general, more flexible generation could deliver ancillary services to the system while having to deliver less energy to the grid at the same time, which would reduce the need to curtail wind output in order to balance the system.

2. *Network technologies*. These include reinforcements and investment in interconnection, transmission and/or distribution networks, as well as advanced network management solutions. Interconnections between neighbouring systems can be used to share flexibility between two systems, while reducing the need for system reserve and response, hence enhancing the ability of the system to accommodate increased deployment of RES.
3. *Energy storage technologies*. Electricity energy storage installations are able to convert electricity into another energy form suitable for storing (kinetic, potential, chemical, compressed air, etc). The currently rather high cost is a limiting factor for deployment of energy storage. However, with higher fluctuations of net demand brought by large-scale deployment of RES in combination with inflexible nuclear and CCS generation, installing energy storage might become economically justified. In cases where a system without storage would have to resort to wind shedding to retain system integrity, it is expected that the additional flexibility provided by energy storage could significantly reduce the volume of curtailed wind output, as shown in [1].
4. *Demand side response (DSR) technologies*. DSR typically involves temporal shifting of the operating schedule of flexible loads (e.g. air conditioners, space heating, dishwashers, washing machines etc.) in order to improve the conditions

in the electricity system. It has not been exploited on a large scale so far, for a number of reasons, such as the need for additional communication infrastructure, weak interest on both the customer and the system side due to the lack of understanding the value of DSR, and the lack of tools to analyse and quantify the benefits from using DSR.

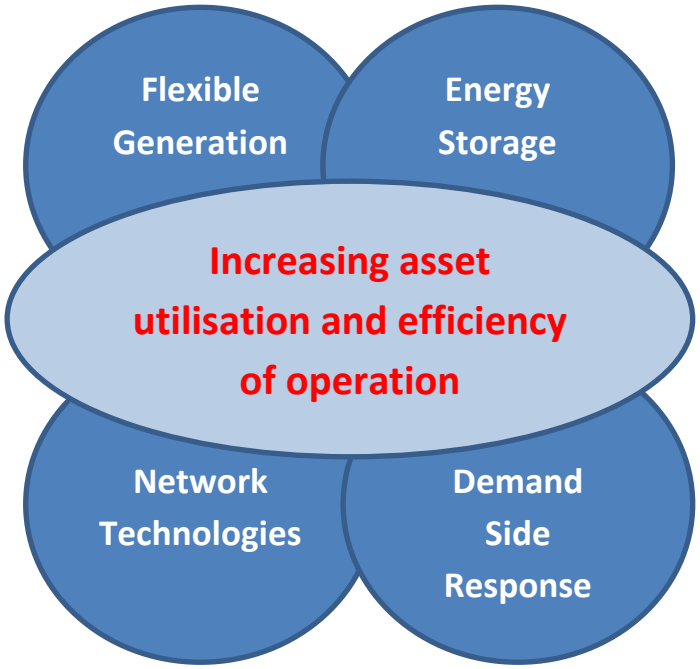

Figure 1-1Flexibility options to increase asset utilisation and efficiency of operation

1.3 Research Questions

This thesis focuses on the development of advanced simulation models and the application of these models to facilitate the understanding the role and the value of alternative flexibility options. The *Research Objectives* of this PhD project can be summarised as:

1. Create a time-domain simulation tool to facilitate a thorough understanding of the operation of future low carbon systems with high penetration RES. RES is characterised by variability, uncertainty and limited inertia capability. Its impact on the system operation is complex due to the inter-temporal links between the system constraints, costs and security consideration [2]. Therefore, it is important to implement an efficient scheduling model, which can optimise system operation by simultaneously scheduling energy production, standing/spinning reserves and inertia-dependent frequency regulation in light of uncertainties associated with RES production and

generation outages. (1) As the variability and uncertainty introduced by wind is more significant than that by demand, the present deterministic rules to schedule various reserves may be inefficient. Stochastic optimisation with mixed integer linear programming (MILP) is required to optimally scheduling standing/spinning reserve [3] [4]. (2) Although the output of wind generation does not significantly change on a second by second basis, there are growing challenges associated with the scheduling of primary reserve. In particular, the degradation of system inertia significantly accelerates the decline of system frequency after generation loss, requiring faster delivery of frequency response [5] [6]. In addition, the actual requirement for frequency response depends on the system inertia, which is driven by the amount of conventional plant scheduled to operate. Given that different realisations of wind energy could significantly change the schedule of conventional plant, this will result in uncertainty in system inertia hours ahead of real time. Therefore, it is necessary to develop a SUC model to optimally schedule both frequency response and standing/spinning reserves, so that the system operation is optimally scheduled across the time scale from seconds to hours.

2. Investigate the role and the value of energy storage in the low carbon power system. Energy storage has the potential to provide multiple services to several sectors in electricity industry and thus support activities related to generation, network and system operation [1]. Hence aggregating the value delivered by energy storage to these sectors is paramount for promoting its efficient deployment in the near future. Stochastic scheduling is particularly suitable for analysing energy storage in a system with high RES penetration [7] [1], since the capacity of energy storage could be optimally split between energy arbitrage and ancillary service provision under various system conditions. Studies in [8] and [9] use historical market prices and assume perfect information of these prices. However, in the future system with high penetration of RES, electricity prices would become more volatile and uncertain, which should been directly modelled when assessing the value of energy storage.

3. Investigate the role and the value of frequency regulation support from wind plants in the low carbon power system. The present grid codes do not require wind plants (WPs) to provide frequency regulation services and therefore high penetration of wind generation could impose a challenge to fulfil the system frequency regulation requirements. In fact, a significant amount of rotational energy is stored in the WPs and at the same time, WPs could provide headroom by de-loading from maximum generation point. Extensive research has been conducted to investigate the limits and capabilities of WPs to provide frequency regulation support. Although the technical impact of frequency regulation support from WPs has been widely studied, the impact on system scheduling and economics of system operation is not yet fully understood. In fact, very little work has been conducted on modelling of system benefits and implications of providing different levels of SI and supporting frequency control. Clearly, there are some key differences between WPs and conventional plants in providing frequency regulation services, and it is important that these are incorporated in optimal generation scheduling models. Firstly, the work in [10] and [11] points out that there is uncertainty associated with the capacity of online WPs for a given level of wind generation production, leading to a challenge to estimate the aggregated SI from WPs. Moreover, as discussed in [12] and [13], additional PFR may be required to support the recovery of original turbine speed. The system scheduling needs to take into account of the recovery effect in order to retain the system security. Finally, in order to provide PFR, WPs need to be de-loaded from optimal operation point. The balance between costs and benefits of PFR provision need to be considered explicitly in the system scheduling. In this context, it is necessary to develop a novel methodology to incorporate frequency regulation support provided both by conventional plants and WPs into system scheduling and therefore, enables the benefits of frequency regulation support from WPs to be quantified.
4. Investigate the role and the value of DSR in the low carbon power system. Wind variability and uncertainty can also be accommodated by DSR.

However, there are two challenging characteristics associated with DSR. Firstly, DSR could simultaneously provide multiple services (e.g. energy arbitrage and frequency response). To obtain the maximum benefit, it is crucial to optimally allocate the capacity of DSR among multiple services. Secondly, the delivery of ancillary services from DSR is followed by an energy recovery period [14]. The accurate assessment of the value of DSR cannot neglect the load recovery and its associated cost. Those characteristics need to be explicitly modelled in order to fully understand the value of DSR. Moreover, there exit various DSR technologies, including electric vehicles, heat pumps, industrial and commercial DSR and dynamic time-of-use tariffs. These technologies have different flexibility levels, response speed and potentials of installed capacity. For the optimal implementation of DSR, it is necessary to understand the benefit of each DSR technology.

5. Investigate the role and the value of enhanced flexibility from conventional generators in the low carbon power system. As one of the options to supply the increased flexibility demand, conventional plants with enhanced flexibility have not received much attention in the research. However, the electrification of transport and heating sector and the retirement of aging plants in Europe require investment to build new power plants. At the same time, it is possible to directly invest in retrofitting the existing plant to increase its flexibility. There also exists arguments regarding whether the flexibility of plants should be taken into account when design the capacity mechanism. Therefore, it is crucial to investigate the role and the value of flexible plants in the future low-carbon power system to guide the investment and market design.

1.4 Thesis Structure

This thesis is organised into six technical chapters to address the research questions identified in section 1.3. Since a wide range of topics are covered from UC methods to difference flexibility features, the relevant literature reviews are contained in each chapter.

Chapter 2 describes the model of stochastic system scheduling tool with inertia-dependent frequency regulation requirements (Question 1). A novel mixed integer

linear programming (MILP) formulation for SUC that optimises system operation by simultaneously scheduling energy production, standing/spinning reserves and inertia-dependent frequency regulation in light of uncertainties associated with wind production and generation outages. Post-fault dynamic frequency requirements (rate of change of frequency, frequency nadir and quasi-steady-state frequency) are formulated as MILP constraints by using a simplified model of system dynamics. Moreover the proposed methodology permits to recognise the impact of wind uncertainty on system inertia. Case studies are carried out on the 2030 Great Britain system to demonstrate the importance of incorporating inertia-dependent frequency regulation in stochastic scheduling and to indicate the potential for the proposed model to inform reviews of grid codes associated with frequency regulation and future development of inertia-related market. This chapter also discusses the advantages of the proposed model in understanding the value of flexibility in the future low-carbon power systems. This chapter is based on a journal paper that has been submitted to IEEE Transaction on Power System [15].

Chapter 3 investigates the value of energy storage (Question 2). This chapter assesses the value of energy storage and informs the business case in the future Great Britain electricity system. In contrast to earlier studies that focus on the benefits for system operation and development, this work analyses the value that energy storage may deliver to the owner. For this purpose, stochastic system and storage scheduling model is proposed and applied to analyse the benefit of energy storage with applications in energy and ancillary service markets. A large set of studies are carried out to quantify the commercial benefits of energy storage. Sensitivity analysis across various scenarios is performed to understand the key drivers for the value of energy storage and how it is affected by energy storage parameters and other factors such as network constraints, prices of energy and ancillary services, and inherent energy system characteristics. A review of current and near-term energy storage technology costs and functionality is also presented. This chapter is based on a journal paper that has been accepted by Proceedings of the Institution of Civil Engineers - Energy [16].

Chapter 4 investigates the role and the value of frequency regulation support from WPs (Question 3). This chapter develops a novel methodology to incorporate the

frequency regulation support from WPs into generation scheduling, therefore enabling the benefits of alternative frequency regulation control strategies to be quantified. Studies are carried out in the future GB power system with different wind penetration levels and frequency regulation requirements. The impact of the uncertainty associated with the capacity of online WPs and the energy recovery effect are also analysed. The results demonstrate that the benefits of frequency regulation support from WPs are significant although these may vary system specific. The proposed models could also inform the development of grid codes associated with frequency regulation support from WPs. This chapter is based on a journal paper that has been submitted to IEEE Transaction on Energy Conversion [17].

Chapter 5 investigates the value of DSR from Thermostatically Controlled Loads (TCLs) (Question 4). This section develops a novel demand side response model (DSRM), which explicitly models and controls the recovery period after frequency regulation provision and thus optimally allocates multiple frequency services to balance the benefit of the demand side frequency support and the cost of supplying extra power with reserve generators during the devices' recovery phase. The proposed method is integrated within a SUC model developed in chapter 2. The studies are carried out on the 2030 GB system and illustrate the effectiveness of our method with respect to alternative implementations. The impact of different recovery pattern and average temperature constraints are also assessed. This chapter is based on a journal paper that has been submitted to IEEE Transaction on Smart Grid [18].

Chapter 6 investigates the value of different DSR technologies (Question 4). This chapter analyses and quantifies the implications of low-carbon technologies (LCTs) and solutions studied in Low Carbon London (LCL) trials for the carbon emissions and renewable integration cost of the broader UK electricity system. Key findings of LCL reports, in particular those characterising the demand profiles associated with electric vehicle (EV) deployment, heat pumps (HPs), industrial and commercial (I&C) Demand-Side Response (DSR), dynamic time-of-use (dToU) tariffs and energy-efficient and smart domestic appliances, are translated into nationally representative demand profiles and their impact on the CO2 performance and wind integration cost of the electricity system is quantified across three proposed scenarios covering 2030-

2050 GB system. Given that the uncertainty of RES is expected to be a major driver for escalating integration cost, the performance of the system is analysed using the proposed scheduling model in chapter 2. As the proposed model is also capable of considering system inertia and frequency response, it is used to further investigate the impact of the provision of ancillary services from alternative sources on the carbon performance and renewable integration cost of the system. This chapter is based on a technical report that has been published online [19].

Chapter 7 investigates the value of enhanced flexibility from thermal plants (Question 5). This chapter examines the value of enhanced flexibility from thermal power plant in the future low carbon energy system. The scheduling model developed on Chapter 2 is performed to calculate the operation cost saving due to improved flexibility. Various flexibility features are defined and analysed across two representative systems showing that the value of plant flexibility is system specific. Sensitivity studies are carried out to understand the impact of different scheduling methods, risk attitudes, frequency regulation requirements and carbon taxes on the value of flexibility. A discussion on market reward for flexibility is also presented. This chapter is based on two papers that have been published and presented in international conferences [20] [21].

Chapter 8 summaries the key finds of this thesis and discusses some potential further work.

1.5 Original Contributions

To address the research objectives, this thesis develops and applies various novel simulation models. The key contributions of this thesis can be summarised as:

- Development of a novel stochastic unit commitment model to optimise system operation by simultaneously scheduling energy production, standing/spinning reserves and inertia-dependent frequency regulation in light of uncertainties associated with RES production and generation outages. For the first time, the dynamics of system frequency evaluation after generation outage is incorporated into stochastic unit commitment model and therefore the system operation is optimally scheduled across the time

scale from seconds to hours. The proposed model is shown to be particularly suitable for analysing the value of flexibility.

- Development of stochastic system and storage scheduling model to assess the value of energy storage may delivery to its owner. The increased variability and uncertainty associated with electricity prices are explicitly modelled and the capability of energy storage to provide multiple services is also assessed.
- Development of demand side response model (DSRM) with explicitly modelling of flexible ancillary service provision from DSR and the associated recovery effect. The proposed DSRM is constructed in such a way that DSR would always guarantee the deliverability of the scheduled response services as the energy deployed is fully paid pack by the end of each time interval. Moreover, the provision of ancillary service can vary at each time step in accordance with the time dependent characteristic of the system requirements
- Development of a novel methodology which incorporates frequency regulation support provided both by conventional plants and WPs into generation system scheduling. The unique characteristics of frequency regulation services provision from WPs is modelled and incorporated into optimal system scheduling model. Therefore, the economic value of frequency regulation support from WPs is quantified for the first time.
- Comprehensive assessment of economic and environmental benefits of various DSR technologies. The value obtained in these calculations represents an important indicator for identifying those DSR technologies that merit the strongest strategic support in order for the theoretical benefits identified in this thesis to materialise in low-carbon systems of the future.
- Comprehensive assessment of the benefits of enhanced flexibility of conventional plants. In particular, lower Minimum Stable Generation (MSG), higher frequency response capability, higher ramp rate, shorter commitment time and idle state capability are considered. A wide range of sensitivity studies are carried out to understand the value of plant flexibilities across

different systems. Impacts of scheduling strategies, risk attitudes, frequency regulation requirements and carbon taxes are also analysed. The results could be used to guide the investment and market design in the future low carbon systems.

2. Stochastic Scheduling with Inertia-dependent Fast Frequency Regulation in the Future Low Carbon Power System

2.1 Introduction

Integration of large share of wind generation increases the requirements for various ancillary services. These additional ancillary services will be mostly delivered through part-loaded generators in combination with fast standing plants. This not only decreases the system efficiency and leads to higher operation cost, but it may also compromise the ability of the system to integrate growing wind generation. In particular, the lack of system inertia exacerbates the need for frequency regulation services in order to maintain the frequency evolution within security boundaries and avoid, in the worst case, emergency demand disconnections. In fact, the lack of inertia already causes wind curtailment [22], [23]. Due to the security concerns, the maximum instantaneous system non-synchronous penetration ratio is limited to 50% in Ireland.

At present, the ancillary services are scheduled following deterministic rules by imposing pre-defined requirements in the generation scheduling procedure. As the uncertainty introduced by wind generation is much more significant than that by demand, scheduling process performed under deterministic rules may be inefficient as indicated in [24]. Stochastic optimisation with mixed integer linear programming (MILP) has been applied to unit commitment (UC) problems dealing with various sources of uncertainty [25], [3]. Scenario reduction techniques are investigated and applied in [3], [4] to alleviate the computational burden of stochastic programming. However, majority of existing research focus on the optimal scheduling of longer-term reserve in the hourly or half-hourly resolution. Recently, UC with more frequently updates and finer time resolution is proposed. In [25], the idea of rolling planning is introduced into Stochastic UC (SUC) to capture the benefit of frequently updated wind forecasts. The sub-hourly dispatch constraints are incorporate into SUC in [26]. Authors in [27] propose a multi-time resolution UC with the capability to consider the system operation up to 5-min interval. Moreover, the work in [28] develops an integrated model to assess the impact of variable generation at multiple timescales.

The finest scheduling interval is 6 seconds for the operation of automatic generation control (AGC).

At the same time, there has been significant interest in directly incorporating post-fault frequency requirements in generation dispatch and scheduling models. The authors in [29] proposed a MILP formulation for UC with frequency regulation constraints. The provision of primary frequency response from each generator is modelled as a linear function of frequency deviation, covering only quasi-steady-state frequency deviation in most cases. Doerthy et al. introduce frequency control in generation dispatch model [30]. Nonlinear frequency constraints are derived by performing a number of dynamic simulations to ensure the RoCoF and frequency deviation will meet the security requirements. The approach presented in [5] develops linear constraints to guarantee frequency response adequacy, which is then added into an optimal power flow formulation. Here, the load damping effect is not considered and system inertia is assumed to be known and not variable. A more recent work [31] incorporated analytical non-linear frequency constraints into a deterministic UC problem. Finally, a frequency-constrained stochastic economic dispatch (ED) model was developed in [6] to incorporate wind uncertainty and frequency regulation constraints. The results demonstrate the dramatic impact of system inertia on the system operation. However, the UC decision is fixed and the constraints to limit the post-fault frequency are nonlinear.

In this context, this chapter proposes a novel MILP formulation for SUC that optimises system operation by simultaneously scheduling energy production, standing/spinning reserves and inertia-dependent frequency regulation in light of uncertainties associated with wind production and generation outages. We identify three key contributions of this work:

1. It introduces a novel MILP formulation for system frequency constraints that ensure the dynamic evolution of post-fault frequency to be within limits associated with the RoCoF, nadir frequency and quasi-steady-state frequency (in accordance with the GB security standards [32]).
2. Through integrating the constraints associated with the dynamic frequency evolution into the stochastic UC, the impact of wind uncertainty on the system

inertia is directly addressed and hence the generation is be optimally scheduled across the time scale from seconds to hours.

3. The developed model is applied to the GB 2030 system in order to understand the impact of:
   1) the degradation in system inertia,
   2) delivery time of frequency response,
   3) changing maximum RoCoF level and
   4) load-damping rate

   on the system operation cost and the ability of the system to integrate wind generation. The proposed scheduling framework could inform (a) the benefits of stochastic scheduling policy; (b) reviews of grid codes associated with frequency regulation and (c) potentially the development of inertia related market, particularly in systems with significant contribution from wind generation.

The rest of this chapter is organised as follows: Section 2.2 introduces the stochastic scheduling model. Section 2.3 describes the inertia-dependent frequency response regulation requirements. The case studies are presented and explained in Section 2.4, while Section 2.5 discusses the advantages of the proposed model in understanding the value of flexibility. Finally, this chapter is concluded in Section 2.6.

2.2 Stochastic Scheduling Model

A stochastic scheduling model with rolling planning is formulated in order to optimally schedule energy production and delivery spectrum number of ancillary services in light of various uncertainties. The UC and ED are solved over a scenario tree (Figure 2-1). The scenarios are weighted according to their probabilities and hence the model optimally balances the cost of committed generation against the expected cost of not meeting demand or other requirements.

2.2.1 Modelling of Stochastic Variables

This section derives the formula for the cumulative distribution function (CDF) of the net demand, which is used to derive values of net demand at each node on the scenario tree. The net demand *t* hours ahead is defined as the demand plus the capacity

that is forced out between the current time and t hours ahead, net of the available wind power. In this way a forced outage is treated as equivalent to an over-prediction of wind power, or an under-prediction of demand, equal to the capacity that is forced out: this treatment is consistent with other studies which model combined forecast errors [71].

2.2.1.1 Modelling of wind uncertainty

We use a univariate, autoregressive model, representing the forecast error in the aggregated wind output as a single value. The model in [33] is applied to simulate the wind output and the associated uncertainty. The normalised wind level $X(k)$ is assumed to follow a Gaussian AR(2) process (2.1) with half-hourly timestep, which is then transformed into a non-Gaussian power output $P^w(k)$ with a range from zero to the installed capacity of wind fleet.

$$X(k) = \varphi_1^x X(k-1) + \varphi_2^x X(k-2) + \sigma^x \epsilon^x(k), \;\; \epsilon^x(k) \sim N(0,1)\ i.i.d. \tag{2.1}$$

$$P^w(k) = W(X(k) + \mu(k \bmod N^d) \tag{2.2}$$

where φ_1^x, φ_2^x are auto-regression parameters, σ^x is the standard deviation of wind level, $P^w(k)$ is the wind power converted from wind level $X(k)$, N^d is the number of timesteps in one day, $W(\cdot)$ is a sigmoid-shaped transformation function (represented by a piecewise linear approximation) and $\mu(j)$ is used to represent a diurnal variation. The auto-regression parameters, standard deviation, transformation function $W(\cdot)$ and additive term $\mu(j)$ are calibrated so that the distribution of the power output, and the diurnal variation of its mean, match historic data [34].

In order to maintain generality and simplify the algebra, we represent the time series here as the equivalent Moving Average (MA) process as:

$$X(k) = \sigma^x \sum_{j=0}^{\infty} \psi_j^x \epsilon^x(k-j) \tag{2.3}$$

where the MA parameters can be derived recursively from the AR parameters as follows:

$$\psi_i = \begin{cases} 0; & j < 0 \\ 1; & j = 0 \\ \varphi_1 \psi_{j-1} + \varphi_2 \psi_{j-2}; & j > 1 \end{cases} \tag{2.4}$$

Let $F(k,i)$ be the median forecast made at timestep k for i timesteps ahead, and therefore the forecast median wind power output is

$$P^{wf}(k,i) = W(F(k,i) + \mu\big((k+i) mod\ N^d\big), \qquad i = 1 \dots N^d \tag{2.5}$$

Let *Z(k, i)* be the forecast error in the normalised wind level, defined according to

$$Z(k,i) = F(k,i) - X(k+i) \tag{2.6}$$

We decompose *Z(k, i)* into a horizon-dependent scaling factor s_i^y and a time series process *Y(k, i):*

$$Z(k,i) = s_i^y Y(k,i) \tag{2.7}$$

where the underlying time-series process *Y(k, i)* can be written as an autoregressive process of order *p* and unit volatility, driven by N(0,1) innovations $\varepsilon^y(k,i)$

$$Y(k,i) = \begin{cases} 0 & i \le 0 \\ \sum_{j=1}^{p} \varphi_j^y Y(k,i-j) + \varepsilon^y(k,i) & i > 0 \end{cases} \tag{2.8}$$

or, equivalently as an MA process whose parameters can be calculated from the autoregressive parameters using (2.4):

$$Y(k,i) = \begin{cases} 0 & i \le 0 \\ \sum_{j=0}^{i-1} \psi_j^y \varepsilon^y(k,i-j) & i > 0 \end{cases} \tag{2.9}$$

The normalised wind forecast error is normally distributed with mean zero and standard deviation:

$$\sigma_i^z = s_i^y \sqrt{\sum_{j=0}^{i-1} (\psi_j^y)^2} \tag{2.10}$$

from which the scale factors s_i^y can be derived to satisfy any desired profile of RMS forecast errors.

2.2.1.2 Modelling of generation outages

Generation outages are assumed to follow Markov process with forced outage rate λ_g and mean time to repair rate μ_g, based on historical plant data. The probability distribution of outages is derived by using a capacity outage probability table (COPT) [35]. This cumulative nodal COPT can be conservatively approximated by considering each unit in group g that is scheduled to run in each timestep prior to node *n* as a separate event with a probability $\lambda_g \Delta t$ of producing a capacity outage of P_g^{max},

so that the COPT for all units in group g can be calculated as a binomial expansion. The cumulative nodal COPT for the whole system can then be obtained by convolving the binomial outage distributions for each unit group. The cumulative COPT formulated here captures the probabilities of capacity outages that accumulate between the current time and the instant before the time interval spanned by node n. This cumulative COPT is denoted as $\left\{\left(V_j^c(n), p_j^c(n)\right)\right\}_j$, where $V_j^c(n)$ is the jth cumulative capacity outage level accumulated before node n (with $j = 0$ corresponding to no outages), and $p_j^c(n)$ is the associated probability.

The number of timesteps during which a unit in group g attempted to run prior to node n is

$$N_g^{tu}(n) = \sum_{n' \epsilon A(n)} N_g^{up}(n') \frac{\Delta\tau(n')}{\Delta t} \tag{2.11}$$

and the PMF of the failed capacity is a binomial distribution $\left\{\left(V_{gj}^c(n), p_{gj}^c(n)\right)\right\}_j$ with the failed capacities

$$V_{gj}^c = P_g^{max} j, \qquad j = 0 \ldots N_g^u \tag{2.12}$$

and probability approximately

$$p_{gj}^c(n) = \binom{N_g^{ut}(n)}{j} \left(\lambda_g \Delta t\right)^j \left(1 - \lambda_g \Delta t\right)^{\left(N_g^{ut}(n) - j\right)} \tag{2.13}$$

Equation (2.13) is a conservative approximation because it assumes that the probability of a unit failing during each timestep is independent of the probability of it failing during any other timestep. In reality, a particular unit cannot fail more than once during the time spanned by the scenario tree. (We are conservatively ignoring the possibility of repairs occurring over such short timescales.) The effect of the approximation will be small as long as the probability of any particular unit failing during the time spanned by the scenario tree is small.

Having calculated the cumulative COPT for each unit group, one can combine them using the algorithm described by Equations (6.22) to (6.25) in [36] to generate an overall cumulative COPT for the whole thermal fleet as

$$\left\{\left(V_j^c(n), p_j^c(n)\right)\right\}_j = \otimes \left\{\left(V_{gj}^c(n), p_{gj}^c(n)\right)\right\}_j \tag{2.14}$$

where $\otimes$ denotes iterative convolution.

The circulation problem regarding COPT construction is solved by iterations as proposed in [36]. The simple iterative scheme is adopted, with an initial UC assuming no outages, the second UC based on the COPT implied by the solution to the first UC, and so on. In practice it was found that no significant reduction in operating costs was achieved by running more than two iterations, so the penalty for using this technique is effectively a doubling of run time.

2.2.1.3 Combined distribution of net demand

The cumulative distribution function (CDF) $C(x;n)$ of the net demand is the total system demand minus the convolution of the probability distribution function (PDF) of realised wind production with the negative cumulative nodal COPT. The CDF for the net demand $C(x;n)$ which is the probability that the demand plus outages net wind power is less than *x*:

$$C(x;n) = \sum_j p_j^c(n)\left(1 - C^w(V_j^c(n) + D(n) - x; \iota(n))\right) \tag{2.15}$$

2.2.2 Scenario Tree

Thousands of scenarios [37] [38] are required to accurately describe the uncertain elements in the system, which presents computational burden and limits the system to be very small. Works in [3] [39] implement scenario reduction techniques [40] to reduce scenario set to a small number. In WILMAR model [41] [42], a large number of scenarios are generated by Monte Carlo simulation and then similar scenarios are merged until pre-defined number reached. However, those scenario reduction algorithms tend to delete the most extreme scenarios, which in fact dominate the requirement for online capacity. Hybrid SUC algorithms [43] [44] are proposed to deal with the possibility of losing extreme scenarios by using additional reserve constraints on top of scenario tree. The same as deterministic method, this exogenous reserve requirement needs careful tuning. Heuristic criteria based scenario selection method is proposed in [38]. Those scenarios are weighted to preserve the moments of hourly wind generation. However, this weighting strategy could bias the expected operation cost. Another scenario generation method is proposed in [45] by constructing and weighting scenario trees based on user-defined quantiles of the wind

forecast error distribution. The authors in [36] extended the methodology to incorporate demand forecast error and generation outages. Compared with Monte Carlo methods, quantile-based method could describe the critical information about the uncertainties by using only a small number of scenarios.

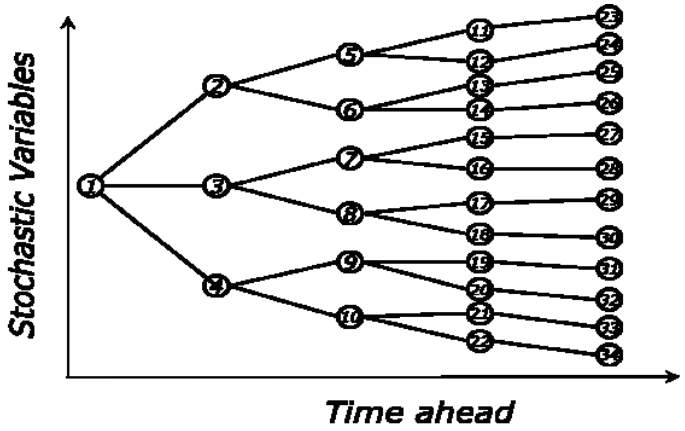

Figure 2-1 Schematic of a typical scenario tree in SUC

Each node n is associated with a user-defined quantile $q(n)$ of the net demand distribution (conditional on the net demand state at the root node), with all nodes on a given scenario having the same quantile. The nodal net demand $P^{nd}(n)$, as calculated at timestep k, is found by inversion of Equation (2.15) using the method of Van Wijngaarden, Dekker and Brent [119]:

$$P^{nd}(n) = C^{-1}(q(n); n) \tag{2.16}$$

where $C^{-1}(q; n)$ is the inverse function of C at node n, and is defined as

$$C^{-1}(q; n) = x \; where \; C(x; n) = q \tag{2.17}$$

Appropriate choices for the scenario quantile levels were discussed in [45]. Since the upper tail of the net demand distribution is likely to yield very high costs (due to load shedding or running of lowest merit plant), the tree should encompass several scenario sat very high quantile levels.

2.2.3 Stochastic Unit Commitment Formulation

The objective of the stochastic scheduling is to minimise the expected operation cost:

$$\sum_{n \in N} \pi(n) \left(\sum_{g \epsilon G} C_g(n) + \Delta\tau(n) \left(c^{LS} P^{LS}(n) + c^{FS} P^{FS}(n) \right) \right) \tag{2.18}$$

Subject constraints as following:

1. System Constraints

The load balance constraint is formulated as below and applied to bus ib in node n:

$$\sum_{g\in G_i} P_g(n) + \sum_{s\in S_i} P_s(n) + P_i^{WN}(n) - P_i^{WC}(n) + P_i^{LS}(n) = P_i^{D}(n) \qquad (2.19)$$

2. Thermal Generator Constraints

The local constraints pertaining to thermal units are set out in this section. The shutdown and start-up decision variables, N_g^{sd} and N_g^{st} , are nominally integer variables, while all other decision variables are continuous.

Some of the constraints at node n refer to subsets of the ancestors of n. The subsets are defined as follows. If a generator in group g starts generating at node n, then it must have been started up at a node in the set

$$A_g^{st}(n) = A(n) \cap \{n' \in N \cup P: \tau\big(a(n)\big) - T_g^{st} < \tau(n') \leq \tau(n) - T_g^{st}\big) \qquad (2.20)$$

If a generator in group g is shut down at node n, it cannot have started generating at any node in the set

$$A_g^{mu}(n) = A(n) \cap \left\{n' \in N \cup P: \tau(n) - T_g^{mu} < \tau(n') \leq \tau(n)\right\} \qquad (2.21)$$

If a generator in group g is started up at node n, it cannot have been shut down at any node in the set

$$A_g^{mo}(n) = A(n) \cap \left\{n' \in N \cup P: \tau(n) - T_g^{mo} < \tau(n') \leq \tau(n)\right\} \qquad (2.22)$$

Total power output and operating costs in each group can be written as

$$P_g(n) = P_g^{msg}\left(N_g^{up}(n) - N_g^{idle}(n)\right) + P_g^{x}(n) \qquad (2.23)$$

$$C_g(n) = C_g^{st}N_g^{sg}(n) + \Delta\tau(n)\left(C_g^{nl}\left(N_g^{up}(n) - N_g^{idle}(n)\right) + C_g^{idle}N_g^{idle}(n) + C_g^{m}P_g(n)\right) \qquad (2.24)$$

Total output above MSG is limited by the number of generating units and the range of power output of each unit:

$$P_g^{x}(n) \leq \left(N_g^{up}(n) - N_g^{idle}(n)\right)\left(P_g^{max} - P_g^{msg}\right) \qquad (2.25)$$

The number of generators that start generating at node n is equal to the number of generators that was started up T_g^{st} previousely:

$$N_g^{sg}(n) = \sum_{a \in A_g^{st}(n)} N_g^{st}(a) \tag{2.26}$$

The number of generators that are generating at node n is equal to the number of generators that were generating at node $n's$ parent, plus the number that started generating at node n, less the number that are shut down at node n:

$$N_g^{up}(n) = N_g^{up}(a(n)) + N_g^{sg}(n) - N_g^{sd}(n) \tag{2.27}$$

The number of generators that are off at node n is equal to the number of generators that were off at node $n's$ parent, plus the number that are shut down at node n, less the number that are started up at node n:

$$N_g^{off}(n) = N_g^{off}(a(n)) + N_g^{sd}(n) - N_g^{st}(n) \tag{2.28}$$

Total number of units which is allow to be shut down at node n is limited to the total number of units which were generating at node $n's$ parent, less the number of units that have been generating for less than T_g^{mu} hours:

$$N_g^{sd}(n) \leq N_g^{up}\big(a(n)\big) - \sum_{a \in A_g^{mu}(n)} N_g^{sg}(a) \tag{2.29}$$

Total number of units which allow to be started up at node n is limited to the total number of units which were off at node $n's$ parent, less the number of units that have been off for less than T_g^{mo}hours:

$$N_g^{st}(n) \leq N_g^{off}\big(a(n)\big) - \sum_{a \in A_g^{mo}(n)} N_g^{sd}(a) \tag{2.30}$$

The number of units which is allowed to be in idle state is limited to the total number of units which are online at node n:

$$N_g^{idle}(n) \leq N_g^{up}(n) \tag{2.31}$$

Ramp rate limits can be modelled as:

$$P_g^x(n) - P_g^x\big(a(n)\big) \leq \Delta\tau\big(a(n)\big)\Delta P_g^{ru} N_g^{up}(n) \tag{2.32}$$

$$P_g^x(n) - P_g^x\big(a(n)\big) \geq -\Delta\tau\big(a(n)\big)\Delta P_g^{rd} N_g^{up}\big(a(n)\big) \tag{2.33}$$

As shown in Figure 2-2 , the amount of frequency response that each generator can deliver is limited by its maximum response capability and the slope f_g^F that links the frequency response provision with the spinning headroom [30]:

$$0 \le R_g(n) \le R_g^{max} \tag{2.34}$$

$$R_g(n) \le f_g^F \left(N_g^{up}(n) P_g^{max} - P_g(n) \right) \tag{2.35}$$

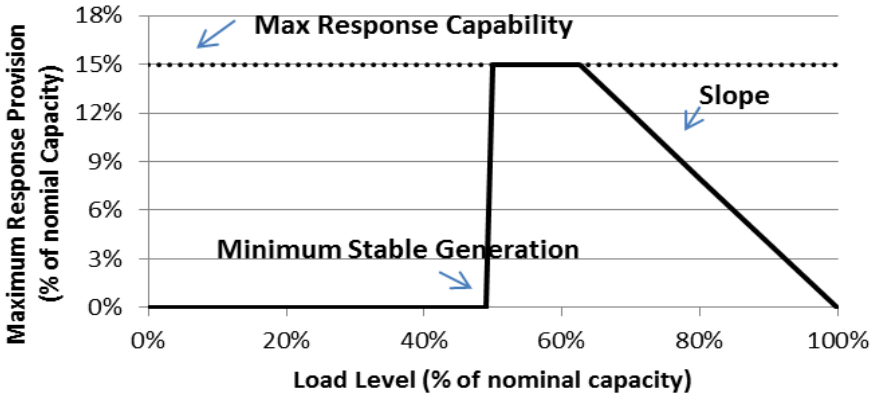

Figure 2-2 Example of response characteristic of conventional thermal plants.

3. Storage Unit Constraints:

The constraints for each storage unit at each node are formulated as below:

Energy constraints

$$E_s^{min} \le E_s(n) \le E_s^{max} \tag{2.36}$$

Operation state constraint (pumping or generating)

$$N_s^{Gen}(n) \in \{0,1\} \tag{2.37}$$

Power output constraints

$$P_s(n) = P_s^d(n) - P_s^c(n) \tag{2.38}$$

$$(1 - N_s^{Gen}(n)) P_s^{cmin} \le P_s^c(n) \le (1 - N_s^{Gen}(n)) P_s^{cmax} \tag{2.39}$$

$$N_s^{Gen}(n) P_s^{dmin} \le P_s^d(n) \le N_s^{Gen}(n) P_s^{dmax} \tag{2.40}$$

Energy balance constraint

$$E_s(n) = E_s(a(n)) + \Delta\tau(n) \left(\eta_s^c P_s^c(n) - \frac{P_s^d(n)}{\eta_s^d} \right) \tag{2.41}$$

Frequency response provision constraints:

$$0 \le R_s \le R_s^{max} \tag{2.42}$$

$$R_s(n) \le \left(N_s^{Gen}(n) P_s^{max} - P_s(n) \right) \tag{2.43}$$

4. Modelling of Demand Side Response

Demand side response (DSR) model is developed by incorporating constraints regarding maximum energy shifted in or out in each time step and total amount of

shifted energy in each day. Maximum energy shifted in or out in one time step can be defined as a proportion of the demand in that step or a proportion of the total demand in the day which that step belongs to. For DSR scheme, the total amount of shifted energy in each day should be zero. The proposed DSR model allows the user to choose a time during each day, when the total amount of shifted energy return to be zero.

A generic model for storage, DSR and combined heat and power (CHP) is developed as shown Figure 2-3. If the red circle and internal demand are ignored, this model can be used to describe the traditional storage. If the discharge route is ignored, this model can be used as CHP storage. If the red circle and discharge route are ignored, this model can be used to simulate flexible EV charging. (Note: Internal demand in the figure represents the original demand before shifting)

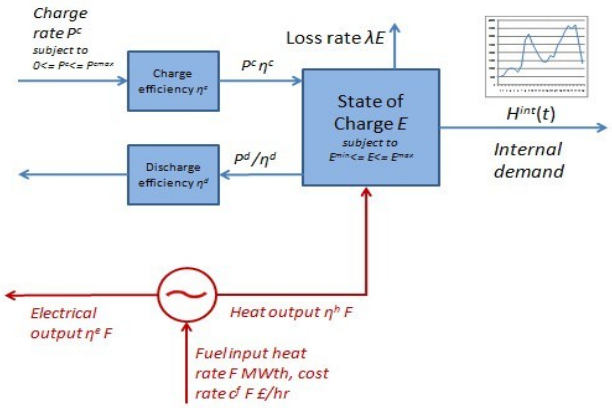

Figure 2-3 A generic model for storage, DSR and CHP

5. Risk Constraints:

Modern power systems are operated in a risk-averse fashion and system operators have different risk attitudes. Robust optimisation approach [46] [47] [48] utilises a user-defined uncertainty set to describe the uncertain elements and optimises the system operation against worst case situation. This approach provides robust solution which is feasible to all the realisations of uncertain elements. However, robust optimisation ignores the different possibilities for each realisation and tends to be conservative, since the worst case happens rarely. A combined stochastic and robust UC is proposed in [49], which allows users-specified weights on stochastic optimisation part and robust optimisation part. Chance constrained SUC is proposed in [50] [51] to enforce a low probability of load shedding. Conditional value-at-risk

(CVaR) [52] has been widely implemented in finance sector to measure risk. It can be formulated as a linear constraint [24], making it more computationally attractive. In this thesis, a simple risk constraint is adopted and incorporated into the model. The risk constraint limits the probability of the load shedding when it is larger than $P_j^{LSallowed}(t)$ below $Prob_j^{LSallowed}(t)$ at hour t:

$$Prob\left(P^{LS}(t) > P^{LSallowed}(t)\right) \leq Prob^{LSallowed}(t) \tag{2.44}$$

The above risk constraint is implemented using the following MILP formulation:

$$Prob\left(P^{LS}(t) > P^{LSallowed}(t)\right) = \sum_{n \in N(t)} \pi(n) * Ri(n) \leq Prob^{LSallowed}(t) \tag{2.45}$$

$$P^{LS}(n) \leq P^{LSallowed}(n) + Ri(n) * M \tag{2.46}$$

where M is a constant number [53] and $Ri(n)$ is a binary variable.

2.3 Modelling of Inertia-dependent Frequency Regulation Requirements

The aim of frequency control is to contain the dynamic evolution of frequency (e.g. following a generator outage) within defined security thresholds. In GB, this is specified by the Security and Quality of Supply Standard (GB-SQSS) [32]. Three criteria are used to set the security standards for the initial transient evolution of frequency (Figure 2-4):

1. Rate of Change of Frequency (RoCoF)
2. Frequency level at Nadir
3. Frequency level at intermediate quasi-steady-state

The RoCoF achieves the highest absolute value just after a disturbance occurs; initially the frequency drop is only limited by the inertial response of conventional generators; currently the standard prescribes that the RoCoF should not exceed 0.125Hz/s [54]. Furthermore, the governor response has to limit the frequency above a minimum value set to 49.2 Hz in case of the largest infeed loss [32]. An extended provision of primary frequency response enables meeting the intermediate quasi-steady-state condition; in the case of GB the frequency should stabilise above 49.5 Hz within 60s.

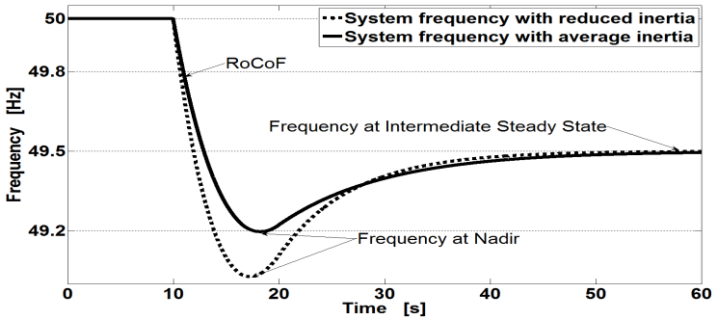

Figure 2-4 System frequency evolution after a contingency.

The growing concern is the reduced system inertia may compromise the performance of frequency regulation. In particular the RoCoF will increase, potentially causing disconnections of distributed generators by actuating RoCoF-sensitive protection schemes, which would further exacerbate the problem. In fact, RoCoF relay protection was found to be a main limitation to achieve high penetration of non-synchronous generation in Ireland [55]. Moreover if frequency drops rapidly, conventional generators may not be fast enough to provide the scheduled primary response [5]; the resulting frequency nadir may activate the Low Frequency Demand Disconnection [32]. As shown in Figure 2-4, The evolution with average inertia (solid) respects the GB security standards, while with reduced system inertia (dotted) these standards may be violated.

2.3.1 Dynamic Model of Frequency Evolution

The time evolution of system frequency deviation can be described by a first order ODE [56]:

$$2H\frac{\partial \Delta f(t)}{\partial t} + D * P^D \Delta f(t) = \sum_{g,s \in \mathcal{G},\mathcal{S}} \Delta P_{g,s}(t) - \Delta P_L \qquad (2.47)$$

where H [MWs/Hz] is the system inertia, D [%/Hz] represents the load damping rate, P^D[MW] is the load level and $\Delta P_{g,s}$ [MW] describes the additional power provided by the generator g or storage s following the generation loss ΔP_L [MW].

In [5] and [6], a conservative approach is adopted and load damping rate is set at zero, which enables derivation of analytical frequency response constraints. However, ignoring the load damping effect would lead to over-scheduling of the frequency response [57]. In Section 2.4.4, we demonstrate the level of load damping has a significant impact on the system operation.

According to the present GB practice, primary frequency response specifies the power increase to be delivered within 10s (T_d) following the contingency [32], while in Ireland the delivery time is 5s [30]. The impact of different delivery time requirements is analysed in Section 2.4.2. Furthermore, in this analysis the governor responses are assumed to be linearly increasing with time ([5], [6]) and thus characterised by a fixed slope until scheduled response is delivered. This model also includes a frequency dead-band Δf_{DB} for the governor [32] that prevents unnecessary response to relatively small frequency deviations. Therefore, the delivery of frequency response can be modelled as:

$$\Delta P_{g,s}(t) = \begin{cases} 0 & if\ t < t_{DB} \\ \frac{R_{g,s}}{T_d} * (t - t_{DB}) & if\ T_d + t_{DB} \geq t \geq t_{DB} \\ R_{g,s} & t \geq T_d + t_{DB} \end{cases} \quad (2.48)$$

where t_{DB} represents the time when frequency deviation reaches the dead-band Δf_{DB}.

In this chapter we propose a formulation to explicitly include the requirements on frequency dynamic evolution within SUC and hence optimally schedule frequency response provision. The differential equation (2.47) is mapped into the SUC model through considering three characteristic periods in the form of constraints associated with the RoCoF, the frequency at nadir and the frequency at quasi-steady-state.

2.3.2 Rate of Change of Frequency (RoCoF)

The time scale that involves the RoCoF constraint is limited to the first couple of seconds following a generation loss. In this short interval, the governor response is still not fully activated (i.e. $\Delta P_g \cong 0$) as the frequency deviation is negligible ($\Delta f \cong 0$). Hence, the maximum value of the rate of change of frequency ($RoCoF_{max}$) is proportional to the power shortage and inversely proportional to the system inertia; this suggests that the minimum level of system inertia *H*, required to satisfy the maximum RoCoF requirement is obtained as:

$$H = \frac{\sum_{g \in \mathcal{G}} H_g * P_g^{max} * N_g^{up}(n)}{f_0} \geq \left| \frac{\Delta P_L}{2RoCoF_{max}} \right| \quad (2.49)$$

where H_g is the inertia constant [s] of generator *g*, P_g^{max} is its capacity [MW] and f_0 [Hz] is nominal frequency.

2.3.3 Frequency Level at Nadir

The frequency nadir is defined as the minimum value achieved by frequency during the transient period. The nadir depends on system inertia, demand and governors' response. The system is assumed to be at nominal frequency (50Hz) in the pre-contingency state [5], and the delivery of frequency response is described by (2.48). By integrating (2.47), the evolution of frequency deviation is obtained as:

$$|\Delta f(t)| = \begin{cases} \left(\frac{\Delta P_L}{D'}\right) \cdot \left(1 - e^{-\frac{D'}{2H}t}\right) & if\ t < t_{DB} \\ \Delta f_{DB} + \left(\frac{\Delta P_L{}'}{D'} + \frac{2R * H}{T_d * D'^2}\right) \cdot \left(1 - e^{-\frac{D'}{2H}t'}\right) - \frac{R * t'}{T_d * D'} & if\ t \geq t_{DB} \end{cases} \quad (2.50)$$

where $D' = D * P^D$, $\Delta P_L{}' = \Delta P_L - D' * \Delta f_{DB}$, $R = \sum_{g,s \in \mathcal{G},S} R_{g,s}$ and $t' = t - t_{DB}$.

The time t^* when the frequency reaches its nadir can be calculated by setting $\frac{\partial |\Delta f(t)|}{\partial t} = 0$:

$$t^* = t_{DB} - \frac{2H}{D'} log\left(\frac{2R * H}{T_d * \Delta P_L{}' * D' + 2R * H}\right) \quad (2.51)$$

The value of frequency deviation at nadir can be found by substituting (2.51) into (2.50), and the maximum frequency deviation $|\Delta f_{nadir}|$ should not exceed the predefined threshold Δf_{max}:

$$|\Delta f_{nadir}| = \Delta f_{DB} + \frac{\Delta P_L{}'}{D'} + \frac{2R * H}{T_d * D'^2} log\left(\frac{2R * H}{T_d * D' * \Delta P_L{}' + 2R * H}\right) \leq \Delta f_{max} \quad (2.52)$$

Rearranging equation (2.52) gives:

$$\frac{2R * H}{T_d} \cdot log\left(\frac{2R * H}{T_d * D' \Delta P_L{}' + 2R * H}\right) \leq D'^2(\Delta f_{max} - \Delta f_{DB}) - D' \Delta P_L{}' \quad (2.53)$$

Proposition: $|\Delta f_{nadir}| \leq \Delta f_{max}$ if the following mixed integer linear constraints are satisfied:

$$\begin{cases} \frac{\sum_{g \in G_{CONV}} H_g * P_g^{max} * y_g}{50} \geq k^* \\ -M\left(1 - N_g^{up}(n)\right) \leq y_g - R \leq M\left(1 - N_g^{up}(n)\right) \\ -M * N_g^{up}(n) \leq y_g \leq M * N_g^{up}(n) \end{cases} \quad (2.54)$$

where M is a large number and k^* is the unique solution from

$$\frac{2k^*}{T_d} \cdot log\left(\frac{2k^*}{T_d * D' \Delta P_L{}' + 2k^*}\right) = D'^2(\Delta f_{max} - \Delta f_{DB}) - D' \Delta P_L{}' \quad (2.55)$$

Proof:

The left-hand side of inequality (2.53) is a monotonically decreasing function of $R * H\ (> 0)$. Therefore, for any given value of D', ΔP_L and Δf_{DB}, there exists a unique value of $R * H$, denoted by k^*, such that

$$\frac{2k^*}{T_d} * log\left(\frac{2k^*}{T_d * D' * \Delta P_L{}' + 2k^*}\right) = D'^2 * (\Delta f_{max} - \Delta f_{DB}) - D' * \Delta P_L{}' \qquad (2.56)$$

Then condition $|\Delta f_{nadir}| \leq \Delta f_{max}$ is satisfied if

$$H * R \geq k^* \qquad (2.57)$$

The system inertia can be calculated by using $H = \frac{\sum_{g\in\mathcal{G}} H_g * P_g^{max} * N_g^{up}(n)}{50}$. Therefore, the requirement on frequency nadir can be formulated as bilinear constraint

$$\frac{(\sum_{g\in\mathcal{G}} H_g * P_g^{max} * N_g^{up}(n)) * R}{50} \geq k^* \qquad (2.58)$$

By defining an additional variable y_g and applying standard reformulation method as in [53], condition (2.58) can be transformed to MILP constraints as shown in (2.54).

■

2.3.4 Frequency Level at Quasi-steady-state

The intermediate quasi-steady-state condition depends essentially on the total amount of frequency response delivered by generators at the time T_d. We denote the maximum allowed quasi-steady-state frequency deviation as Δf_{max}^{ss}; hence, for given amplitude of generation loss ΔP_L, this frequency deviation can be found, by assuming in (2.47), that RoCoF is effectively zero i.e. that the frequency has reached a constant level:

$$|\Delta f^{ss}| = \frac{\Delta P_L - R}{DP^D} \leq \Delta f_{max}^{ss} \qquad (2.59)$$

This allows quantifying the required frequency response to satisfy the quasi-steady-state frequency criterion as:

$$R \geq \Delta P_L - D * P^D * \Delta f_{max}^{ss} \qquad (2.60)$$

Unlike the other two constraints, the quasi-steady-state constraint does not depend on system inertia.

2.3.5 Frequency Regulation Requirements in the Future GB Low Carbon System

In the present GB system, the amount of required frequency response is based on the demand level, which is primarily driven by the quasi-steady state frequency threshold. However, the increased rating of the largest plant and the growing penetration of wind energy will make constraints associated with transient frequency evolution significantly more relevant. In this subsection we demonstrate the change in frequency response requirement from being determined by quasi-steady-state frequency limit, to being driven by nadir frequency limit. Assuming a constant of inertia H_g=5s and an average generators' loading level (80% of the units' capacity), the current quasi-steady-state frequency driven response requirement (red in Figure 2-5) is compared with the nadir frequency driven response requirement (black). In the past, given the largest plant rating of 1.32GW, response requirement driven by the quasi-steady-state frequency (red solid) is always binding, i.e. being above the frequency nadir driven requirement (black solid). On the other hand, after the new 1.8GW nuclear plant is commissioned, frequency nadir driven response requirement would dominate the overall requirement when demand is lower than 30GW in the system without wind (dashed) or when demand is lower than 45GW in the system with 20GW wind output (dotted).

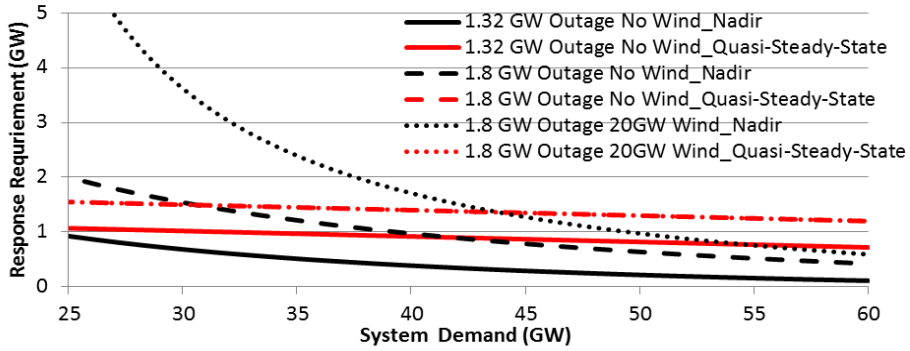

Figure 2-5 Nadir (black) vs quasi-steady-state (red) response requirement.

Another key concern is the impact of wind uncertainty on the scheduling of system frequency regulation. The requirements of frequency regulation depend on the system inertia, which will in turn be driven by the amount of synchronised conventional plant and the system demand. Different realisations of wind production could significantly

change the schedule of conventional plants, resulting in different levels of system inertia.

Stochastic scheduling explicitly models the uncertainty in wind production by using the scenario tree. As shown in Figure 2-1, commitment decisions are made in each node of the tree based on the realisation of wind energy production, which also provides the level of system inertia. In each time step, the system inertia could vary significantly depending on wind realisation in each node of the scenario tree. Figure 2-6 shows maximum (solid) and minimum (dotted) levels of system inertia in 4-hour ahead. Although it is possible to select a conservative estimation of system inertia at each time step (always the minimum level), this would over-schedule frequency regulation, potentially degrading efficiency of system operation.

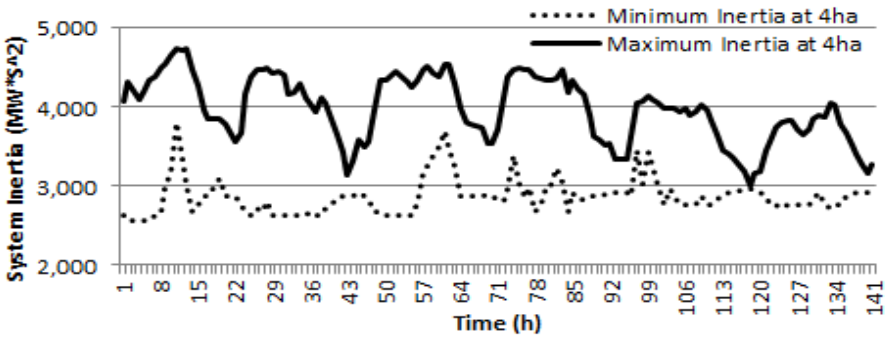

Figure 2-6 Example of maximum (solid) and minimum (dotted) system inertia in 4-hour ahead.

2.4 Case Studies

In this section, the proposed frequency regulation inclusive scheduling method is firstly compared with conventional methods. Then we demonstrate the impact of delivery time of frequency response, the maximum RoCoF and the load damping rate on the operation cost and the ability of the system to absorb wind; the importance of taking into account the inertia capability of generators in UC is also discussed.

Simulations of annual system operation are performed using the GB 2030 scenario [1]. The maximum demand is 59.4 GW, total conventional generation capacity is 70GW and the installed wind capacity is assumed to be 35GW (30% wind penetration). Existing 2.6 GW pump-hydro storage plant with 10GWh energy storage capacity and 75% round efficiency is also included in the generation mix. This storage plant provides up to 500 MW of frequency response. Table 2-1 summarises the characteristics of conventional plants [58].

The value of lost load ($VOLL$) and penalty on the shortage of frequency response are set at 30,000 £/MWh. The reference settings for delivery time($T_d = 10s$), frequency dead-band($\Delta f_{DB} = 15mHz$) and load-damping rate ($D = 1\%/Hz$) are chosen according to the GB practice [32]. The proposed requirement on RoCoF (0.5Hz/s) for the future GB system [54] is adopted.

The case studies were carried out over a twelve-core Inter 3.46GHz Xeon processor with 12GW RAM. The optimisation was solved by using FICO Xpress 7.1, which was linked to a C++ simulation application via the BCL interface [59].

Table 2-1
Characteristics of Thermal Plants Used in the Study

	Nuclear	Coal	CCGT	OCGT
Number of plants	**6**	**40**	**70**	**30**
Rated Power (MW)	**1800**	**500**	**500**	**200**
Min Stable Gen (MW)	**1800**	**250**	**250**	**50**
No-load cost (£/h)	**0**	**3364**	**7809**	**8000**
Marginal cost (£/MWh)	**10**	**72**	**51**	**110**
Startup cost (£)	**n/a**	**90000**	**32000**	**0**
Startup time (h)	**n/a**	**6**	**4**	**0**
Min down time (h)	**n/a**	**4**	**4**	**0**
Inertia Constant (s)	**5**	**5**	**5**	**5**
Max Response (MW)	**0**	**75**	**75**	**40**
Response Slope	**0**	**0.3**	**0.4**	**0.6**
Emission(kgCO2/MWh)	**0**	**925**	**394**	**557**

2.4.1 Value of the Proposed Scheduling Method

High penetration of wind generation not only reduces the inertia of the system, but also introduces the uncertainty in system inertia. As shown in Figure 2-6 the different realisations of wind power could lead to significant different levels of system inertia. Scenario-tree based stochastic scheduling model provides a platform to recognise the effect of unknown inertia caused by the wind uncertainty. The benefit of stochastic scheduling of reserve has been wildly recognised. This section explores the importance of scheduling frequency response by taking into account the impact of wind uncertainty on system inertia. Three different scheduling modes are compared; the first two follow traditional methods, the third is the one proposed in this chapter.

1. Deterministic scheduling (DS): reserve requirements are calculated dynamically but only based on single scenario [3] with a quantile of 0.96 and the inertia-dependent frequency response requirement is calculated based on this single scenario.

2. Stochastic scheduling with deterministic inertia (SS_1): the traditional stochastic approach is applied as in [36]. However, the frequency response requirement is deterministic and conservative; it is calculated using the worst-case scenario, thus covering the minimum available system inertia in each time step.
3. Stochastic scheduling with explicitly considering the impact of wind uncertainty on system inertia (SS_2): this scheduling method differs from SS_1 as, at each time step, the frequency response requirement is calculated for each scenario based on the associated system inertia.

The system performance with different methods is shown in Figure 2-7. As expected, both the stochastic methods reduce the operation costs and CO_2 emission compared to the DS case. In particular, the SS_1 provides approximately 1.2% operation cost reduction and 1% emission reduction, while the proposed method (SS_2) can further reduce the operation cost by more than 0.8% and the emission by more than 2%.

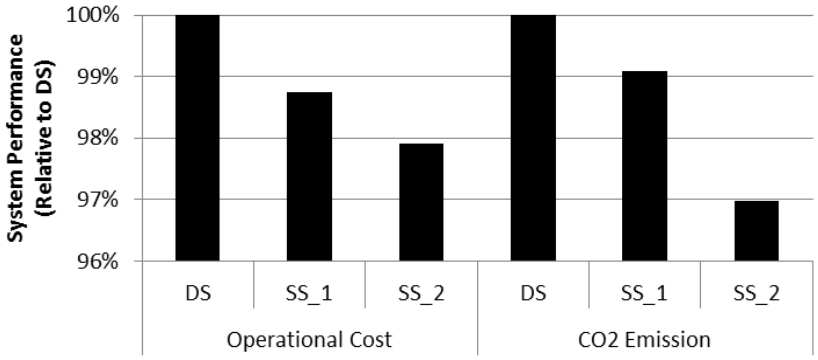

Figure 2-7 System performance comparison under different scheduling methods

Table 2-2 provides the details of system operation based on different scheduling methods. Compared with conservative approach (SS_1), directly considering the impact of wind uncertainty on system inertia allows to optimally scheduling high-cost but flexible plants (OCGT) to provide frequency response for the scenarios with low probability but very high response requirement. Therefore, the total spinning headroom is reduced, more wind generation is integrated and lower operation cost is achieved. It is also worth mentioning that the proposed method significantly reduces

the production of high-emission coal plants; therefore CO_2 emission of the system is dramatically reduced.

The computation time for each case is also presented in Table 2-2. The simulation was carried out for a year with half-hourly rolling and a duality gap of 0.1%. There are 17520 MILP optimisations in total. It took about 3.7 hours to solve the deterministic scheduling; while the computation times are much higher for both stochastic scheduling methods. Moreover, SS_2 takes considerable longer time than SS_1, due to the fact that SS_2 models the inertia-dependent frequency response constraints in all scenarios. While SS_1 only model them in the worst-case scenario. As a comparison, the same study was carried out by using SUC with commonly-used constant frequency response requirement; it takes about 22 hours to solve the problem.

Table 2-2
Detailed Results of System Operation

	DS	SS_1	SS_2
Operation Cost (£/MWh)	**38.15**	**37.67**	**37.36**
Curtailed Wind (% available wind)	**8.78**	**7.90**	**7.48**
Average spinning headroom (MW)	**8913**	**8560**	**7851**
COAL: Production (TWh)	**11.3**	**9.83**	**7.92**
COAL: Frequency Response (MW)	**292**	**245**	**201**
CCGT: Production (TWh)	**149.3**	**150.1**	**151.4**
CCGT: Frequency Response (MW)	**1231**	**1262**	**1334**
OCGT: Production (TWh)	**0.09**	**0.39**	**0.67**
OCGT: Frequency Response (MW)	**3**	**10**	**41**
Storage: Average state of charge (%)	**92**	**71**	**65**
Storage: Frequency Response (MW)	**490**	**472**	**476**
Computation Time (hours)	**1.6**	**25**	**27**

Similar studies are carried out with different wind penetration levels. As shown in Figure 2-8, when the wind penetration level is moderate, there is no significant economic benefit (difference between dotted and solid) from explicitly considering the impact of wind uncertainty on system inertia. On the other hand, when the wind penetration level reaches 20% or above, significant operation cost saving can be obtained by using the proposed method.

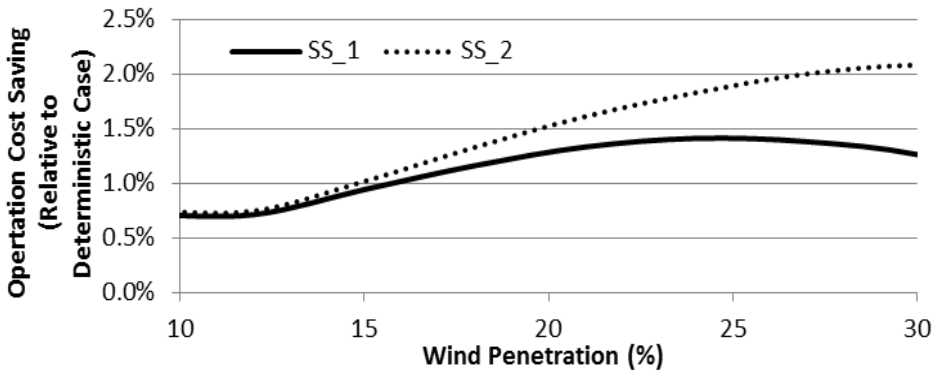

Figure 2-8 Annual operation cost saving from different operation methods: SS_1 vs SS_2.

2.4.2 Impact of Delivery Time of Frequency Response

In the future, with a larger maximum plant rating and reduced inertia, frequency will achieve the nadir much faster; therefore, in order to contain this drop, governor response would need to be delivered faster. This sub-section illustrates the impact of frequency response delivery time T_d on the system performance. The maximum response capability and the slope for each generator are assumed to remain the same as in Table 2-1, but the delivery time is varied from 10s to 3s. The results in Figure 2-9 show an operation cost reduction (solid) by up to 3% from decreasing the delivery time; in parallel, the need for curtailing wind (dotted) reduces by up to 50%. The benefits due to the reduction of delivery time show a clear saturation effect after 5s. This is because when the frequency delivery is fast enough to secure the nadir, the required additional power injection starts to be bounded by quasi-steady-state frequency requirement. These results are consistent with the discussions presented by National Grid [60].

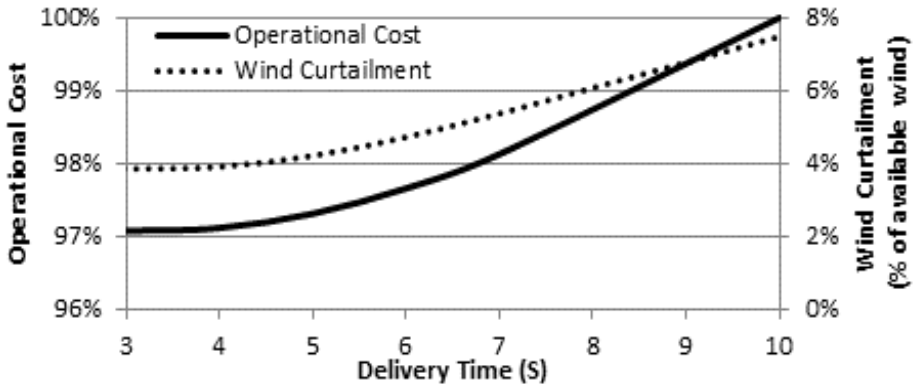

Figure 2-9 Impact of reducing the delivery time on system operation cost and wind curtailment.

2.4.3 Impact of RoCoF Settings

A large RoCoF due to reduced system inertia would force disconnection of distributed generation, leading to further system stresses. It is not clear yet how to choose appropriate RoCoF protection settings for the future GB system with high penetration of RES. Therefore, this section investigates the impacts of varying the maximum RoCoF from 0.5 Hz/s to 0.2Hz/s. As shown in Figure 2-10, the 0.2 Hz/s setting would lead to extremely high operation cost (solid) and wind curtailment (dotted). It is also worth noting that the benefits of relaxing maximum RoCoF beyond 0.4Hz/s will be limited. This conclusion supports the development of new recommendation to change the RoCoF protection settings for new and existing DG [54].

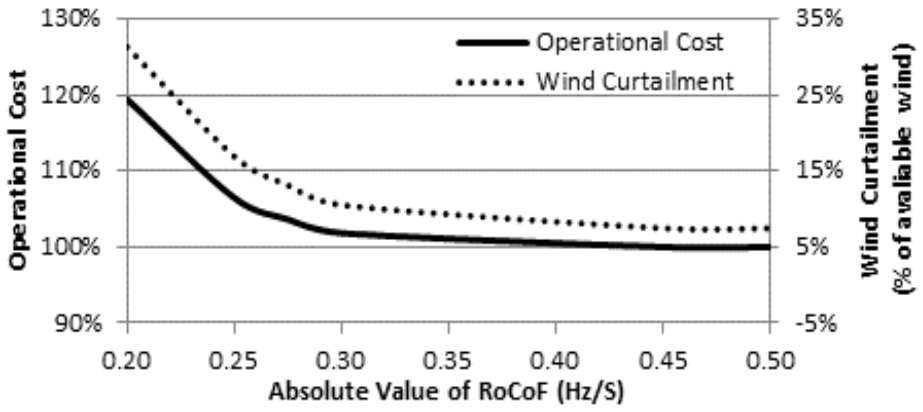

Figure 2-10 Impact of maximum RoCoF setting on the operation cost and the wind curtailment.

2.4.4 Impact of Load Damping Rate

This sub-section aims to investigate the impact of reducing the load damping rate from 1%/Hz to 0%/Hz. As shown in Figure 2-11, the increase of operation cost (solid) up to 4.2% follows a linear trend with the reduction of load damping rate; while the wind curtailment could linearly increase from 7.5% to 10.7 %. Although the overall damping effect may decline in the future due to the increased use of power electronics interfaces, neglecting it in the scheduling process could increase the generation cost and limit the ability of the system to accommodate wind generation. In fact, it would be beneficial to stimulate alternative provision of damping effect in the future system.

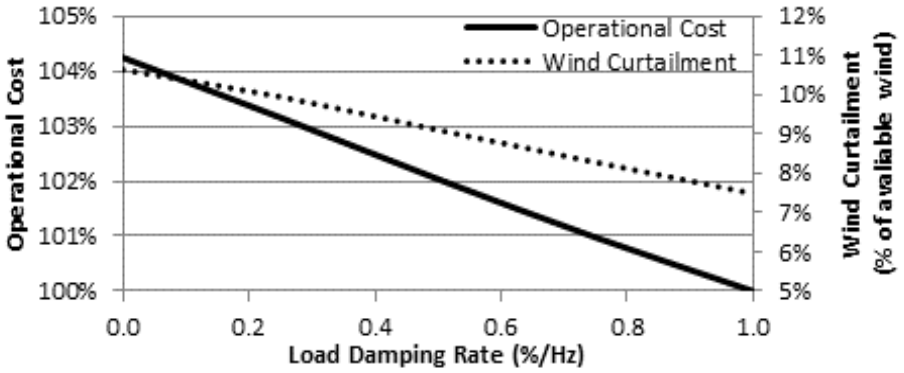

Figure 2-11 Impact of load damping rate on the system operation cost and wind curtailment.

2.4.5 Recognition of Different Inertia Capability of Generators

This sub-section demonstrates the benefits of recognising the generator's inertia in the scheduling process, which may inform the development of inertia market, as proposed in [61]. For this purpose, 5GW of CCGT plant are assumed to be characterised by higher inertia (8s) and slightly higher marginal cost. Two simulations are carried out, one with and another without recognising the inertia capability of plants. Results in Table 2-3 show that if the generators' inertia is explicitly considered, the scheduling process will commit more plants with higher inertia and their energy production will significantly increase, from around 4TWh to 24TWh in the study analysed. We also observe an increase in the total operation cost when the inertia is not fully recognised in the scheduling process as this will lead to increase in the amount of part-loaded plants to respect the RoCoF and nadir constraints. By being able to exploit the high inertia capability of some plants, a further 1TWh of wind can be integrated.

Table 2-3
Impact of Inertia Recognition on the Energy Production

(TWh)	With Recognition of Inertia	Without Recognition of Inertia
Nuclear	88	88
CCGT	134	155
CCGT_High Inertia	24	4
COAL	2	2
CCGT	0.5	0.5
Integrated Wind	96	95

2.5 Advantages of the Proposed Model in Understanding the Value of Flexibility

This section discusses the advantages of the proposed model in understanding the value of flexibility in the future low-carbon power systems. As examples, the impacts

of stochastic scheduling on the value of storage and the impact of inertia-dependent frequency regulation requirement on the value of response provision are assessed.

2.5.1 Impact of Stochastic Scheduling on the Value of Energy Storage

Stochastic scheduling is particularly suitable for analysing energy storage in a system with high RES penetration [7] [1], since the capacity of energy storage could be optimally split between energy arbitrage and ancillary service provision under various system conditions. Figure 2-12 presents the difference in the value of energy storage being evaluated using conventional deterministic scheduling and the stochastic scheduling approach. It will clearly be very important to optimally allocate the storage resource between providing reserve and conducting energy arbitrage, which only stochastic scheduling can facilitate. Stochastic scheduling is therefore superior to its deterministic counterpart, because the allocation of storage resources between energy arbitrage and reserve varies dynamically depending on the system conditions.

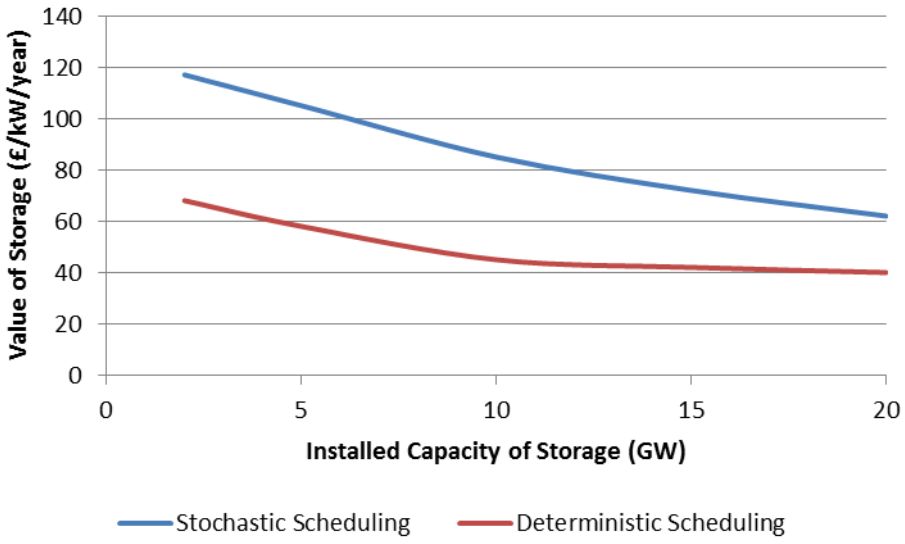

Figure 2-12 Value of storage: Stochastic Schedule VS Deterministic Schedule

In this particular case, we observe that with 2 GW of storage when considering a particular scenario, stochastic scheduling increases the value of storage by more than 75%, while for the installed capacity of 20 GW of storage this would be around 50%. It is due to the fact that deterministic scheduling keeps too much energy in the storage system as reserve and therefore loses the chances to do energy arbitrage. In conclusion, it is essential to utilise stochastic scheduling to fully capture the value of flexibility provided by energy storage.

2.5.2 Impact of Inertia-dependent Frequency Response Requirement on the Value of Frequency Response Provision

This sub-section focuses on quantifying the impact of incorporating inertia-dependent frequency regulation requirement on the value of frequency response provision (including DSR and fast storage). 5% of total demand at any given time is assumed to contribute to primary response provision. The value is assessed by comparing the annual system operating cost with and without the contribution of DSR to frequency regulation. Detailed assumptions could be found in [62].

Two different approaches are considered with respect to scheduling frequency regulation. With *constant requirement*, it is assumed that the volume of frequency response required in the system is determined in the same manner as in the today's system dominated by conventional generators, and therefore does not vary from hour to hour. *Inertia-dependent requirement* on the other hand is quantified for each time interval in our study based on the level of system inertia in that hour.

Figure 2-13 suggests that the value of DSR is several times higher in the case of inertia-dependent response requirement. Moreover, by directly taking into account of the inertia reduction, the value of response provision increases significantly from 2020 to 2030 due to the increased integration of RES. On the other hand, if only constant requirement is applied, there is not notable increase of the value.

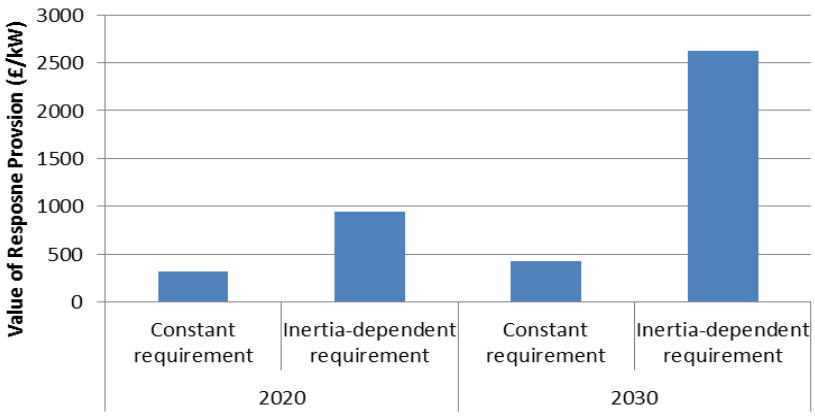

Figure 2-13 Value of response provision from demand side

Figure 2-14 further disaggregates the value of response provision across times of day. With constant response requirement, the value of responsive demand is slightly higher during daytime. The reason is that during night, the storage is normally pumping, which is sufficient to provides the bulk of the required response. With

inertia-dependent response requirement on the other hand, the value of responsive demand is much higher during night-time, when the synchronised capacity is low, thus requiring more frequency response.

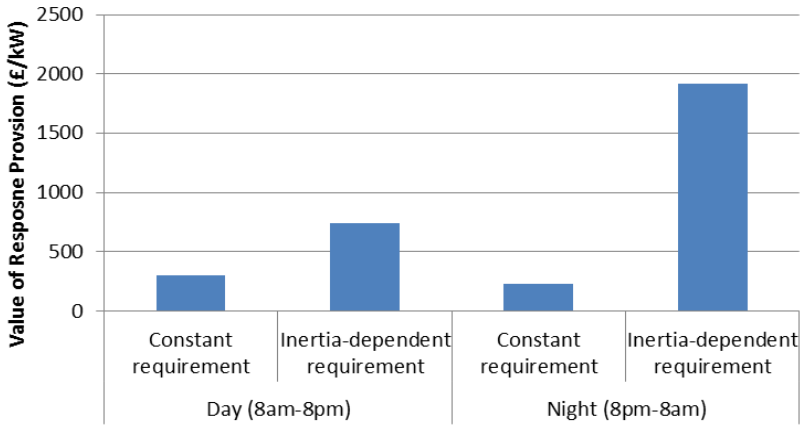

Figure 2-14 Value of response provision from demand side across times of day

2.6 Conclusion

At the present, in most jurisdictions frequency response requirements are primarily based on quasi-steady-state consideration. However, a growing share of wind generation, which does not provide inertial response, will make frequency control more challenging. In this chapter we propose a simplified system frequency evolution model and derive a set of mixed integer linear constraints in order to ensure that the system dynamic performance meet the security requirements. These constraints are then incorporated into a stochastic UC model. This novel framework allows the impact of wind uncertainty on system inertia to be directly addressed, which avoids over-scheduling the frequency response. Numerical results show the benefits of the proposed method compared with traditional methods in terms of operation cost savings and wind curtailment reduction.

Moreover, the model proposed enables the impact that different settings of frequency response delivery time, RoCoF limit and load damping rate would have on the system operation cost and on the wind curtailment to be assessed. The results obtained regarding the RoCoF and delivery time can provide economic evidence to support appropriate reforms of the grid code. Furthermore, we demonstrate the value of recognising different inertia capabilities of generators in the scheduling process.

The advantages of the proposed model in understanding the value of flexibility are also discussed. As examples, the impacts of stochastic scheduling on the value of storage and the impact of inertia-dependent frequency regulation requirement on the value of response provision are shown to be significant.

There are several areas of enhancing the proposed framework. The developed model assumes a fixed delivery time for all the generators while considering different speeds of individual generators in delivering scheduled frequency response will be important to provide appropriate incentives for speedy delivery of frequency response.

Furthermore, synthetic inertia from wind turbines is believed to play an important role in supporting the frequency performance in future low carbon power system [63]. However, it is very challenging to incorporate synthetic inertia into a UC model, since there is uncertainty associated with aggregated synthetic inertia capability from wind turbines even for a given level of wind power production [64]. The proposed model could be potentially extended to incorporate these multiple uncertainties in the future.

3. Value of Energy Storage in the Future GB Low Carbon Power System

3.1 Introduction

In recent years, concerns over climate change have increased the demand for renewable energy sources (RES) and other low carbon generation technologies such as nuclear plants. With respect to balancing capabilities, these technologies are less flexible than traditional fossil fuel plants. Therefore, the increased balancing requirements due to high RES penetration have to be provided by other sources. In this context, energy storage (ES) will potentially play an important role in supporting the integration of RES.

Extensive studies have been conducted to understand the value of ES. Previous work evaluated its capability to perform energy arbitrage [65] and provide ancillary services [66]. Multiple-service provision from ES was investigated in [1] [67]. Stochastic scheduling is particularly suitable for analysing ES in a system with high RES penetration [7], since the capacity of ES could be optimally split between energy arbitrage and ancillary service provision under various system conditions.

The above studies provide insights into the overall benefits of ES to the system, while other studies assess the techno-economic performance from the investor's point of view. Authors in [8] estimate the profit of ES in the PJM market, but by arbitrage-only. The profit of ES with combined services provision was studied in CAISO by [9]. Those studies use historical market prices and normally assume perfect information of these prices. However, in the future system with high RES penetration, electricity prices would become more volatile and uncertain.

This chapter focuses on an assessment of the value that distributed ES may deliver to the owner. This thesis quantifies the value of ES in energy and ancillary services markets. The site-specific value of ES is also analysed. For this purpose, stochastic system and storage scheduling model is prosed and applied

Sensitivity analysis across various scenarios has been carried out to analyse the key drivers for the value of ES and how it is affected by ES parameters and other factors such as prices of energy and ancillary services, network constraints and inherent

energy system characteristics. The assessment in Section 3.2 and Section 3.3 is carried out with the technology-agnostic approach. The storage is only represented through a limited number of generic key characteristics, such as power rating of storage (charging and discharging), round trip efficiency, and energy storage capacity. This allows a wide range of technologies to be mapped onto the results. Then Section 3.4 provides a review of the costs and performance of some particular storage technologies. Based on the results of Section 3.2-3.4, the potential storage technologies can be identified.

3.2 Assessment of the Value of Energy Storage in the Energy and Ancillary Services Markets

A set of studies have been carried out to investigate the applications of ES for multiple commercial activities in energy and ancillary services (balancing, short-term operating reserve (STOR) and frequency response (FR)) markets. The objective of these studies is to investigate the changes in the value of ES driven by changes in the generation mix and the corresponding energy and ancillary service prices. Therefore, the value of ES is assessed for the present system, as well as two future low-carbon systems (2030) with different levels of flexibility (as shown in Table 3-1):

1. The Present System: the system is dominated by fossil fuel plants. The analysis is performed using historical price data from the spot market in 2012 [68].
2. The future inflexible system: the system is characterised by high penetration of RES and base-load plants, as well as low capacity of Open Cycle Gas Turbines (OCGTs).
3. The future flexible system: this system contains the same level of RES as the inflexible system but with lower capacity of base-load plants and higher capacity of OCGTs.

Table 3-2 shows the technical, economic and emission characteristics of generation technologies. The operating cost of generators is divided into: variable, no-load, and start-up costs. The fuel and carbon prices are obtained from [69]. RES is assumed to

submit negative bid prices for a curtailment (equal to a Renewables Obligation Certificates (ROCs) value of 50 £/MWh). The capacity of CCGT/OCGT is equally allocated among three categories with different variable costs.

Table 3-1 Generation Mix in the Present and Future System

(GW/%)	Base load	Coal	CCGT	OCGT	Storage	Wind
Present System	15.3(19%)	22.8(29%)	27.2(35%)	4(4%)	2.7(4%)	6.9(9%)
Future Flexible System	20(19%)	0(0%)	30(29%)	20(19%)	2.7(3%)	30(30%)
Future Inflexible System	30(29%)	0(0%)	37(36%)	3(3%)	2.7(3%)	30(30%)

Table 3-2 Characteristics of Generators in the Future system

	P^{max}/P^{min} (MW)	Noload Cost (£/h)	Variable Cost (£/MWh)	Startup Cost (£)	Startup Time (h)	Response (MW)	Min up/down time (h)	Emission (kg/MWh)
Base	500/500	303	7.1	N/A	N/A	0	N/A	0
CCGT	500/250	8357	70/85/100	20500	4	100	4	394
OCGT	140/56	4200	250/350/450	0	1	70	1	557

3.2.1 Assessment Framework

The study is carried out in 2 stages (Figure 3-1). The first stage is to derive the electricity prices using the stochastic system scheduling model. In the second stage, the stochastic storage scheduling model determines the operation of ES to maximise the expected profit based on the price information from the system scheduling model. During the second stage, the capacity of ES under investigation is assumed to be small enough that can be modelled as a price taker [8].

a. Stochastic generation scheduling model and settlement

The stochastic generation scheduling model [70] minimises the expected operating cost across all the possible realisations of uncertain elements. The full range of possible realisations is firstly discretised into a set of representatives by user-defined quantiles, and then the corresponding probabilities $\pi(n)$ can be calculated by using the trapezium rule. These representatives and the associated probabilities are used to build a scenario tree. The optimisation is subject to dynamic constraints for thermal and bulk storage units. Operating reserve requirements are endogenously optimised within the model. The scheduling is performed on a rolling basis, in which only here-and-now decisions are fixed and all subsequent decisions are discarded.

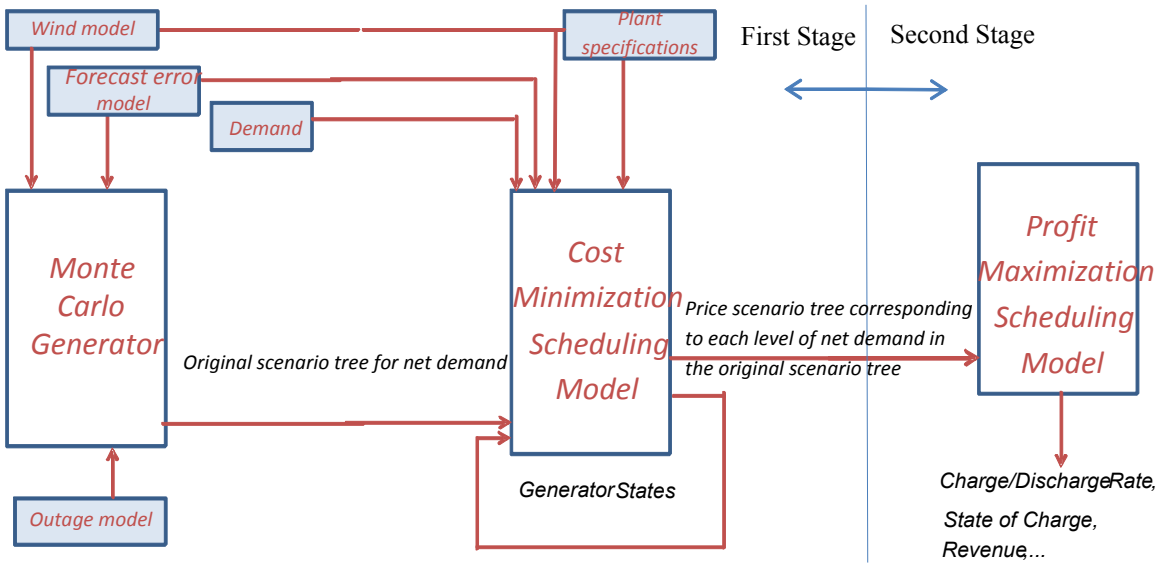

Figure 3-1 Assessment framework to evaluate distributed ES

Alternative settlement schemes have been proposed for the stochastic system scheduling [71]. The energy-only real-time pricing scheme is adopted in this chapter, which has been implemented by [72] to investigate the value of demand side flexibility. Under this scheme, all the compensation is based on the actual state of the system. After the commitment decisions are made, the model calculates the optimal dual variables in each node of the scenario tree. In order to provide a prediction for the real-time price, it is necessary to remove the probabilities from these optimal dual variables: if $p(n)$ is the optimal dual variable for node n and $\pi(n)$ is the probability of reaching node n, the forecasted price for node n can be calculated as $p(n)/\pi(n)$. A similar scenario tree can be built, containing the forecasted real-time prices and the associated probabilities for each node. For the arbitrage-only case, the price is calculated in a single scenario which describes the most-likely value of stochastic variables in day-ahead. This assumption corresponds to the day-ahead energy only market. In addition, FR and STOR services are assumed to be contracted ahead of operation scheduling on an annual or monthly basis.

b. Profit maximisation scheduling model of ES under price uncertainty

The storage scheduling model optimises the operation of ES to maximise its expected profit based on the price scenario tree. The scheduling is also performed using rolling planning. After all the uncertainties are realised, the final prices in each timestep are obtained and used to settle the market.

The objective is to maximise the expected profit:

$$\sum_{n\in N}(\pi(n)\big(Pr_{RT}(n)\big(P_s^d(n)-P_s^c(n)\big)+Pr_{Res}*P_s^{Response}(n)+Pr_{STOR}*P_s^{STOR}(n)\big)\big) \tag{3.1}$$

subject to storage physical constraints include: (i) charge rate limits (Equation 3.2) and discharge rate limits (Equation 3.3); (ii) stored energy balance constraints (Equation 3.4); (iii) constraints associated with the amount of energy that can be stored (Equation 3.5).

$$N_s(n)P_s^{cmin} \le P_s^c(n) \le N_s(n)P_s^{cmax} \tag{3.2}$$

$$(1-N_s(n))P_s^{dmin} \le P_s^d(n) \le (1-N_s(n))P_s^{dmax} \tag{3.3}$$

$$E_s(n)=\rho_s E_s\big(a(n)\big)+\left(\eta_s^c P_s^c(n)-\frac{P_s^d(n)}{\eta_s^d}\right) \tag{3.4}$$

$$E_s^{min} \le E_s(n) \le E_s^{max} \tag{3.5}$$

Provision of FR and STOR requires ES to provide extra power for 30 minutes and 2 hours respectively. Therefore, additional constraints are developed for ES to keep enough headroom and stored energy, if contracted to provide these services.

Ancillary service provision constraints include: (i) maximum FR capability (Equation 3.6) and STOR service capability (Equation 3.7); (ii) storage headroom constraints associated with response provision (Equation 3.8) and STOR provision (Equation 3.9); (iii) stored energy constraints associated with response provision (Equation 3.10) and STOR provision (Equation 3.11).

$$0 \le P_s^{Response}(n) \le P_s^{ResponseMax} \tag{3.6}$$

$$0 \le P_s^{STOR}(n) \le P_s^{STORMax} \tag{3.7}$$

$$P_s^{Response}(n) \le \Big(\big(1-N_s(n)\big)P_s^{dmax}-P_s^d(n)+P_s^c(n)\Big) \tag{3.8}$$

$$P_s^{STOR}(n) \le P_s^{dmax}-P_s^d(n)+P_s^c(n)-P_s^{Response}(n) \tag{3.9}$$

$$0.5*P_s^{Response}(n) \le E_s(n)-E_s^{min} \tag{3.10}$$

$$2*P_s^{STOR}(n) \le E_s(n)-E_s^{min}-0.5*P_s^{Response}(n) \tag{3.11}$$

The optimisation is solved by using a mixed integer linear programming solver developed by FICO [59] which is linked to a C++ simulation application via the BCL interface.

3.2.2 Value of Energy Storage in the Energy and Ancillary Service Markets

The above assessment framework is applied to investigate the applications of ES for multiple commercial activities in energy and ancillary service markets. Unless otherwise specified, the following studies assume that the energy capacity of ES is large enough for discharging at maximum output for 4 h and the round-trip efficiency is 75%.

a. Impact of increased RES and generation inflexibility

In this section, the value of ES is analysed in the proposed scenarios. For future systems, two cases are studied:

(1) ES performs arbitrage-only in the day-ahead energy market: the scheduling of ES is made and fixed in the day-ahead market, based on the prices calculated by the most-likely forecast of uncertain variables.

(2) ES participates in both the day-ahead energy market and the real-time balancing market: the scheduling of ES is made based on the real-time price scenario tree, and updated on a rolling basis.

The value of ES is calculated by dividing the revenue of ES over its lifetime with the energy capacity (kWh). As shown in Figure 3-2, the value is between £100 (current) - £650 (future) per kWh, which is higher in future systems because of the increasing volatility in real-time prices caused by the high RES penetration. The value of ES in the present system is in line with the results presented in [8]. Moreover, by providing balancing services, the additional value obtained by ES is significant. Due to the difficulty of system balancing (high real-time price) and high RES curtailment (negative real-time price), the price volatility in the inflexible system is higher and therefore the corresponding value of ES is also higher.

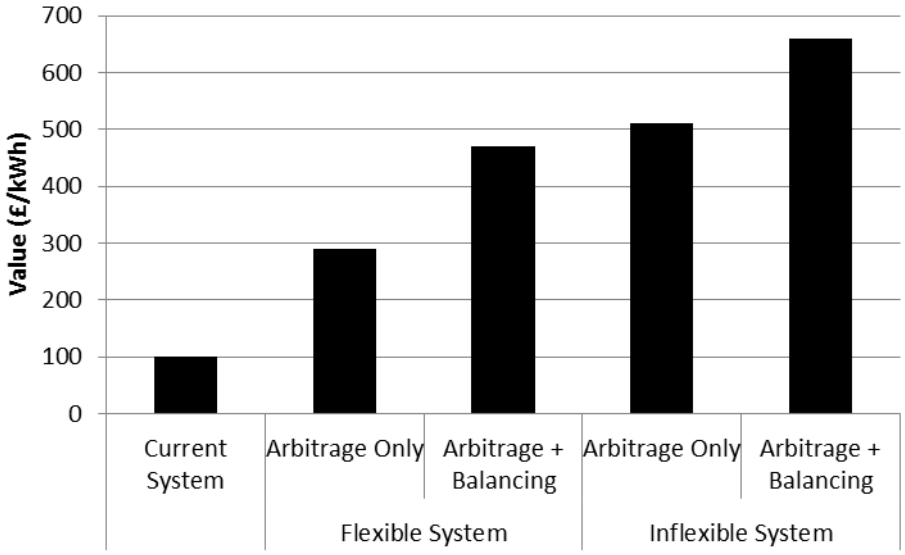

Figure 3-2 Value of ES across different systems

b. Impact of energy capacity and efficiency on the value of ES

Studies are conducted to understand the dependency of the value of ES on the energy capacity and the round-trip efficiency. The result is expressed as a ratio between the value with a specified energy capacity/efficiency and the value of ES in the base case.

Figure 3-3 shows that the value (£/kWh) drops when the energy capacity is higher. This suggests that the demand to keep the energy in ES for a long period is relatively low. Clearly, this is likely to be system-specific; as in some systems, it may be required to have a large energy reservoir.

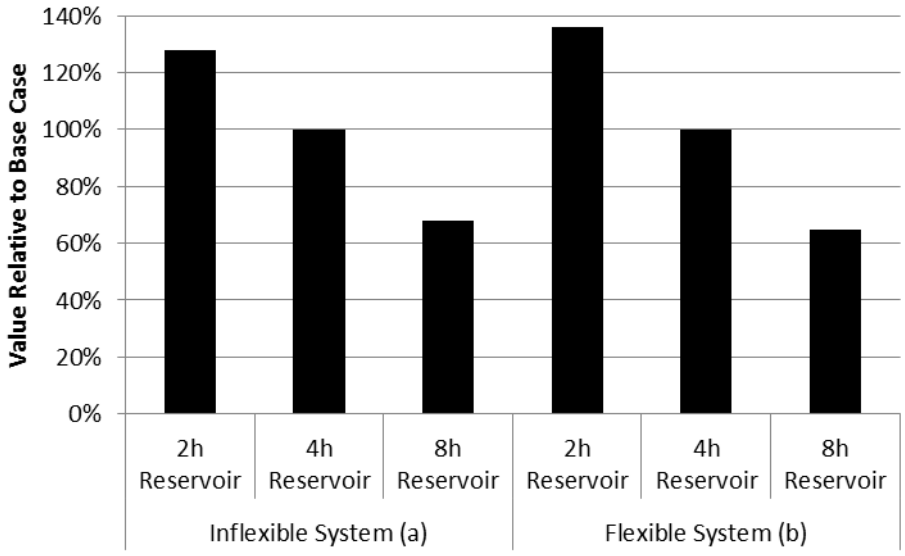

Figure 3-3 Impact of energy capacity on the value of ES

For the impact of the round-trip efficiency, as discussed by [73], negative prices may provide incentives to increase losses. Hence, ES with lower energy efficiency could obtain a higher value. This case is illustrated in the inflexible system (Figure 3-4 (a)). In the flexible system (Figure 3-4 (b)) and systems without ROCs (Figure 3-5), curtailment of RES is less and therefore negative prices occur less often. The improved efficiency increases the value but only marginally.

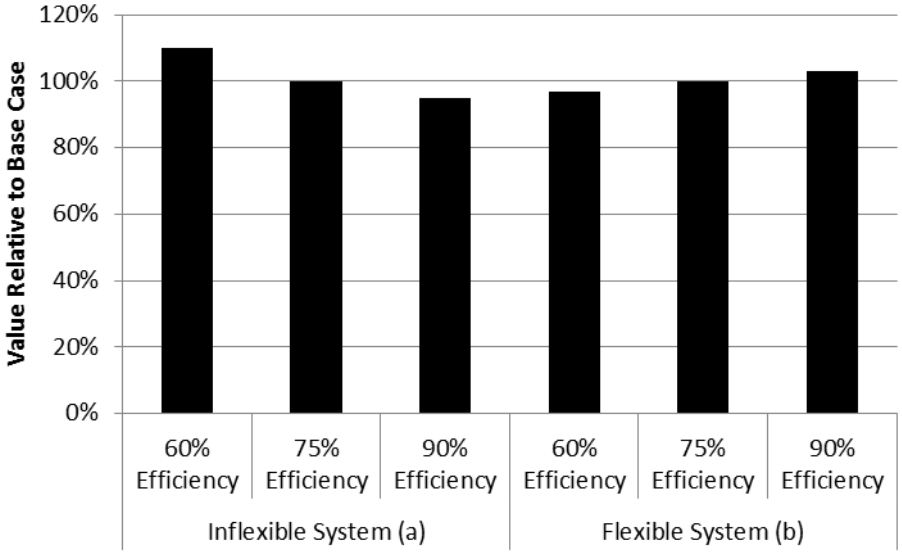

Figure 3-4 Impact of round-trip efficiency on the value of ES (case studies with ROCs)

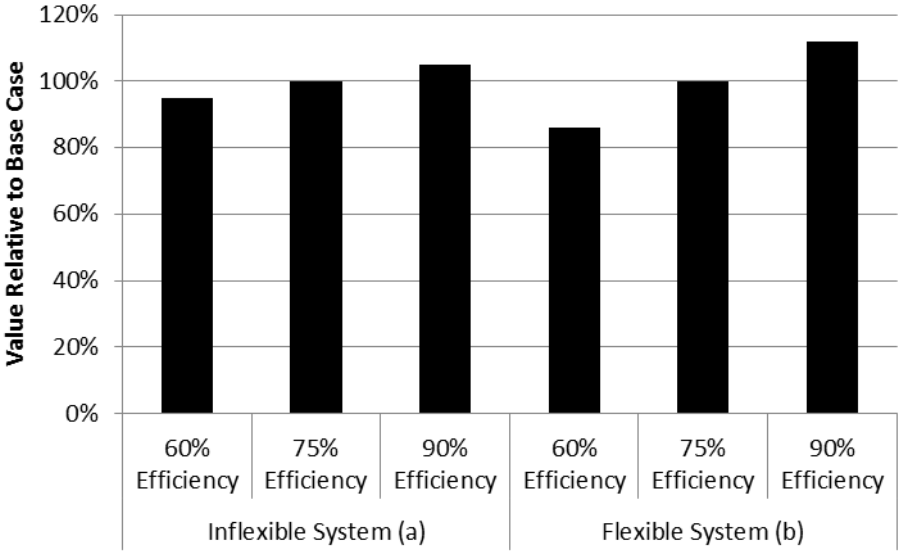

Figure 3-5 Impact of round-trip efficiency on the value of ES (case studies without ROCs)

c. Impact of penetration level of ES and competing technologies

It is important to note that the value of storage investment will depend on the flexibility of the system. This implies that the value of the first investment that adds

system flexibility will be higher than the value of subsequent investment. In order to illustrate this phenomenon, we carried out a set of different studies that add 5 GW of storage on top of the storage in the base case. The studies were carried out on the future inflexible and flexible systems. The results are shown in Figure 3-6.

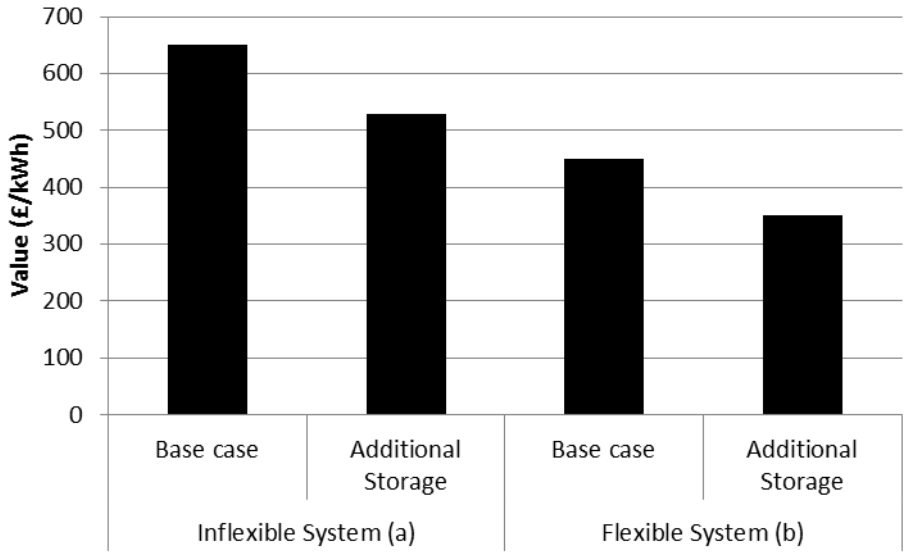

Figure 3-6 Value of subsequent storage investment

The results show that the value of subsequent storage investment decreases in both flexible and inflexible systems. This is expected since the system now becomes more flexible and therefore additional storage will have lower value. For example, the value of subsequent 5GW of storage in the inflexible system decreases from £650/kWh to £530/kWh in the inflexible system. Similarly, the value reduces from £450/kWh to £350/kWh in the flexible system.

Another sensitivity study was carried out to investigate how the value of storage will change if there is enhancement on the flexibility of CCGT plants. This is related to the reduction in the synchronisation time of CCGT from 4 h to 2 h, reduction in minimum up time from 4 h to 2 h and the reduction in the minimum stable generation limit from 50% to 20%. The studies were carried out for both inflexible and flexible future systems. The results are presented in Figure 3-7. The results are consistent with the previous findings. Improving the flexibility of the system will actually decrease the value of the storage.

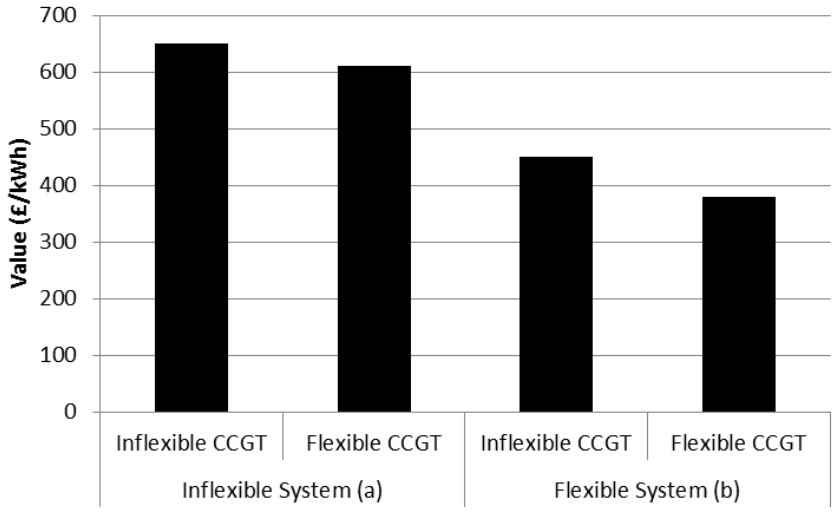

Figure 3-7 Impact of flexible CCGT on the value of storage

d. Value of ES by providing multiple ancillary services

In order to maximise the revenue, ES can also provide additional commercial services including FR and STOR. For specific time windows (between 7 and 9 am and between 5 and 9 pm are chosen in this study), part of ES's capacity are dedicated to providing these services. A certain amount of stored energy is also required to ensure the deliverability. The studies analyse the value of ES in the future inflexible system by using a range of market prices for FR (10 - 50 £/MW/h) and for STOR (5 - 25 £/MW/h), as well as various percentage (0-75%) of storage capacity allocated for these services.

The results in Figure 3-8 (a) indicate that by providing the extra FR service, the value of ES can be enhanced, especially if the market price is attractive (e.g. £50/MW/h). Due to the additional operation constraints, the value obtained from energy and balancing market decreases, but not significantly since the service is provided only for few hours a day.

For the STOR service (Figure 3-8 (b)), the ability of ES to offer this service can also improve its value, although this depends on the market prices. Reduction in the revenue from energy and balancing activities caused by STOR provision is higher than that by FR provision because of a longer service provision requirement. The results in Figure 3-8 (b) also demonstrate that for some market prices, there exists an optimal capacity to provide STOR service (e.g. 25% in the 15 £/MW/h case).

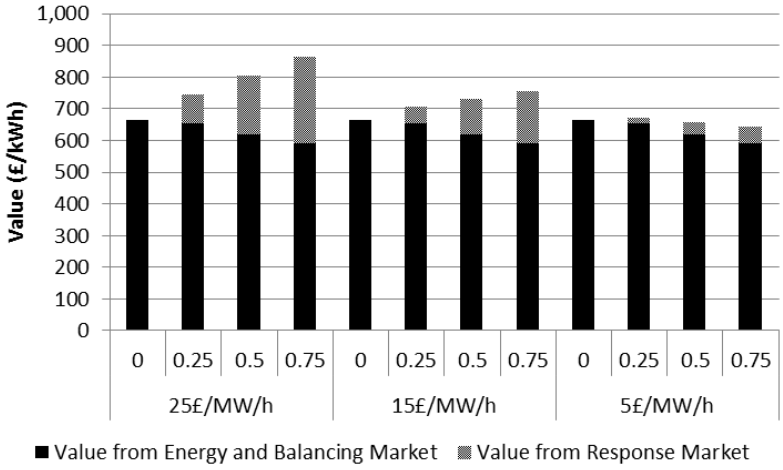

(a) Frequency Response

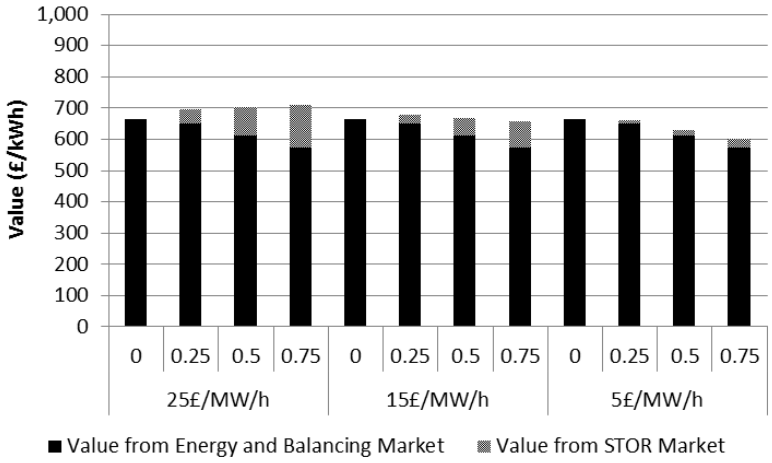

(b) STOR Service

Figure 3-8 Value of ES from real-time market and ancillary service market

3.3 Assessment of the Site-specific Value of Energy Storage

This set of studies quantifies the value of distributed ES installed at specific sites without the reinforcement of the local network. Therefore, ES may have to reduce its charge rate from optimal value during some hours with low price and high demand. As a consequence, ES may also lose some opportunities to discharge during some high price hours due to energy limits. The same model as in Section 3.2 is applied, but with the additional local network constraint:

$$D(n) + P_s^c(n) - P_s^d(n) \leq P_{DN}^{Max} \tag{3.12}$$

Three potential sites for ES applications are considered:

- A university (UoL) with a peak demand of 11MW

- An hospital (GI) with a peak demand of 4 MW
- A pharmaceutical company (AZ) with a peak demand of 8.8 MW

Due to the local network constraint, the operation of ES must be optimised taking into account the customer's load profiles at these specific sites. The profiles will depend on the nature of customer's activities and use of electricity. For example, the electricity load in a university during the evening and early morning is much lower compared to the load at day-time. While this is a general trend, the difference may be less significant for a hospital that runs 24 h. In this study, the load profiles were taken from the metered data.

The size of the various storage systems used in the following study is between 2MWh and 38MWh.The results in Figure 3-9 suggest that for a relatively small size ES, the value is not site-specific. In these cases, the network constraints are not binding and do not affect the storage operation.

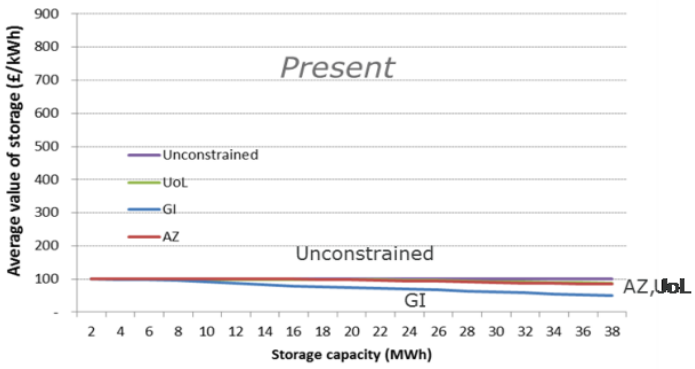

(a) Present System

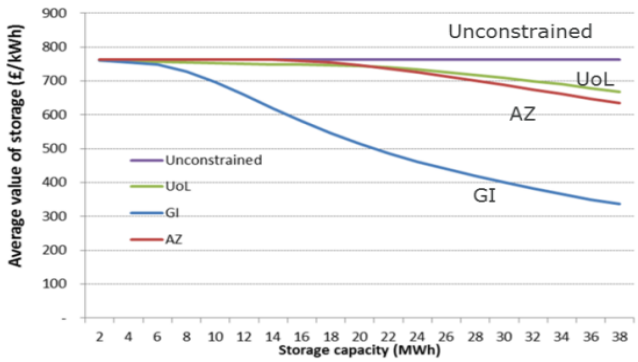

(b) Future system - Inflexible

Figure 3-9 Value of ES in different sites

When the storage capacity increases up to a threshold, the effect of network constraints becomes visible. This threshold depends on the load profiles and the capacity of the local network. Among the three sites, GI has the lowest capacity then AZ and UoL. Thus, the threshold for GI is the lowest one, followed by AZ and then UoL. Figure 3-9 also suggests that, for the present system (a), the network capacity impact is relatively small as the price typically correlates well with the demand. However, in the future system (b) with a significant amount of RES, the prices will be more volatile and the correlation between the demand and the prices will also be affected by the output of RES. Hence, the effect of the network constraint becomes much more significant. The optimal sizing of ES is a challenging task and a cost-benefit analysis is necessary to inform the optimal investment.

3.4 Review of Energy Storage Technologies

This section reviews the technologies best suited for grid-scale distributed ES from kW to MW in power and a few hours in energy capacity. The current status as well as projected performance and costs in 2020 are discussed. The DOE/EPRI Electricity storage handbook [74] provides an excellent overview of current ES technology status and costs, which has been used as the basis of the current cost data. This is further informed by the 2012 PNNL report [75] along with data in [76] and [77], which provides some current cost and performance data and some projections up to 2020.

Figure 3-10 attempts to rank each of the technologies reviewed in terms of key characteristics, with red meaning that the technology is less suitable or has significant disadvantages, green meaning that it is more suitable and/or has important advantages and amber meaning that it displays some of both.

Technology	Power density	Energy density	Cycle life	Self discharge	Round trip efficiency	Capital cost	C-rate	Depth of discharge	Commercial Maturity
Lead acid									
Advanced Lead acid									
Li-ion									
NiMH									
Flow battery V-V									
NaS									
ZEBRA									
Zinc air									

Figure 3-10 Characteristics of reviewed ES technologies.

Several technologies offer current ES costs of < 300 £/kWh, namely conventional lead acid (190 £/kWh), sodium sulphur (NaS) (230 £/kWh), and zinc air (120 £/kWh). However all have disadvantages, namely limited life, charge and discharge rate and the lack of deep discharge capability of conventional lead acid, the need to maintain the operating temperature of sodium sulphur which results in a high self-discharge and its availability only in the MW/MWh range, and the current lack of maturity of zinc air. NiMH appears to be an expensive option for distributed ES at around 610-1100 £/kWh. Therefore the technologies best suited today for highly distributed ES at the kW/kWh range appear to be the advanced lead acid batteries and lithium ion batteries, with Li-ion offering higher rates of charge/discharge. For applications into the 100's kW/kWh range, NaS, sodium-nickel chloride (ZEBRA) and flow batteries are all promising, with 1MW systems available at 230 £/kWh for NaS, 320 £/kWh for ZEBRA, and 460 £/kWh for vanadium flow batteries. Neither advanced lead acid nor lithium ion appears to compete effectively at the MW scale in terms of cost. Zinc air offers the prospects of costs down to 120 £/kWh at this power level, but requires scale up and improvement in charge/discharge rate and cycle life.

Costs of some technologies are expected to be reduced dramatically by 2020. Li-ion pack costs will be halved to 240 £/kWh driven by increasing volumes for electric vehicles (EVs). NaS and ZEBRA costs remain unchanged at 230 £/kWh and 300-600 £/kWh as there are only limited supplier, and there is no external driver for growth. Vanadium flow battery costs will be reduced to around 240 £/kWh, driven by significantly improved performance (currently being demonstrated in research labs). Advanced lead acid battery costs remain unchanged at around 420-840 £/kWh as there is no major external driver for volume, and the sector is already mature. NiMH costs remain unchanged or even increased as it is no longer developed for automotive applications. Zinc air remains a promising low cost option but still struggles to deliver a high cycle life.

3.5 Conclusion

This chapter presents the analysis for distributed ES with the application to energy and ancillary services markets. A large set of studies has been carried out to

understand the value of ES and the key drivers that affect the value across different scenarios.

The results suggest that in the energy and ancillary services markets, the value of ES is mainly driven by the temporal arbitrage opportunities created by volatility in either or both day-ahead and real-time (balancing) energy prices. The value is between £100/kWh and £650/kWh, which is higher in the future system due to increased price volatility caused by high RES penetration. On top of energy and balancing services, ES can also provide additional ancillary services e.g. FR. If the market prices for those services are attractive, they can add up to £200/kWh to the value of ES. The value of ES is shown to be site-specific when there is an active network constraint. The effect of network constraint becomes much more significant in the future system where the coincidence level between the demand and the prices is reduced due to the output of RES.

Due to high costs associated with current storage technologies, none of reviewed technologies appears to be cost-effective in the present power system. The most effective technologies today are Li-ion battery (£480/kWh) for kW/kWh application and NaS (£230/kWh) for 100's kW/kWh application, both of which are much higher than the value (£100/kWh) quantified in the present system. However, with the expected dramatic reduction of the costs and significantly increased value (£280/kWh - £860/kWh) in the future system, some technologies such as (Li-ion, Vanadium flow, NaS, ZEBRA, Advance lead acid) may become attractive. Zinc air remains a promising low cost option, but still struggles to deliver a high cycle life. NiMH (610-1100 £/kWh) appears to be an expensive option for ES, even in the future system.

4. Assessment of the Role and the Value of Frequency Regulation Support from Wind Plants

4.1 Introduction

Integration of large share of renewable energy resources (RES) increases requirements for various ancillary services to support real-time balancing of demand and supply. In particular, as the integration of wind generation displaces conventional plant, the system inertia provided by the rotating mass reduces, which already causes concerns regarding the frequency stability [60]. The rate of change of frequency (RoCoF) will increase, potentially causing disconnections of distributed generators by actuating RoCoF-sensitive protection schemes. This would further exacerbate the problem. RoCoF relay protection actually has been found to be a main limitation to achieve high penetration of non-synchronous generation in Ireland [55]. Moreover if frequency drops rapidly, conventional generators may not be fast enough to provide the primary frequency response (PFR); the resulting frequency nadir could activate the costly under frequency load shedding.

On the other hand, a significant amount of rotational energy is stored in the wind plants (WPs). Extensive research has been conducted to investigate the limits and capabilities of variable speed wind turbines (VSWT) to provide frequency regulation support. A supplementary control loop could be incorporated into the WPs controller to provide frequency regulation similar to conventional plants. Authors in [78] show that VSWT with proposed controller could even provide more synthetic inertia (SI) than a fixed-speed wind turbine. Studies in [79] analysed the impact of operating speed and power output on the contribution of WPs to short-term frequency regulation. The authors in [80] assessed SI and PFR capability of different turbine technologies, while the maximum temporary extra active power support from a commercial multi-megawatt VSWT is quantified in [81]. In additional, the delivery of frequency regulation support from HVDC-connected offshore wind farms is discussed in [82] and [83].

The impact of frequency regulation support from WPs on the system frequency performance has been assessed in different systems. The results suggest that the

RoCoF and frequency nadir could be significantly improved, but it depends on the system specifications and the design of the controller. The study in [84] analyses the impacts of WPs participating in U.S Western Interconnection and concludes that wind penetration level and the PFR capability of conventional plants are key factors in determining the effectiveness of frequency regulation support from WPs. The authors in [12] present an investigation on impacts of SI and droop parameters on the system frequency response performance. The simulation results suggest too aggressive design of SI and droop response does not further reduce the frequency nadir, but leads to a delay of the system frequency reaching steady-state condition. Moreover, the recovery period after SI provision could cause second frequency nadir and therefore, the authors in [13] proposed a modified control algorithm to mitigate the recovery effect.

Although the technical impact of frequency regulation support from WPs has been widely studied, the impact on system scheduling and economics of system operation is not yet fully understood. Since there exist alternative options (e.g Relaxing RoCoF [55] or DSR [58]) to relieve the concerns over frequency stability, it is important to fully understand the associated economic and environmental benefits through the simulation of system operation. The economics and revenue of PFR provision from WPs has been studied in WI [85] and Spanish system [86], but the values of SI provision and combined provision of SI and PFR are still to be quantified. Moreover, when designing WPs controllers it is important to take into account the actual system needs, which may vary depending on a number of factors including wind penetration level. The benefits and drawbacks of alternative designs of frequency regulation support from WPs need to be assessed.

In fact, very little work has been conducted on the modelling of system benefits and implications of providing different levels of SI and supporting frequency control. Clearly, there are some key differences between WPs and conventional plants in providing frequency regulation services, and it is important that these are incorporated in optimal generation scheduling models. Firstly, the work in [10] and [11] points out that there is uncertainty associated with the capacity of online WPs for a given level of wind generation production, leading to a challenge to estimate the aggregated SI from WPs. Moreover, as discussed in [12] and [13], additional PFR may be required to

support the recovery of original turbine speed. The system scheduling needs to take into account of the recovery effect in order to retain the system security. Finally, in order to provide PFR, WPs need to be de-loaded from the optimal operation point. The balance between costs and benefits of PFR provision need to be considered explicitly in the system scheduling. In this context, this chapter develops a novel methodology to incorporate frequency regulation support provided both by conventional plants and WPs into generation system scheduling and therefore, enables the benefits of frequency regulation support from WPs to be quantified. We identify three key contributions of this work:

1. It proposes a simplified model for the aggregated SI provision from WPs with the capability to consider the uncertainty associated with the number of online WPs and the additional PFR required due to the recovery effect.
2. This chapter introduces a novel stochastic unit commitment model, which takes into account of SI and PFR from WPs. The SI and PFR are linked with the system operation through the constraints associated with the limits of RoCoF, nadir frequency and quasi-steady-state frequency.
3. The benefits of frequency regulation support from WPs are assessed in the future GB system with different wind penetration levels and frequency regulation requirements. The impacts of the uncertain capacity of online WPs and the recovery effect are also investigated. The need of the frequency regulation support from WPs and the optimal design of the controllers are shown to be system-specific.

This modelling approach can therefore quantify the benefits of WPs supporting system frequency control and also inform the development of future grid codes and market mechanisms associated with frequency regulation. The rest of this chapter is organised as follows: Section 4.2 discusses the modelling of frequency regulation support from WPs. Section 4.3 describes the proposed scheduling model to assess the benefits of SI and PFR provision from WPs. The case studies are presented and explained in Section 4.4, while Section 4.5 concludes the chapter.

4.2 Modelling of Frequency Regulation Support from Wind Plants

The VSWT can be equipped with additional frequency controller to provide system frequency regulation support. The SI controller responses to RoCoF and provides only transient response, which is most effective in fast frequency changes. Droop control, on the other hand, provides permanent response, is effective in relatively slower events, and permits participation of WFs in PFR. Combined SI and droop control could reduce both the transient excursions of the frequency and its steady-state error [80].

4.2.1 Synthetic Inertia Provision from Wind Plants

According to the principals of inertia control, an additional control loop could be incorporated into WP controller to response to the derivative of frequency change (4.1). Unlike conventional plants, SI of WPs is dominated by the design of the controller. The physical limits of WPs must be respected. Otherwise, based on actual system characteristics, the controller should be designed to maximise the system benefits.

$$\Delta P_W^{Inertia} = -\underbrace{K_{inertia}}_{2*H_{Wind}} \frac{\partial \Delta f}{\partial t} \tag{4.1}$$

The SI provided by WP depends on a number of stochastic variables, including the wind speed, the wind turbulence, mechanical states of the drive train and so on. However, the aggregated SI from WPs in the large scale system may be obtained from the averaged SI from each WP [10]. In fact, the capacity of online WPs is the key factor in determining the aggregated SI. The work in [11] illustrates the uncertainty associated with capacity of online WPs for a given level of wind generation by using historical data from wind farms in Ireland. Figure 4-1 shows the maximum, average and minimum capacity of online WPs for a given level of system-wise wind generation. The figure suggests that there exists large uncertainty regarding the capacity of WPs being online. This raises the question of reliability associated with the reliance on the SI, given the risk-averse attitude of system operators.

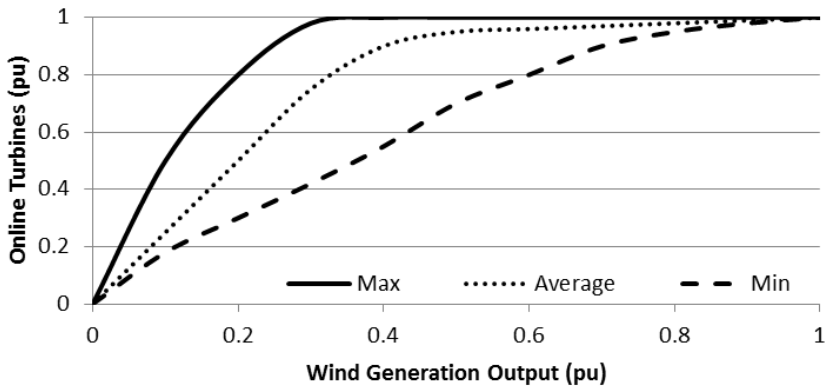

Figure 4-1 Variable speed wind turbines operating above minimum speed

Below rated wind speed, the provision of SI is followed by a recovery period, causing the power output of the WPs temporarily below the original operation point. As studied by [12], the recovery period could delay the system frequency from reaching steady-state condition, in the worst case, causing second frequency nadir. In the Hydro Quebec system [87], the specification requires the maximum generation reduction during recovery phase to be lower than 20% of nominal power. In fact, as urged in [13], the recovery period after providing SI may lead to an increased demand on PRF. However, it is complicated to qualify exactly how much of the additional PRF should be scheduled to supply the required energy to accelerate WPs. To demonstrate the effect of energy recovery and the benefit of reducing it, two simplified relationships between additional PFR at steady state and the time constant of SI are assumed (Figure 4-2).

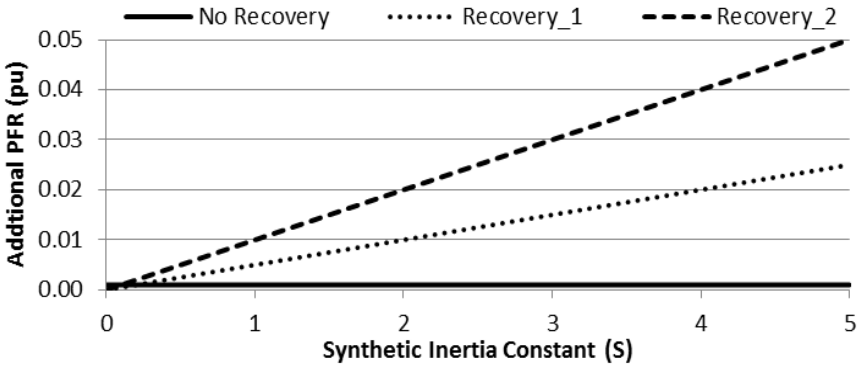

Figure 4-2 Assumptions on recovery effect of SI provision

4.2.2 Primary Frequency Response Provision from Wind Plants

Similar to the speed governors of conventional generators, a droop control can be incorporated into WP controller to response to the frequency change.

$$\Delta P_W^{PFR} = -K_{droop}\Delta f \quad (4.2)$$

WPs must be de-loaded from optimal operation point to provide sufficient headroom in order for the droop function to be active in under-frequency events. During normal operation conditions, the controller is set to provide headroom by generating less power than what is available. Different de-loading approaches have been proposed and can be classified as pitching techniques and over-speeding techniques. The maximum PFR is the maximum potential output and actual output of the wind turbine. 5% or 10% headroom is normally chosen in the technical studies [85]. However, in order to achieve the optimal system operation, the cost of de-loading of WPs and the benefit of PFR provision need to be balanced by the scheduling tool.

4.3 Scheduling of System Operation with the Frequency Regulation Support from Wind Plants

A stochastic scheduling model with inertia-dependent frequency regulation requirements is formulated in order to assess the benefits of frequency regulation support from WPs. The model is capable of optimising system operation by simultaneously scheduling energy production, standing /spinning reserves and inertia-dependent frequency regulation. The unit commitment and economic dispatch are solved over a scenario tree. The scenarios are weighted according to their probabilities and hence the model optimally balances the cost of committed generation against the expected cost of not meeting demand. The detailed model of SUC is presented in Section 2.2. The following section extends the inertia-dependent frequency regulation requirements proposed in Section 2.3 to incorporate the contribution from wind plants.

4.3.1 Inertia-dependent Frequency Regulation Requirements with Contribution from Wind Plants

The inertia-dependent frequency response requirements was developed in section 2.3, which is extended in the section to incorpate the frequency response contruitbion from WPs.

The time evolution of system frequency deviation can be described by a first order ODE [56]:

$$\underbrace{(2H_{Conv}+2H_{Wind})}_{2H^*}*\frac{\partial\Delta f(t)}{\partial t}+D*P^D*\Delta f(t)=\underbrace{\sum_{g,s\in\mathcal{G},S}\Delta P_{g,s}(t)+\Delta P_W(t)}_{\Delta P^*}-\Delta P_L \tag{4.3}$$

where H_{Conv} (H_{Wind})[MWs/Hz] is the inertia from conventional plant (WPs), D [%/Hz] represents the load damping rate, P^D[MW] is the load level, $\Delta P_{g,s}(\Delta P_W)$ [MW] describes the extra power provided by conventional generators/storage (WPs) following the generation loss ΔP_L [MW].

In this analysis the PFR from conventional plants and WPs are assumed to be linearly increasing with time and thus characterised by a fixed slope until scheduled PFR is delivered at T_d [5]. This model includes a dead-band Δf_{DB} that prevents unnecessary response to relatively small frequency deviations. Therefore, the delivery of PFR can be modelled as:

$$\Delta P^*=\begin{cases}0 & if\ t<\ t_{DB}\\ \underbrace{\frac{R_{g,s}+R_w}{T_d}}_{R^*}*(t-t_{DB}) & if\ T_d+t_{DB}\geq t\geq\ t_{DB}\\ R_{g,s} & t\geq\ T_d+t_{DB}\end{cases} \tag{4.4}$$

where t_{DB} represents the time when frequency deviation reaches the dead-band Δf_{DB}.

1) Rate of change of frequency (RoCoF)

The time scale that involves the RoCoF limit is only the first couple of seconds following a generation loss. In this short interval, the governor response is still not fully activated as the deviation of frequency is very small. Hence, the minimum level of system inertia H^*, required to satisfy the maximum RoCoF requirement ($RoCoF_{max}$) is obtained as:

$$H^*=\frac{\sum_{g\in\mathcal{G}}H_gP_g^{max}N_g^{up}(n)+H_{SI}*P_{online}^{WN}(n)}{f_0}\geq\left|\frac{\Delta P_L}{2RoCoF_{max}}\right| \tag{4.5}$$

2) Frequency level at nadir

The frequency nadir is defined as the minimum value achieved by frequency during the transient period. The nadir depends on system inertia and governors' response. The system is assumed to operate at nominal frequency (50Hz) in the pre-contingency state, and the delivery of frequency response is described by (4.4). By integrating (4.3), the frequency nadir can be calculated as

$$|\Delta f_{nadir}| = \Delta f_{DB} + \frac{\Delta P_L{}'}{D'} + \frac{2R^* * H^*}{T_d * D'^2} log\left(\frac{2 * R^* * H^*}{T_d * D' * \Delta P_L{}' + 2 * R^* H^*}\right) \quad (4.6)$$

where $D' = D * P^D$, $\Delta P_L{}' = \Delta P_L - D' * \Delta f_{DB}$, $t' = t - t_{DB}$ and $R^* = \sum_{g,s \in \mathcal{G},S} R_{g,s} + R_w$.

Following the proposition in Section 2.3.3, the frequency nadir requirement with SI contribution from WPs can be obtained as:

Proposition: $|\Delta f_{nadir}| \leq \Delta f_{max}$ if the following mixed integer linear constraints are satisfied:

$$\begin{cases} \dfrac{\sum_{g \in \mathcal{G}} H_g * P_g^{max} * y_g + H_{SI} * P_{online}^{WN}(n)}{f_0} \geq k^* \\ -M\left(1 - N_g^{up}(n)\right) \leq y_g - R^* \leq M\left(1 - N_g^{up}(n)\right) \\ -M * N_g^{up}(n) \leq y_g \leq M * N_g^{up}(n) \end{cases} \quad (4.7)$$

where M is a large number and k^* is the unique solution from

$$\frac{2k^*}{T_d} \cdot log\left(\frac{2k^*}{T_d D' \Delta P_L{}' + 2k^*}\right) = D'^2(\Delta f_{max} - \Delta f_{DB}) - D' \Delta P_L{}' \quad (4.8)$$

3) Frequency level at quasi-steady-state

The quasi-steady-state condition depends essentially on the total amount of PFR delivered at the delivery time T_d. Given the quasi-steady-state frequency deviation limit Δf_{max}^{ss}, this frequency deviation can be found, by assuming in (4.3), that RoCoF is effectively zero i.e. that the frequency has reached a constant level:

$$|\Delta f^{ss}| = \frac{\Delta P_L - R^*}{D P^D} \leq \Delta f_{max}^{ss} \quad (4.9)$$

This allows quantifying the required PFR to satisfy the quasi-steady-state frequency criterion as:

$$R^* \geq \Delta P_L - D * P^D * \Delta f_{max}^{ss} \quad (4.10)$$

There may exit additional PFR due to the provision of SI from WPs. By defining this additional PFR as R_{add}^{WN}, the PFR requirement in steady state can be described as

$$R^* \geq \Delta P_L - D * P^D * \Delta f_{max}^{ss} + R_{add}^{WN} \quad (4.11)$$

4.4 Case Studies

In this section we quantify the system benefits of different levels of frequency regulation provided by WPs. This analysis is aimed at informing cost-benefit case for developing controllers for providing frequency regulation by WPs, including the value

of providing SI, importance of controlling wind turbine speed recovery and the benefits of combined provision of SI and PFR.

4.4.1 Description of the System

Simulations of system benefits of different levels of frequency regulation provided by WPs are performed in the context of GB future scenario with different penetration levels of wind generation. The maximum demand is nearly 60 GW, total conventional generation capacity is 70 GW and the installed wind capacity is varied, 20, 40 and 60GW, corresponding to 20%/40%/60% wind penetration level. A 2.6 GW pump-storage plant with 10GWh energy capacity and 75% round efficiency is also included in the generation mix. The characteristics of conventional plants are presented in Table 2-1 [58]. The reference settings for delivery time($\mathrm{T_d} = 10\mathrm{s}$), RoCoF limit ($\mathrm{RoCoF_{max}} = 0.25\ \mathrm{Hz/s}$), frequency dead-band($\Delta f_{DB} = 15\mathrm{mHz}$) and load-damping rate ($D = 1\%/\mathrm{Hz}$) are chosen according to GB standards [32]. The impact of relaxed RoCoF limit [54] is also assessed. In the base case study, the average number of online WPs is utilized as in [10]; the time constant of SI is assumed to be 5s; and the recovery effect is ignored. The optimization was solved by using FICO Xpress [59], which was linked to a C++ simulation application via BCL.

4.4.2 System Benefits of SI Provision from WPs

This section assesses the system benefits of SI provision from WPs, in terms of reducing the frequency regulation cost and reaching high wind penetration level. Firstly, the impact of increased capacity of WPs without SI on the annual frequency regulation cost is assessed. As shown in Figure 4-3, when 60GW of WPs are installed, the annual cost increase about 10 times when compared with the system without WPs. This increased cost is associated with more part-loaded operation of conventional plants and moreover the increased wind curtailment. The relaxation of RoCoF limit from 0.25Hz/s to 0.5 Hz/s is shown to be capable to significantly alleviate the challenge of frequency regulation provision. In fact, with relaxed RoCoF limit, the system can integrate 20GW of WPs without causing significant increase in the frequency regulation cost. However, frequency regulation cost still increases more than 3 times when the stalled capacity of WPs reaches 60GW.

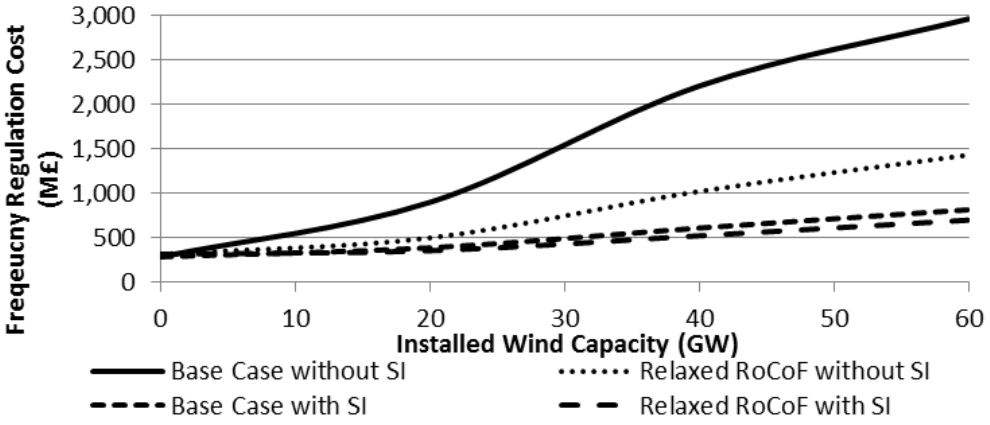

Figure 4-3 Impact of WPs on the frequency regulation cost

SI is shown to be more effective than the relaxation of RoCoF limits in reducing the cost associated frequency regulation provision. With the SI capacity, only marginal cost increases would occur when upto 40GW of WPs is installed. However, SI would not completely eliminate the increase of frequency regulation cost in the system with very high capacity of WPs. The results also suggest that with SI capability, the benefit of RoCoF relaxation is limited.

The SI capability of WPs also plays an important role in achieving high level of wind penetration. Figure 4-4 shows the wind penetration level with different installed capacities of WPs. The results suggest that without SI capability, the penetration of wind generation increases linearly with the installed capacity of WPs, but saturated after reaching 30%. In particular, when the installed capacity of WPs increases from 40GW to 60GW, the penetration only increases by 3%, implying a large amount of wind curtailment. On the other hand, with the SI capability, wind penetration could increase by about 10%, reaching over 40%.

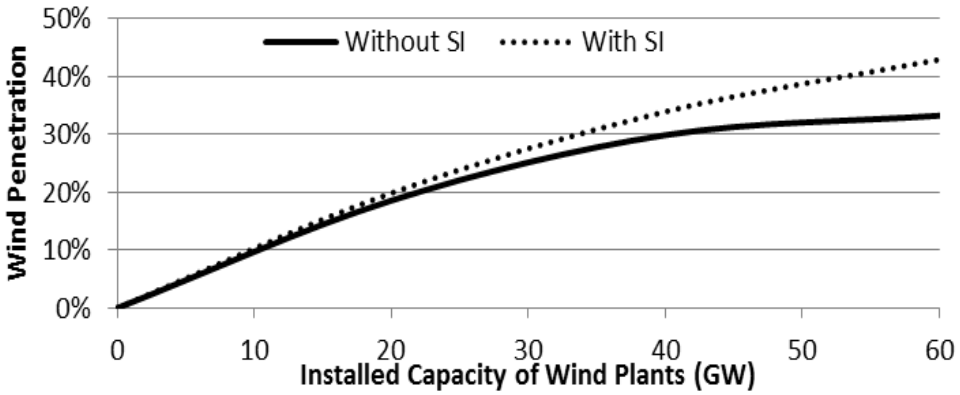

Figure 4-4 Impact of SI on the ability of the system to reach high wind penetration

4.4.3 Value of SI with Different Technology Penetration Levels

This section explicitly quantifies the economic value of equipping SI capability to WPs. Since it is not likely that all the WPs will provide SI in the future, especially for the WPs which are already in operation or under construction; this section, in particularly focuses the marginal operation cost saving as a function of the volume of WPs with the SI capability. The presented results can be used as a reference in cost-benefit analysis aimed at determining the amount of WPs to be equipped with SI capability.

As shown in Figure 4-5, the value of SI is in general high with moderate technology penetration level, but decreases linearly with increased capacity of WPs capable of providing SI. The value shows a significant jump when the installed wind capacity increased from 20GW to 40GW; while the further increase is moderate when the capacity increases to 60GW. The results also suggest that it may not be necessary to require all WPs to provide SI, since the marginal value of the service is very low after 30GW of WPs with this function.

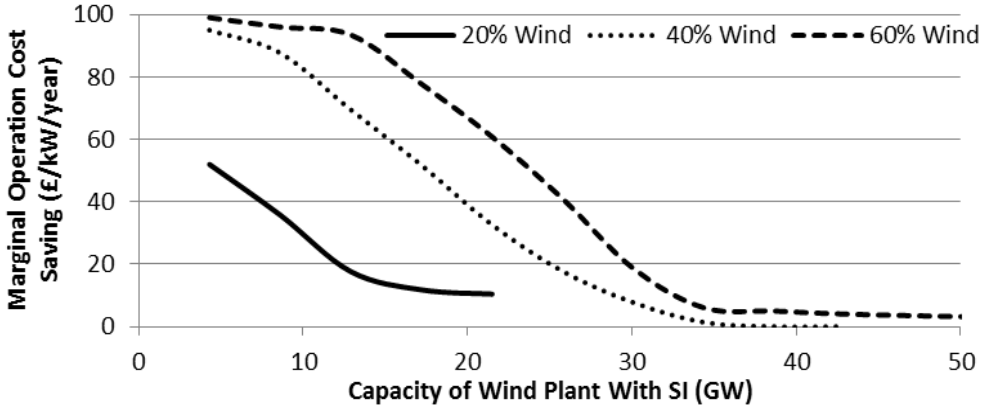

Figure 4-5 Marginal operation cost saving from SI (with 0.25Hz/s RoCoF)

As already discussed in GB, the relaxation of RoCoF limit could be implemented to support the integration of wind generation, which might significantly reduce the need for WPs to provide SI. Therefore, the similar study is carried out with relaxed RoCoF limit. The result in Figure 4-6 suggest that the value of SI would reduce with a factor of 5; however the first 10GW of WPs could still reduce the operation cost by more than 20£/kW/year in the system with more than 40GW of WPs.

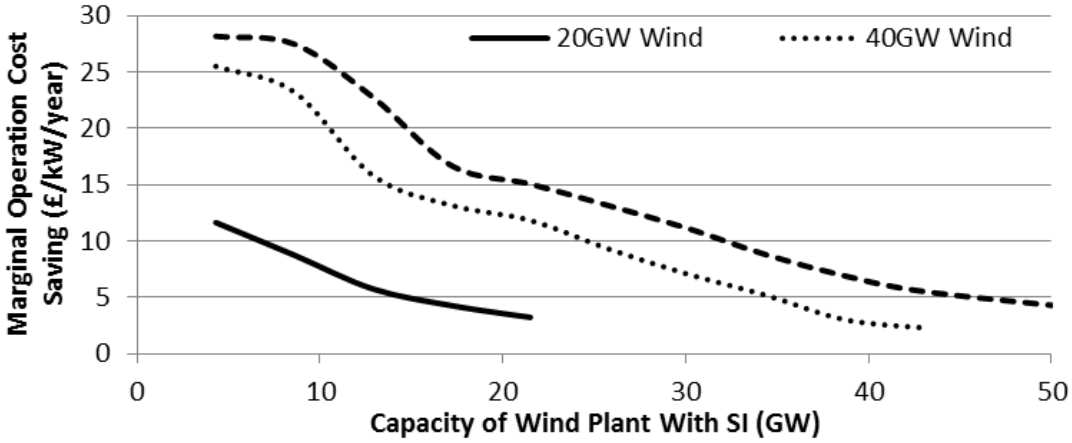

Figure 4-6 Marginal operation cost saving from SI (with 0.5Hz/s RoCoF)

The results in Figure 4-5 and Figure 4-6 suggest that given an annualised cost associated with SI capability, the optimal amount of WPs to be equipped with SI capability is system specific. The installed capacity of WPs and frequency regulation requirement are two of key deciding factors.

4.4.4 Impact of Uncertain Capacity of Online WPs

As discussed in Section 4.2, there exists uncertainty associated with the capacity of WPs being online. The results presented so far are based on average value. However, due to the risk-averse attitude, the system operators would make conservative assumptions regarding the minimum capacity of WPs being online. This section investigates the impact of this uncertainty on the benefit of SI.

Figure 4-7 shows the operation cost saving in the system with 40GW of WPs by using assumptions of maximum, average and minimum capacity of WPs being online (as shown in Figure 4-1). With low level of WPs equipped with SI capability, the conservative assumption could reduce the benefit of SI provision by 40% when compared with the case using average capacity. While with the increased penetration of WPs with SI capability, this uncertainty shows much less impact. In the case that all the WPs are capable to provide SI, conservative assumption only leads to 5% benefit reduction. The results also provide evidence that in the system with relatively low penetration of WPs with SI capability, there exist very significant value in providing information to system operators regarding the actual capacity of WPs being online.

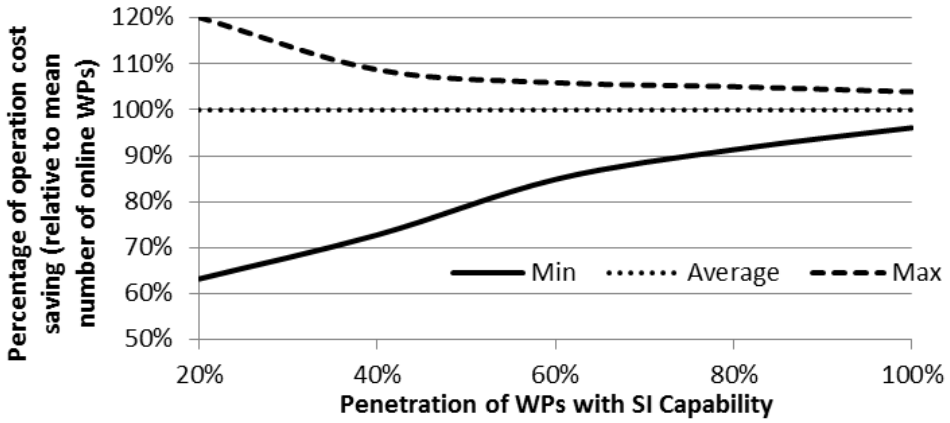

Figure 4-7 Impact of uncertainty associated with online WPs on the benefit of SI.

4.4.5 Impact of Recovery Period of Wind Plant Speed

Another challenge associated with SI provision from WPs is the recovery period of the wind turbine original speed; without careful design of the controller, this effect may lead to a detrimental impact on the system operation. This section analyses this effect in the system with 40GW WPs, with particular focus on the impact of different SI parameters.

The results in Figure 4-8 show that the more severe the recovery effect is, the less benefit the SI brings. However, the reduction is in general moderate in the system with tight RoCoF limit. This is due to that fact that tight RoCoF limit actually constrains the system operation and large amount of conventional plant would be committed only to provide required inertia. Those part-loaded plants could provide large amount of headroom; hence, the additional PFR due to SI provision could be easily supplied without incurring high costs.

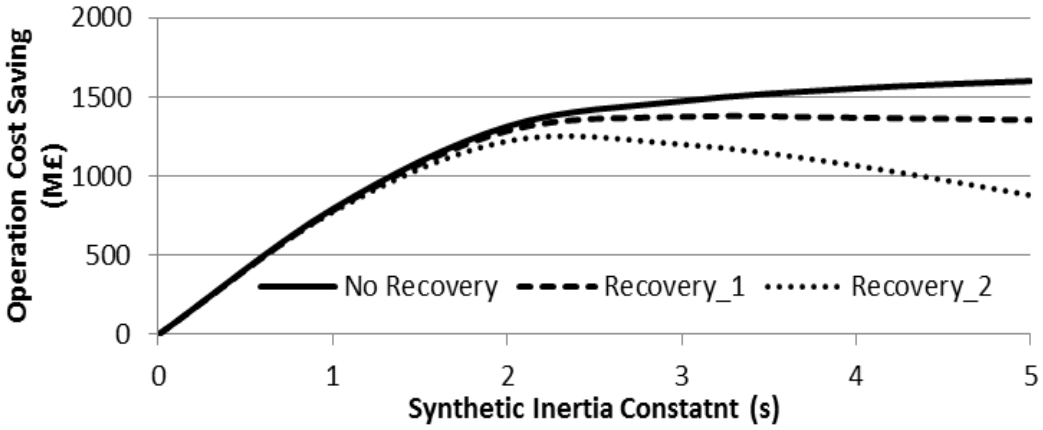

Figure 4-8 Impact of recovery effect on the value of SI

Similar studies are carried out for the system with relaxed RoCoF limit. The results in Figure 4-9 show that recovery effect could largely offset the benefit of SI provision if the controller is designed to be very aggressive. Moderate SI contribution from WPs helps to secure the frequency limit in the nadir and at the same time, the resulting additional PFR in the quasi-steady-state is moderate and could be easily met. On the other hand, more aggressive designs would lead to increase in costs of additional PFR in the quasi-steady-state which exceed the benefit that SI brings to secure the frequency nadir, and therefore the total benefit would decline

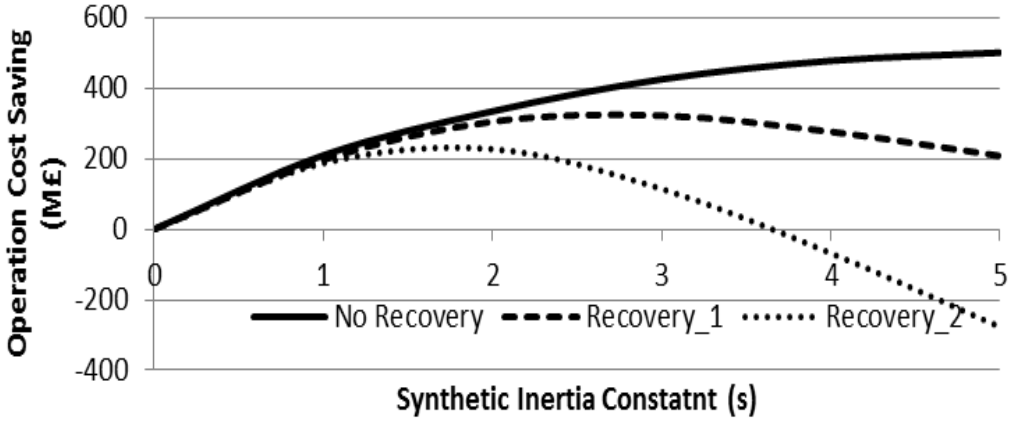

Figure 4-9 Impact of recovery effect on the value of SI (Relaxed RoCoF limit)

The results in Figure 4-8 and Figure 4-9 also suggest that there exists an optimal time constant of SI which would achieve maximum operation cost saving. This optimal time constant depends on the magnitude of recovery effect and the frequency regulation requirement. It is also worth to note that the maximum operation cost saving is 500 M£ without recovery effect but only 200M£ with high recovery effect. This suggests a significant benefit to design a SI controller with reduced recovery effect as proposed in [63].

There are proposals to develop tuneable controller for SI, which allows the time constant to be modified according to the system needs under different system conditions. Table 4-1 compares the system operation cost saving from fixed SI controller with optimal time constant and tuneable SI controller. The result suggests a considerable benefit of tuneable controller over fixed controller, especially when there exist severe recovery effect.

Table 4-1
Operation Cost Saving of Different SI Controllers

	Fixed Controller	Tuneable Controller
No Recovery (M£)	500 M£	500
Recovery_1 (M£)	322	406
Recovery_2 (M£)	224	338

4.4.6 Value of Combined Provision of SI and PFR from WPs

The capability of WPs to provide combined SI and PFR is analysed in this section. The operation cost savings for SI only, PFR only and SI+PFR are shown in Figure 4-10. With the tight RoCoF limits, the capability of WPs to provide PFR shows very limited value, since the system operation under this condition is constrained by the RoCoF limits. Large amount of conventional plants would need to be part-loaded to supply the required inertia. Significant headroom from conventional plants would be then available to provide PRF; hence the value of WPs providing PFR would be very low. On the other hand, with relaxed RoCoF, PFR only could achieve similar savings as SI only, while the combined provision would lead to a further 10% saving.

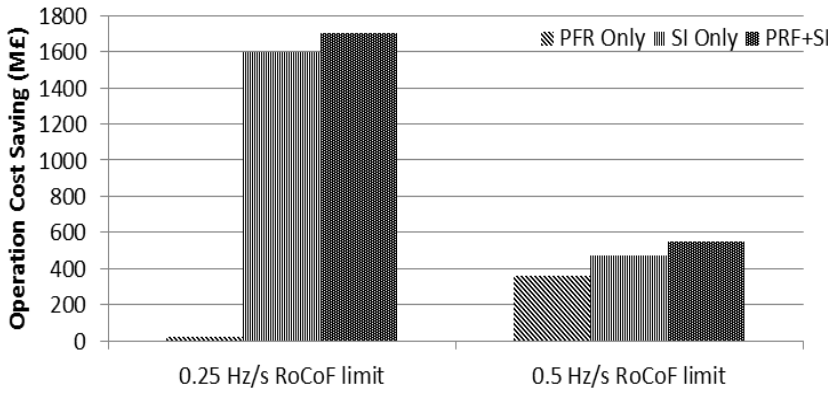

Figure 4-10 Operation cost saving from frequency support from WPs

The above results suggest that combined PFR and SI would deliver marginal additional benefits when compared with control schemes that deliver SI only. However, as already discussed, the recovery effect may lead to an increase in PFR requirements in the steady state, which would make the combined provision more desirable. Figure 4-11 shows that with the high recovery effect, the maximum saving is increased from 1200M£ in SI only to 1650M£ in the combined provision. In this particular case, combined PFR and SI almost eliminate the recovery effect since it archived similar operation cost saving as the case without recovery effect (Figure 4-8).

Moreover, the combined provision also impacts the optimal time constant of SI, which is changed from 2.2s in SI only to 3.8s in combined provision.

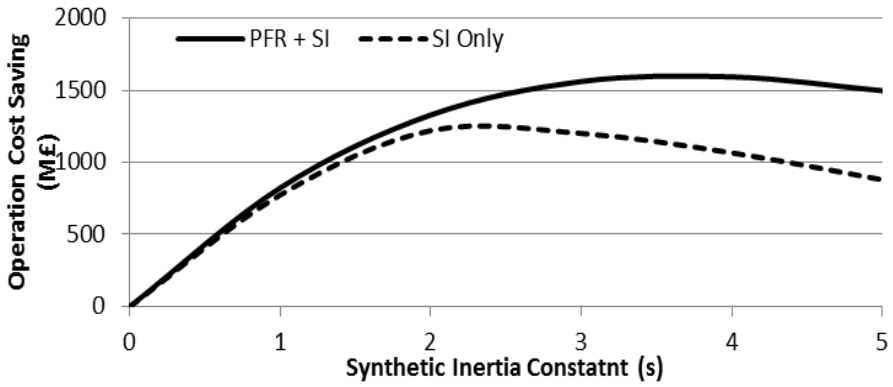

Figure 4-11 Impact of recovery effect on the value of combined SI and PFR

4.5 Conclusion

This chapter proposes a novel stochastic scheduling formulation with the capability to schedule system operation taking into account the frequency regulation support from WPs. The proposed model is applied to assess the benefits of SI and PFR provision from WPs in the future GB electricity system with different wind generation levels and frequency regulation requirements.

The results suggest the SI could effectively reduce the system operation cost in the system, especially with high penetration of wind generation. In addition, marginal operation cost saving of SI provision from WPs is investigated, which could be used to support cost-benefit analysis for determining the amount of WPs to be equipped with SI capability. The relaxation of RoCoF limit significantly reduces the demand on the SI provision from WPs. The impact of uncertainty in the capacity of WPs being online on the operation cost saving is shown to be significant only in the system with low penetration of WPs with SI capability. Moreover, the effects of recovery period are system specified. There is moderate impact of recovery period in the system with tight RoCoF limits. While in the system with relaxed RoCoF limit, very aggressive design of SI capability could even increase the operation cost. In fact, there exists an optimal time constant of SI that would achieve the maximum operation cost saving. This optimal time constant depends on the installed capacity of WPs, the magnitude of recovery effect and the frequency regulation requirement. The results also suggest that there would be significant benefits in reducing the recovery effect of SI provision. The

tuneable controller of SI leads to higher benefits than fixed controller of SI if the recovery effect is severe.

The analysis carried out also demonstrates that there would be no value for WPs in providing PFR in the system with the present RoCoF limit. But when the relaxed RoCoF is applied, PFR provision could achieve similar cost saving as SI provision. Combined provision of SI and PFR shows marginal extra benefits over SI only. However, the additional PFR due to severe recovery effect could significantly increase the demand on the combined provision.

There are several possible areas of further enhancing this analysis. First of all, this chapter only considers the uncertainty associated with online capacity of WPs when determining the aggregated SI capability. In fact, as discussed in [63], a more detailed model could be developed by taking into account of probability distribution of wind speeds and wind ramps. Further research is needed to model more accurately the relationship between SI contribution and additional PFR in the steady-state and incorporate this in the system scheduling.

Moreover, although the results suggest a significant benefit of frequency regulation support from WPs to the system operation, it is still unclear how this benefit can be captured by the owner of WPs under present market framework. Similar to the inertia market as proposed in [85], a framework for rewarding the provision of frequency regulation by WPs should be assessed.

5. Scheduling of Flexible Demand-side Response from Thermostatically Controlled Loads (TCLs)

5.1 Introduction

The integration of large shares of renewable energy sources (RES) leads to an increased amount of various ancillary services. Traditionally part-loaded or fast-standing plants supply these services. However, if generation side remains the only source for system control and flexibility, the cost of integrating RES will rise, limiting the actual ability to absorb them. An alternative approach suggests that demand side response (DSR) may facilitate the fulfilment of system requirements. Initial research [88, 89, 14] has investigated the value for DSR providing reserve in joint energy/reserve markets; however, the generalised DSR model used does not consider the physical constraints of any particular demand side technology.

An interesting subset of appliances for DSR encompasses thermostatically controlled loads (TCLs); under certain boundaries, TCLs are not time-critical and can sustain small alterations to the regular duty cycle. The authors in [90] quantified the value for system scheduling if TCLs provide primary control. TCLs could also enhance the system operation by performing energy arbitrage [91]. Similar studies, but based on different technologies (battery storage/EVs), revealed the benefits of selecting optimal portfolios of multiple services [92]. However achieving appropriate level of coordination with TCLs is not straightforward as individual appliances have, typically, only two power states (on and off) whereas the desired response is continuous [93]; hence, the control frameworks in [90, 91] enabled only individual services. An initial platform for a simultaneous provision of multiple services (energy arbitrage and frequency response) from TCLs is proposed in [94]. Although this control framework allows for accurate control over both short and long term time scales, its application to the economic dispatch problem did not fully considered the effect of TCLs´ energy recovery on the system operation after the response supply. However, the accurate assessment of the DSR value and a reliable provision of demand side services cannot neglect the load recovery and its associated cost. The energy recovery could be performed by means of extra power consumption after the

deployment of the response services. In [14] this power absorption is modelled as a function of the previous power reduction through a generic constant parameter; however, the energy level after the payback period cannot be calculated. The extra power consumption is suppressed in [90] by means of an ad-hoc control strategy, although the ability to cancel the payback costs a slow energy recovery; this design automatically prevents TCLs from supplying medium term response services, limiting the contribution of TCLs only to primary response.

The main contribution of this chapter solves the challenge addressed; we develop a demand side response model (DSRM) that accurately includes the dynamics of the load recovery pattern and calculates the associated post fault energy levels. This novel model, integrated in a system scheduling routine, calculates the optimal allocation of energy consumption and response service provision of a heterogeneous population of TCLs that minimises the system operational cost. The optimal solution balances the actual cost of committing extra generation reserve to assist the load recovery against the benefit of demand side frequency services. The provision of frequency response can vary at each time step in accordance with the time dependent characteristic of the system requirements [95]. These requirements depend on the level of inertia that, in turn, reflects the high variability of wind. The proposed DSRM is constructed in such a way that TCLs would always guarantee the deliverability of the scheduled response services as the energy deployed is fully paid pack by the end each time interval; this characteristic makes the supply of DSR services highly reliable and comparable with generators' standards. In addition, the feasibility of the TCLs´ energy profile is guaranteed by means of the accurate decentralised control described in [96]. The proposed DSRM is incorporated into an advanced stochastic unit commitment (SUC) model, based on the framework developed in [95]; it optimises the system operation in the light of uncertainties associated with renewable production and generation outages. This SUC model also takes into account the impact of reduced system inertia on the frequency regulation requirements.

The rest of this chapter is organised as follows: Section 5.2 derives the aggregate model and the control for TCLs. Section 5.3 presents the stochastic unit commitment

model with flexible demand response from TCLs. The simulation results based on GB 2030 system are provided and explained in Section 5.4

5.2 Modelling of Aggregated Heterogeneous TCLs

A large heterogeneous population of TCLs is described as a leaky storage unit with associated envelope constraints in [97]. The envelope parameters, labelled with the hat, do not represent a particular "real" device within the cluster; they just bound the flexibility of the whole TCLs' population. Hence, a cluster of $N \gg 1$ different TCLs can be described as an energy storage unit where the energy level S(t) [MWh] is defined as:

$$\frac{dS(t)}{dt} = -\frac{1}{\hat{\tau}} S(t) + P(t) \tag{5.1}$$

with $\hat{\tau} = min_a\, \tau^a$ the thermal time constant [h] where the superscript a is used for appliance-specific parameters.

Moreover $P(t) \equiv \hat{P}_0 \Pi(t)$ [MW] is the power consumed; $\hat{P}_0 = \sum_a P_0^a$ [MW] is the aggregate steady state power consumption and $\Pi(t)$ is a relative power curve ($\Pi_0 = 1$ for a steady state condition). In addition, the quality of service on individual appliances imposes energy bounds on the aggregate capacity.

$$\hat{S}_{min} = \max_a S_{min}^a \leq S(t) \leq \hat{S}_{max} = \min_a S_{max}^a \tag{5.2}$$

Energy bounds cannot adequately respect the primary function of the TCL (cooling/heating) as the devices would be stuck at all times at the lower or upper energy bounds. Therefore, we force the mean value of the energy across a time window of interest w to equal $\hat{S}_0 = \hat{P}_0 \hat{\tau}$, the steady state energy level.

$$\frac{1}{w} \int_w S(t) \mathrm{dt} = \hat{S}_0 \tag{5.3}$$

5.2.1 Controller Constraints

The decentralised control method in [96] enables individual TCLs to track a relative power curve Π(t) so that the aggregate power consumption targets such a profile in expectation:

$$E[P(t)] \cong \hat{P}_0 \Pi(t) = P(t) \tag{5.4}$$

The controller implementation introduces limits on the accessible range of power consumption levels. This implicitly defines the minimum and maximum power limits

$$\widehat{\mathrm{P}}_{min} = \max_{a} \mathrm{P}^{a}_{min} \;\leq\; P(t) \;\leq\; \widehat{\mathrm{P}}_{max} = \min_{a} \mathrm{P}^{a}_{max} \tag{5.5}$$

The respect of constraints (5.2) and (5.5) is sufficient to guarantees the feasibility of the response, avoiding the need for device-level simulations. With this strategy, TCLs can follow a power profile $P(t)$and simultaneously deliver response services, so long as their simultaneous provision does not violate appliances' constraints.

5.2.2 Main Characteristics of the DSRM

The demand side response model (DSRM) introduced in this chapter exhibits three main characteristics:

- *Flexible response provision:* the TCLs energy and power consumption at each interval are variable; this characteristic enables a flexible provision of response services in accordance with the time-dependent system requirements [95]. During those hours characterised by low net demand (system demand minus the wind production) the response requirements would be typically high due to an overall shortage of inertia. A growth in the TCLs' power absorption allows for a larger provision of frequency response services. Note that this behaviour is in synergy with the aim of energy arbitrage as, under these system conditions, the energy cost would be typically low, facilitating the increase of the TCLs' energy level. With high net-demand instead, TCLs tend to reduce the power consumption and thus lowering the available response buffer; this action reflects the lower system response requirements during those hours (many conventional generators already online and thus high system inertia). Again, this action aligns with the arbitrage's aim as TCLs would be consequently scheduled to facilitate the system demand shaving, due to temporally high costs.
- *Accurate energy recovery:* the DSRM allows for full controllability of the payback phase; after the provision of secondary response, TCLs can consume an extra amount of power compared to the scheduled power consumption for that interval. The amplitude of this additional power peak is precisely calculated based on the amount and duration of the secondary response and the duration of the energy recovery

window. The extra power consumption allows TCLs´ energy recovery to be more flexible; moreover it is drained during the less time-critical interval of reserve service and thus it supplied by additional generators; hence, from the system point of view the fast reserve requirement rises. We point out that the provision of secondary control by TCLs cannot be seen as an autonomous option to the secondary response supplied by generators; it is only able to postpone the generators' supply from a time window, when this supply would be very expensive, to another one, during which delivering the same amount would be easier. Hence, the use of TCLs to provide medium-term response (with the consequent load recovery) could be seen as a way to arbitrage between generators' response requirement, which is in itself an expensive service, and reserve requirement, which is cheaper, by decreasing the former and increasing the latter.

- *Energy profile and security services reliability:* although the probability of having a generator outage is generally very low, the probability of having an outage at each step is independent from the event's realisation at previous steps. In case of a failure at step k, if the TCLs´ recovery phase does not end by the beginning of interval $k+1$, it will not be possible to absorb the scheduled power consumption and to provide the scheduled response, without the risk of violating devices' temperature constraints. System security is thus not guaranteed, in which case, additional generation capacity would need to be engaged, entailing extra cost. The DSRM is based on the premise that the energy deployed while providing frequency services at the generic time interval k has to be fully paid back by the end of the same interval. This implies that at the beginning of interval $k+1$, the TCLs´ energy level will equal the regular energy level scheduled for the 'normal operation'; the devices would be fully capable to provide the response services scheduled for interval $k+1$. This way, TCLs' reliability would be really comparable to the one of generators, which is normally ready to provide response shortly after reserve providers have taken over the balancing from response providers. As an example, the poor reliability affecting so far demand side resources, forced the system operator PJM to limit up to 20% the provision of 'frequency regulation requirement' from DSR [98].

5.2.3 Mathematical Formulation of the DSRM

Equation (5.1) can be solved at generic step k across the interval [0,t] of length Δt by implementing alternative consumption profiles(constant power $P(t) = P_i$ or a linear power $P(t) = \rho_i \vartheta + q_i$). These two generic solutions below (5.6a-b) will be used to formulate the DSRM.

$$S_k = S_{k-1} \cdot e^{-\frac{\Delta t}{\hat{\tau}}} + \hat{\tau} P_k \cdot \left(1 - e^{-\frac{\Delta t}{\hat{\tau}}}\right) \tag{5.6a}$$

$$S_k = S_{k-1} e^{-\frac{\Delta t}{\hat{\tau}}} + \hat{\tau} \rho_k \Delta t + \hat{\tau} \left(1 - e^{-\frac{\Delta t}{\hat{\tau}}}\right) (q_k - \hat{\tau} \rho_k) \tag{5.6b}$$

where S_{k-1} and S_k are the energy levels at the beginning and end of interval k, respectively.

Considering the generic solutions (5.6a-b), the DSRM (see Figure 5-1) can be constructed to govern the energy consumption and the frequency response provision (with consequent payback) of TCLs at all the steps i of length Δt_1 of the optimisation horizon. This interval is divided into three further sub-intervals of length $\Delta t_2, \Delta t_3, \Delta t_4$, respectively.

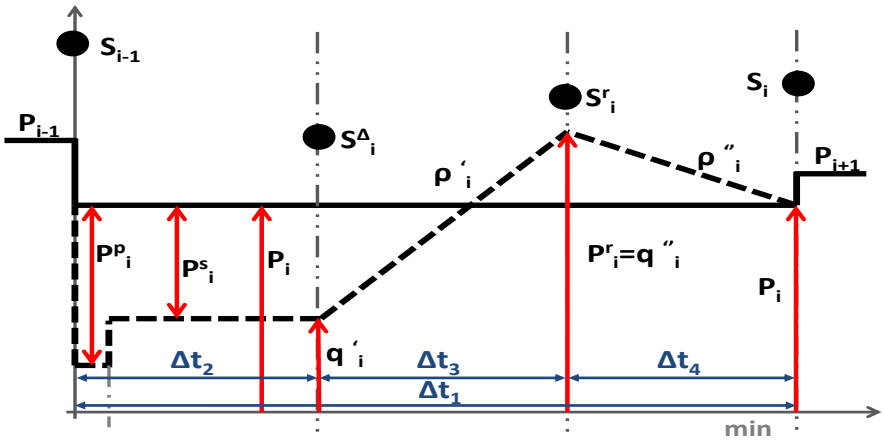

Figure 5-1 Multiple services model for demand response

The initial and final energy levels are S_{i-1} and S_i [MWh] and the amount of power actually absorbed by the TCLs population is P_i [MW]. These quantities are limited by (5.2) and (5.5). The included services are primary (P_i^p [MW]) and secondary (P_i^s [MW]) response as described in Sec. III-A. After the deployment of primary response the total TCLs consumption cannot drop below $\hat{P}_{min}$; adequate reserve for primary response allocations is enforced by (5.7).

$$0 \leq P_i^p \leq P_i - \widehat{\mathrm{P}}_{min} \tag{5.7}$$

For this short-term service the energy check at the end of the provision is neglected as the simulation results suggest the resulting energy decrease is marginal. The same minimum power requirement is applied to secondary response:

$$0 \leq P_i^s \leq P_i - \widehat{\mathrm{P}}_{min} \tag{5.8}$$

The power decrease is sustained for Δt_2. Equation (5.9) ensures that the energy level after the secondary response provision will not be below the lower energy bound. Therefore, the energy storage level S_i^{Δ} respects:

$$S_i^{\Delta} = \gamma_2 S_{i-1} + \beta_2 P_i - \beta_2 P_i^s \geq \widehat{\mathrm{S}}_{min} \tag{5.9}$$

Afterwards the energy recovery phase starts and thus the power consumption increases with a fix slope ρ_i' $[\frac{\mathrm{MW}}{\mathrm{min}}]$ from the intercept q_i' [MW]. In the end of time interval $\Delta \mathrm{t}_3$, if secondary response is delivered, the power consumption P_i^r will be greater than P_i; again P_i^r and S_i^r cannot exceed the maximum power and energy level, respectively;

$$P_i^r = L_1 S_{i-1} + L_2 P_i + L_3 P_i^s \leq \widehat{\mathrm{P}}_{max} \tag{5.10}$$

$$S_i^r = H_1 S_{i-1} + H_2 P_i + H_3 P_i^s \leq \widehat{\mathrm{S}}_{min} \tag{5.11}$$

It is worth to point out that P_i^r and S_i^r are calculated such that, within Δt_4, from the intercept q_i'' with a slope ρ_i'', the power consumption and stored energy return to originally scheduled level P_i and S_i, respectively. L_1 and L_2 are proved to be 0 and 1in the appendix; this implies that the additional amount of power to add to the contingency reserve requirement, P_i^{ar}, only depends on the amount of secondary response allocated by means of L_3.

$$P_i^{ar} = P_i^r - P_i = (L_2 - 1)P_i + L_3 P_s = L_3 P_s \tag{5.12}$$

In particular, considered a time interval $\Delta \mathrm{t}_1$ and fixed the secondary response commitment (Δt_2), the energy to payback is univocally determined, while L_3 and hence P_i^{ar} vary with Δt_3 as $\Delta t_3 + \Delta t_4 = const = \Delta t_1 - \Delta t_2$. A fast recovery ($\Delta t_3$ small) leads to small $\mathrm{P_i^{ar}}$ although it increases the rapidity in the power provision from reserve generators. On the other side, a large $\Delta \mathrm{t}_3$ drastically increases the amount of reserve to supply. A case study in Sec 5.4.3 illustrates the impact of this trade off on

the system operational cost. Finally, note that this result is in step with previous works [14, 99]. However, the relation between the power reduction and the consequent power to pay back was only expressed through a generic constant parameter empirically estimated, whereas, in this work, this relation is mathematically derived.

The average energy of TCLs needs to remain close to its steady state $\hat{S}_0$. In this context we first define $n_{\theta,\theta+i}^{(\sigma)}$ as the node at time step $t = \theta + i$ included in the scenario σ of the scenario tree and with root at time step $t = \theta$. Figure 5-2a helps to understand the notation introduced. The red arrow is pointing at the node located at time step $t = \theta + 1$, included in the scenario $\sigma = 1$, with root at time step $t = \theta$. The associated equality constraint (5.13) is obtained by inserting (5.1) in (5.3) and using (5.12) to eliminate $P_T(n)$in each interval in accordance with precious notation and takes the form.

$$\frac{1}{w}\left[\varphi S\left(n_{\theta,\theta}^{(\sigma)}\right) + \sum_{i=1}^{w-1} S\left(n_{\theta,\theta+i}^{(\sigma)}\right) + \chi S\left(n_{\theta,\theta+w}^{(\sigma)}\right)\right] = \hat{S}_0 \tag{5.13}$$

$$\varphi = \left[\frac{\tau}{\Delta t} - \frac{e^{-\frac{\Delta t}{\tau}}}{\left(1 - e^{-\frac{\Delta t}{\tau}}\right)}\right] \tag{5.14}$$

$$\chi = \left[\frac{1}{\left(1 - e^{-\frac{\Delta t}{\tau}}\right)} - \frac{\tau}{\Delta t}\right] \tag{5.15}$$

It is worth pointing out that $\varphi + \chi = 1$. At time $t = 1$, the system is also scheduled taking into account constraint (5.13); the TCLs' energy levels (stochastic variables) are solved over a scenario tree (Figure 5-2b, black) and they represent the optimal are consumption for the first 24 hours.

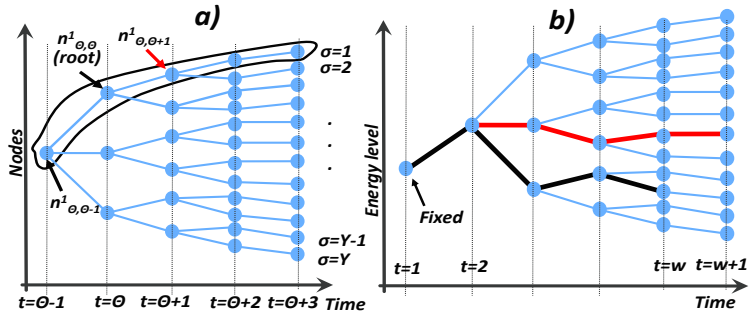

Figure 5-2 Node's identification (a); schematics of a scenario tree in SUC (b).

The application of rolling planning implies that, at $t = 2$, the system is rescheduled for the time window of length w that goes from $t = 2$ to $t = \mathrm{w} + 1$; new optimal TCLs energy levels are calculated (Figure 5-2b, red). The application of (18) in this new time window would not recognise the TCLs state of charge at $\mathrm{t} = 1$ (already fixed). In general, it results that the devices would always have the possibility to postpone the energy recharge required to actually satisfy (5.13). As energy and temperature are proportional quantities, TCLs will always be on average warmer (with refrigeration units in mind). Hence, we modify (5.13) so that the optimal solution at each time step is 'aware' of the energy levels already reached by the TCLs to obtain the constraint:

$$\frac{1}{w+p}\left[\varphi S\left(n_{\theta,\theta-p}^{(\sigma)}\right) + \sum_{i=1-p}^{w-1} S\left(n_{\theta,\theta+i}^{(\sigma)}\right) + \chi S\left(n_{\theta,\theta+w}^{(\sigma)}\right)\right] = \hat{S}_0 \quad (5.16)$$

In this case, at the generic time step $t = \theta$ the system is still solved over the following w time steps, but the average energy constraint takes into consideration also all p 'past' energy levels, that are not variables but fixed quantities. The impact on system cost savings and on the TCLs quality of the service of modifying the average energy constraint (5.13) with (5.16) due to rolling planning is illustrated in Sec.5.4.4.

5.3 Stochastic Unit Commitment Model

We implement the multi-stage stochastic unit commitment (SUC) with rolling planning proposed in chapter 2. The solution is obtained over a scenario tree; the scenarios are weighted according to their probability to realise. Hence, the solution is the optimal balance between the costs of committing generation against the expected cost of not meeting demand. The SUC model optimises the system operation by simultaneously scheduling energy production, inertia-dependent primary response, load-dependent secondary response, contingency reserve and operational reserve, in the light of uncertainties associated with renewable production and generation outages. The fundamental framework in [95] is extended to incorporate the DSRM that permits to exploit TCLs flexibility. The objective of the stochastic scheduling is to minimise the expected generation operation cost:

$$\sum_{n\in N}\pi(n)\left(\sum_{g\epsilon\mathcal{G}}C_g(n)+\Delta\tau(n)C_{LS}P_{LS}(n)\right) \tag{5.17}$$

subject to typical load balance constraint and local constraints for the thermal units. Details on these constraints and the equations describing generation costs are presented in chapter 2. The primary $R_g^P(n)$ and secondary response $R_g^S(n)$ characteristics of the generating units are modelled according to the machine load level:

$$0 \le R_g^P(n) \le N_g^{up}(n)R_g^{Pmax} \tag{5.18a}$$

$$R_g^P(n) \le f_g^P N_g^{up}(n)\left(P_g^{max}-P_g(n)\right) \tag{5.18b}$$

$$0 \le R_g^S(n) \le N_g^{up}(n)R_g^{S,max} \tag{5.19a}$$

$$R_g^S(n) \le f_g^S\left(N_g^{up}(n)P_g^{max}-P_g(n)\right) \tag{5.19b}$$

Constrains (5.18b) and (5.19b) suggest that the same spinning headroom is allowed to delivery primary and secondary response as current GB practice [100]. The contingency reserve characteristic $R_g^R(n)$ of generator is modelled as the power increase from a generator at its maximum ramp rate until the predefined delivery time t_R, and it is also bounded by the spinning headroom of each generator:

$$0 \le R_g^R(n) \le N_g^{up}(n) * r_g^{max} * t_r \tag{5.20a}$$

$$R_g^R(n) \le N_g^{up}\left[P_g^{max}-P_g(n)-\max\left(\frac{R_g^P(n)}{f_g^P},\frac{R_g^S(n)}{f_g^S}\right)\right] \tag{5.20b}$$

Constrain (5.20b) requires that the spinning headroom scheduled for response should not to be used for contingency reserve in order to allow the recovery of response provision for next time step.

The inertia-dependent fast response requirements for the SUC are calculated based on the security thresholds of the rate of change of frequency ($RoCoF_{max}$) and the frequency deviation Δf_{max} . The RoCoF achieves the highest absolute value just after the disturbance occurs; in this narrow time span, the frequency drop is only limited by the inertial response of conventional generators. Therefore the minimum required level of system inertia $H(n)$ obtained as:

$$H(n) = \frac{\sum_{g \in \mathcal{G}} H_g * P_g^{max} * N_g^{up}(n)}{f_0} \geq \left| \frac{\Delta {P_L}^{max}}{2RoCoF_{max}} \right| \quad (5.21)$$

where H_g is the inertia constant [s] of generator g, f_0 is nominal frequency (50Hz) and $\Delta {P_L}^{max}$[MW] the amplitude of the maximum generation loss.

The frequency nadir depends on system inertia, governors' governor response and TCLs response. The scheduled primary response of generators and TCLs is assumed to linearly increase with time by t_p and, after this time, is constant. This choice can be actually implemented for TCLs by means of the control strategy considered [96]. The aim is now ensuring that $|\Delta f_{nadir}(n)| \leq \Delta f_{max}$ at each node n; following equivalent steps as in [95], the primary response requirement $P^P(n) = \sum_{g \in \mathcal{G}} R_g^P(n) + P_T^P(n)$, that satisfies the constraint on frequency nadir has to respect:

$$P^P(n) \geq \Delta P_L - D * P_D(n) * \Delta f_{max} \quad (5.22a)$$

$$P^P(n) * H(n) \geq k^*(\mathrm{n}) \quad (5.22b)$$

Constraint (5.22a) imposes that static condition of RoCoF equal to zero when frequency is at the nadir. The complete derivation of (5.22b) can be found in Sec.2.3.4; In particular, the constraint on frequency nadir is respected if:

$$\frac{2 * P^p(n) * H(n)}{t_p} \cdot log\left(\frac{2 * P^p(n) * H(n)}{t_p * D * \Delta {P_L}^{max} + 2 * P^p(n) * H(n)}\right) \leq D^2 * \Delta f_{max} - D * \Delta {P_L}^{max} \quad (5.23)$$

The left-hand side of inequality (5.23) is a monotonically decreasing function of $P^p(n) * H(n)$ (positive quantity). Therefore, for any given value of D and ΔP_L^{max}, it exists only a unique value $k^*(n) = P^p(n) * H(n) \Rightarrow \Delta f_{nadir}(n)| = \Delta f_{max}$ .The bilinear constraint (5.22b) is then transferred to a mix integer linear formulation by applying standard reformulation method as in [53]. The provision of secondary response permits to stabilise the frequency deviation at least at maximum intermediate steady state value Δf_{max}^{iss}; the combined action of secondary response and fast reserve brings frequency back to f_0. The intermediate steady-state frequency deviation is obtained, by assuming that RoCoF is zero; hence the service requirement is expressed by:

$$P^S(n) \geq \Delta {P_L}^{max} - DP_D(n)\Delta f_{max}^{iss} \quad (5.24)$$

Finally, contingency reserve is required to assist the frequency recovery by taking over for frequency responsive plants and hence restoring their response capability. TCLs´ energy recovery also affects the required reserve as the extra power absorbed by the devices is supplied by reserve generators. The following requirement is therefore applied:

$$P^R(n) \geq \Delta {P_L}^{max} + P^{ar}(\mathrm{n}) \tag{5.25}$$

5.4 Case Studies

Simulations of annual system operation are performed using the GB 2030 scenario [95]. The maximum demand is 59.4 GW, total conventional generation capacity is 70GW and the installed wind capacity is assumed to be 35GW (30% wind penetration). Table 2-1summarises the characteristics of conventional plants as in [90]; wind farms do not provide inertial response and frequency services as current practice.

C_{LS} is set at 30000£/MW; t_P (5 seconds) and the maximum RoCoF (0.5 Hz/s) reflects National Grid (NG) proposals for future low carbon system. The load damping rate is 1%/50Hz as in [95]. Δf_{max} is set at 49.2 Hz whereas Δf_{max}^{iss} is -0.5 Hz. The duration of each time step of the SUC is Δt_1= 30 minutes; we set Δt_2= 10 minutes, and finally we select $\Delta t_3 = \Delta t_4 = \Delta t_2$. The impact of varying this setting is investigated in Section 5.4.3. Reference parameters for domestic fridge-freezers are taken from [101]; the matching of a first order model used in this chapter to higher order dynamic models in [101] provide a satisfactory fit in regular devices' operating conditions. The parameters were varied by ±10% to establish the data for an heterogeneous set of 55 million [94] of appliances; in particular,$\hat{\tau} = 4.5$ h,$\hat{\mathrm{S}}_{\max} = 10.5$ GWh,$\hat{\mathrm{S}}_{\min} = 9.0$ GWh, $\hat{\mathrm{P}}_{\min} = 1.2$ GW and $\hat{\mathrm{P}}_{\max} = 5.1$ GW.

5.4.1 System Operational Cost Savings due to DSRM

This section explores the value of scheduling the system incorporating the DSRM proposed in this chapter. Hence four scheduling methods are compared between them and with the inflexible case (S_ID) in which TCLs are treated as regular loads (constant consumption/ no response). All of these methods share the SUC formulation in Sec. IV whereas the TCLs contribution is different.

1. *Scheduling with constant response/no recovery (S_CRNR):* the TCLs energy/power consumption is constant as in [90]; the devices maintain at all times an energy buffer sufficient to deliver a maximum response equal to can provide up to a limited amount of response ($\hat{P}_0 - P_{min}$). Afterwards they recover the steady state consumption without absorbing extra power $\left(q_i'' = P_i = \hat{P}_0,\ \forall \mathrm{i}\right)$. However, from preliminary simulations (data not shown) we infer that, under this criterion, if TCLs provide the maximum amount of secondary response permitted, ($\hat{P}_0 - P_{min}$), it will take around 6 hours (12 time steps) to recover the energy level. Therefore after a generator failure, TCLs would not be able to provide again the scheduled response without the risk of violating the temperature constraints for the next 5.5 hours. The secondary response availability at each time step has to be limited to $(\hat{P}_0 - P_{min})/12$. This constraint is not applied to primary response as the energy deployment is negligible. This method always overschedules the energy buffer compared to the actual maximum response limit.
2. *Scheduling with flexible response/no recovery (S_FRNR):* Similar to S_CRNR but TCLs can adjust their energy/power consumption and hence maintain only the energy buffer required for the response committed. The recovery is not permitted ($q_i'' = P_i$ =variable ∀i) and hence the maximum response is still limited.
3. *Scheduling with DSRM (S_DSRM):* this method incorporates the demand side characteristics and constraints provided in Section 5.2.
4. *Scheduling with flexible response ignoring the recovery (S_FRIR):* similar to S_DSRM but it ignores the effect of energy recovery; generators are not scheduled to provide additional reserve, therefore the secondary response from TCLs results to be a cost-free service as in [88, 89].

The annual operational cost and the percentage of wind curtailment with the S_ID are 12.5 b£ and 9.7%, respectively. The performances obtained with the four methods listed above are shown in Figure 5-3.

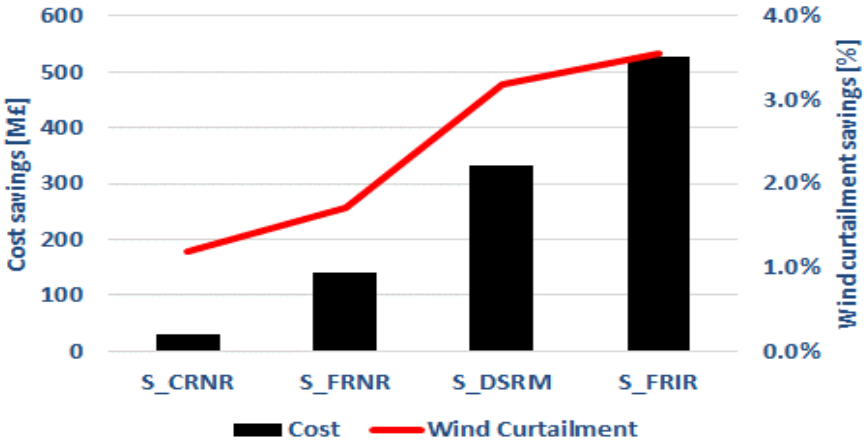

Figure 5-3 Cost savings (black bars) and wind curtailment savings (red line).

The cost savings provided by S_CRNR are marginal. The flexibility in the energy consumption and therefore also in the frequency response introduced in the S_FRNR allows for partially augmented savings. It results that most of the significant savings obtained with our method (S_DSRM) derive from the introduction of the energy payback that enables a much larger participation of secondary response from TCLs at the expense of higher reserve requirements. The largest savings are reached by the S_FRIR method; this confirms that, ignoring the cost of TCLs energy recovery results in over-estimating the TCLs value. However, this method is highly not reliable, as generators would not be able to follow the demand recovery, causing another frequency drop. Figure 5-4 demonstrates the benefits of the flexible consumption/response and the inclusion of energy recovery; the graphs represent the system operation for 36 hours.

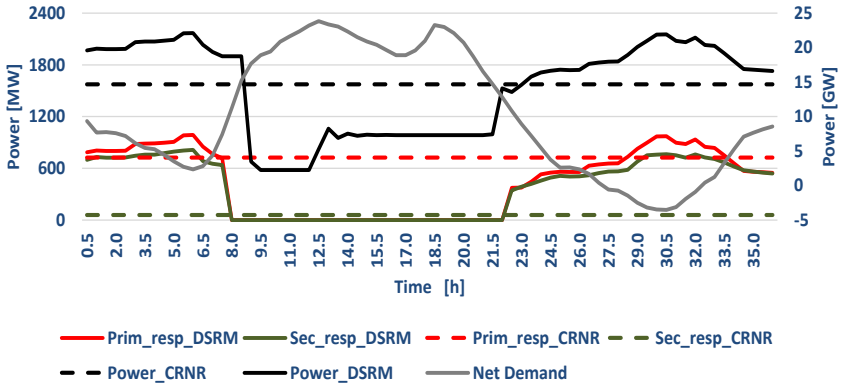

Figure 5-4 Actual consumption, primary and secondary response allocation for TCLs.

The grey solid line is the net demand. The black lines illustrate to the TCLs actual power consumption, the red lines to the available primary response and the green ones

to the available secondary response; solid lines refer to S_DSRM, the dashed to S_CRNR. It is clear how the S_DSRM allocates more primary and secondary response when the net demand is low (high frequency requirements); note how the actual consumption is much higher than the steady state (hours 1-7 and 28-35). Conversely, when the net demand is high (low security requirements), the allocation of response services drops, as well as the power consumption (hours 8-21). This behaviour shows the synergies between energy arbitrage and flexible response provision previously mentioned; in fact when the net demand is low, the energy cost would be typically low and TCLs would generally absorb more energy. Moreover, the cost is held low only if TCLs also provide large amount of response (high system requirements) otherwise supplied committing generators. The synergy is established as high consumption enables high amount of response available. On the other side, high energy costs correspond to high net demand situations; TCLs reduce the consumption facilitated by small response requirements. However considering the S_CRNR, the response is kept available even when it is not needed, and cannot be increased when it would be largely beneficial. Moreover, the absence of recovery permits only a marginal contribution of secondary response. It is worth to point out that, the flexible energy consumption allows for a large and flexible primary response contribution. However, only the possibility to absorb extra power during the recovery period enables likewise provision of secondary response; in fact the maximum secondary response capacity would be otherwise limited to a small fraction of the maximum power reduction as in S_CRNR and S_FRNR. The importance of this equal availability for primary and secondary response is highlighted in the next sub-section.

5.4.2 Individual or Simultaneous Provision of Response Services

After the comparison with other methodologies, we now focus the proposed method (S_DSRM). Figure 5-5 shows the contribution to system operational cost savings due to the TCLs primary and secondary support either individually provided either, as in the reference S_DSRM, together. Two settings for the maximum time to deliver primary response, t_d, are compared; 5 seconds for the reference Case A and 10 seconds for Case B.

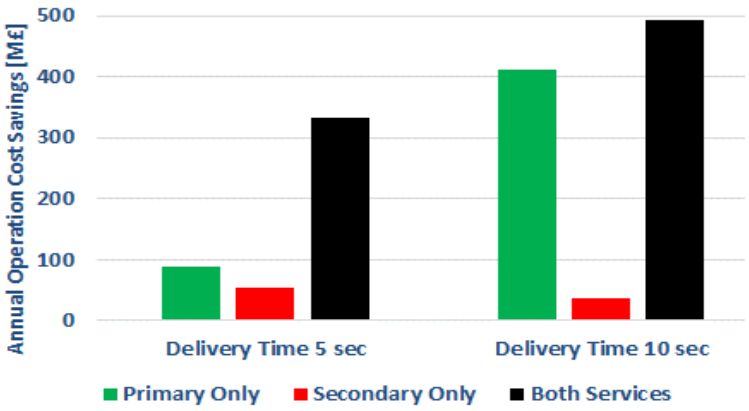

Figure 5-5 Response services contribution to system annual cost savings.

It is worth to point out that in Case B the speed of provision of primary response from generators is halved but the amount of response available remains constant. In a previous work [95] we have demonstrated that the 2030 GB requirements for primary response would be much higher than those for secondary response if T_d is kept equal to 10 seconds (current operation); on the other side, with $T_d = 5$ seconds the primary and secondary requirements are comparable, as also suggested by NG in [60]. Hence, for Case A it is important that TCLs provide both services together otherwise there would be no value for the system if individually supplied. As the requirements are comparable, if TCLs procure only primary response, several generators would still have to be committed to supply the secondary response (being also able to give primary control). This would be in contrast with the aim of demand side response which tries to de-commit part-loaded generators to make a more efficient network operation. The system operation shown in Figure 5-4 confirms this characteristics; in fact, primary and secondary response are either both committed (similar amount) either both not used. Due to the fact that much higher primary response is required than secondary response in Case B, TCLs could also provide only primary response and still achieve important cost savings. Note that the system in Case B is in general more inflexible and therefore the value for overall TCLs support is higher compared to the one in case A (black bars). However the annual operation cost of system B is significantly higher than that in system A.

5.4.3 Sensitivity to the Recovery Pattern

The relation between the additional reserve required due to TCLs recovery and the secondary response from the devices is regulated by the function $L_3 = f(\Delta t_3)$. For a given time interval Δt_1 and for a given secondary response commitment Δt_2, this function only depends on Δt_3. The sensitivity of the operation cost savings to the energy recovery pattern is shown in Table 5-1 where the reference case, Case A (Δt_3=10mins), is compared with Case B (Δt_3=5mins) and Case C (Δt_3=15mins).

Table 5-1
Sensitivity of the Operation Cost to the Energy Recovery Pattern

	Case A	Case B	Case C
Annual cost savings [M£]	**331**	**297**	**314**

The outcomes show that the best solution is the result of a trade-off between the amount of the additional reserve and the speed in the provision of this service. The average reference setting Δt_3=10mins is the most cost effective solution. Reducing Δt_3 decreases the amplitude of P_i^{ar}, but requires a faster provision of the reserve from the generators; in fact, these units will face technical limitations (ramping constraints); the system will have to schedule more available units, increasing the operation cost. Conversely, with a large Δt_3, the power limitations on reserve machines due to the ramping constraints decrease; this setting would still turn into the most cost effective solution although the amount of extra reserve increases. However, the secondary response actually committed is now sometimes limited by the upper bound of (5); this issue cuts down the advantages of this setting.

5.4.4 Average Energy Constraint

This section extends the discussion regarding the need for TCLs average energy to remain close to its steady state $\hat{S}_0$. Three scheduling methods (all with rolling planning) are considered with different implementations of the constraint on the average state of charge (SOC). Case A implements constraint (21) while Case B (reference case) implements (22). The last option, Case C, guarantees that the average SOC of each real day of the year equals $\hat{S}_0$. Figure 5-6 shows that the highest cost saving (black bars) is achieved by Case A. However, this method makes an unfair use of the TCLs energy storage; in fact the annual average SOC is around 4.5% lower than $\hat{S}_0$ (mean error, green).

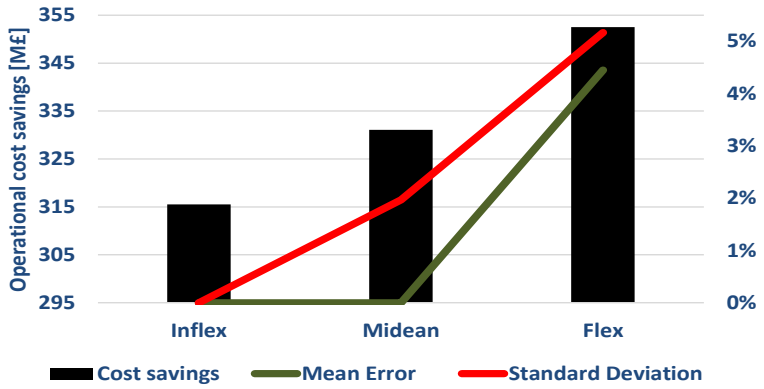

Figure 5-6 Comparison of the scheduling methods based on cost savings, mean error and standard deviation of the pdf of the average daily SOC.

The mean error is nil for Case B and C therefore the average SOC is maintained in the long term. However, although with Case B, the daily average SOC is not strictly guaranteed over each real day, the standard deviation of the pdf of the average SOC (red line) for each actual day of the year is low (1.9%). In fact, Case B permits to operate the refrigerators slightly warmer over one day, if the response requirements are low and slightly colder in another day characterised by higher system requirements. The augmented flexibility of Case B enables larger cost savings compared to stricter Case A. Note that the energy level and the temperature are in proportional relation.

5.5 Conclusion

In this chapter we have introduced a novel model for demand side response (DSRM) from a heterogeneous population of thermostatically controlled loads. We identify three key ingredients that characterise the methodology developed; the first one reflects the ability to adjust the actual energy consumption highlighting the intrinsic TCLs flexibility. In fact, these devices are able to increase the energy/power consumption in order to deliver more response services during those periods with high system response requirements (low net demand). If the reverse case happens, an overall reduction of energy/power consumption is allowed. This behaviour results to be in synergy with the possibility for TCLs to make energy arbitrage, increasing the consumption in presence of low energy cost (net demand low) and reducing the absorption during those period with high energy costs (high net demand). The second characteristic regards the demand side energy payback; the proposed DSRM allows for a full controllability of this phase; during the recovery, TCLs can absorb an extra

amount of power supplied by reserve generators. Therefore, the demand side value is calculated considering the cost of this increment. Moreover, we demonstrate that the extra power consumption only depends on the amount of secondary response allocated. The last feature deals with the reliability of the response support from TCLs; the devices can always guarantee the deliverability of the scheduled response at the generic step $i+1$. If response services are actually provided at interval i, the energy will still recover the pre-fault level scheduled for $i+1$ by the end of the interval i.

The mathematical formulation of the DSRM in Section 5.2.3 is included in the SUC model proposed in Chapter 2. The results of the case study attest the value of the demand side response; moreover, the comparison with other approaches for demand response proves the effectiveness of our methodology. In particular, the large cost savings obtained are due to the flexible response provision and especially due to the inclusion of the recovery phase, suppressed in other frameworks. In fact, the inclusion of the payback period allows for large secondary response provision and the value of this is shown in Section 5.4.2 that suggests the need for a simultaneous and comparable provision of primary and secondary response. The relation between the additional reserve required and the secondary response from TCLs is given by a quasi-linear function L_3 that depends only on Δt_3 if Δt_1 and Δt_2 are fixed. In Section 5.4.3 we verify that the optimal setting for Δt_3 would be an intermediate value; small values are penalised by strict generators' rump rates constraints while, for large values, the TCLs consumption is limited by the maximum TCLs power threshold. Our ongoing research is focused on the linearization of L_3 that would make $\Delta t_3(n)$ a decision variable. Hence, the TCLs recovery would become fully optimised and flexible. Finally in Section 5.4.4 we discuss the impact that rolling planning in the scheduling routine has on the TCLs quality of the service. We compare three methods; one of this is not doable as the average SOC (temperature) is lower than the steady state value; both the other two methods are valid with associated benefits and drawbacks.

6. Assessment of the Benefits of Different Demand-side Response Technologies

6.1 Introduction

The challenges introduced by intermittent wind generation present significant opportunities for the flexibility service providers such as Demand-Side Response (DSR). In time, it is possible that new sources of DSR connected to the distribution network (i.e. residential customers, controlled charging of electric vehicles, and controlled heating load) could play a significant role, given that their flexibility can potentially reduce the negative economic and environmental impact of intermittency of wind and PV generation. In this context, this chapter analyses and quantifies the implications of low-carbon technologies (LCTs) and solutions studied in the Low Carbon London (LCL) trials for the carbon emission and wind integration cost within the broader GB electricity system. Therefore, the key specific objectives of this study can be summarised as follows:

1. Analyse the benefits of LCTs trialled in LCL in reducing carbon emissions and wind integration cost in the broader GB electricity system for a range of long-term development scenarios. In particular, the LCTs investigated include: electric vehicles (EVs), heat pumps (HPs), industrial and commercial (I&C) DSR and dynamic time-of-use (dToU) tariffs for residential customers.
2. Evaluate the carbon benefits of smart operation of LCTs in the context of electricity system decarbonisation and increased share of intermittent RES.
3. Quantify the economic benefits of carbon savings from smart DSR operation in terms of lower requirements to invest in zero-carbon generation capacity in order to achieve the same carbon emission target.
4. Analyse the benefits of smart operation of LCTs in reducing system integration cost of wind, including balancing cost associated with wind intermittency and investment cost associated with back-up capacity to ensure system security.

The key link between the technology-specific, bottom-up LCL trials and system-level studies presented in this chapter is the effective shape of electricity demand seen by large-scale generation for different deployment levels of trialled low-carbon

solutions, but also the potential of these solutions to provide ancillary services to the system, in particular frequency response and reserve. Compared to previous published work, the uncontrolled charging or heating patterns are now based on measured populations, and the ability to shift has been updated based on insights from LCL. The possibility to source these services from the demand side rather than from centralised generation can significantly reduce the cost of operating the future power system and the resulting environmental burden.

The impact of various low-carbon solutions and technologies is investigated for several future system development scenarios, with particular emphasis on different possible evolution trajectories of wind and other intermittent renewable generation capacity. Given that the uncertainty and limited inertia capability of intermittent renewable output are expected to be a major driver for escalating integration cost and system emission, the performance of the system is analysed using Advanced Stochastic Unit Commitment (ASUC) model proposed in chapter 2 that is able to dynamically allocate spinning and standing reserve depending on the conditions in the system. As the ASUC model is also capable of considering system inertia and frequency response, we further investigate the impact of the provision of frequency regulation from alternative sources on the carbon performance and wind integration cost of the system.

6.2 Overview of Low Carbon London Solutions with Potential for Carbon Reduction

In this section we provide an overview of technologies investigated in LCL trials and specify their key characteristics with respect to the carbon reduction potential.

6.2.1 Low Carbon London trials

A number of technologies and solutions have been trialled within the LCL project that are expected to make a visible impact on the carbon emissions from the broader energy system. In this chapter we focus in particular on the following four LCTs:

- Electric Vehicles (EVs)
- Heat Pumps (HPs)
- Dynamic Time-of-Use (dToU) tariffs
- Industrial and Commercial Demand-Side Response (I&C DSR)

a. Electric vehicles

A detailed description of EV trials conducted in LCL is given in Report B1 [102]. The trial included residential and commercial vehicles and monitored their charging at both their home or office charging points, as well as at a number of public charging stations. The report quantified some of the key parameters of EV demand relevant for network planning and system analysis such as typical demand profiles and diversified peak demand for a given number of EVs.

As an illustration, the fully diversified average and peak day demand profiles for residential EV users are shown in Figure 6-1. The average profile represents the charging demand for an average day, while the peak profile has been obtained by extrapolating the diversity characteristic of EV peak demand towards a very large number of vehicles, where the coincidence factor approaches 20%. Given that the typical (non-diversified) charging power for a single residential charging point is around 3.5 kW, this results in a diversified peak EV demand of 0.7 kW. This information has been used to construct annual hourly demand profiles that were used as an input into the ASUC model used for this study.

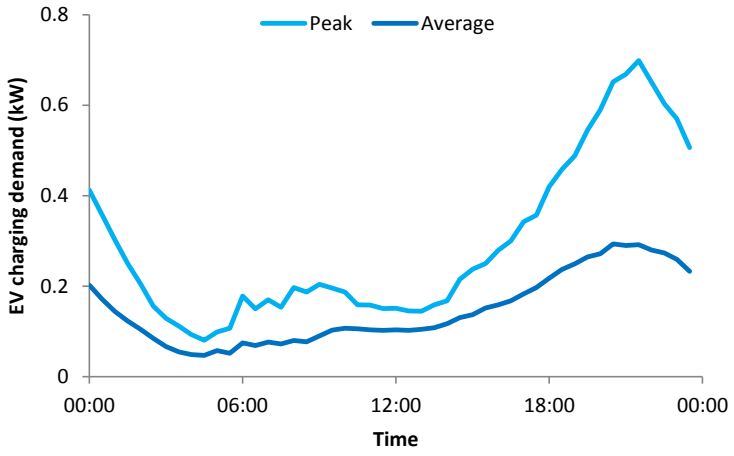

Figure 6-1 Average and peak EV charging demand profiles from LCL trials

LCL Report B1 has further assessed the flexibility of EV demand, i.e. how much of EV charging demand may be shifted in time in order to support the electricity system but without compromising the ability of the EV users to make their intended journeys. The analysis of smart charging in Report B1 suggested that between 70% and 100% of EV demand can be shifted away from peak hours. Based on the results of that analysis, we estimate that up to 80% of EV demand could be shifted away to other times of day while supporting the same journey patterns. This flexibility parameter is used as input into the ASUC model in order to allow it to make optimal scheduling decisions on when flexible EVs should be charged from the system operation perspective.

b. Heat pumps

LCL trials also involved the monitoring of residential heat pumps, as described in Report B4 [103]. Given that the trials only involved two dwellings, a 2-bedroom and a 4-bedroom home, the trial results were used to calibrate the likely non-diversified peak of residential heat pump load, however in order to construct a fully diversified profile of national-level HP demand, we used inputs from previous studies such as the ENA report [104], Micro-CHP Accelerator trial [105] or recent studies carried out for Carbon Trust [1], Department of Energy and Climate Change [106] and Climate Change Committee [107]. All of these assumed a gradual improvement in building insulation levels, and estimated the hourly profiles based on representative temperature fluctuations for the UK. The diversified peak day demand is shown in Figure 6-2 for illustration.

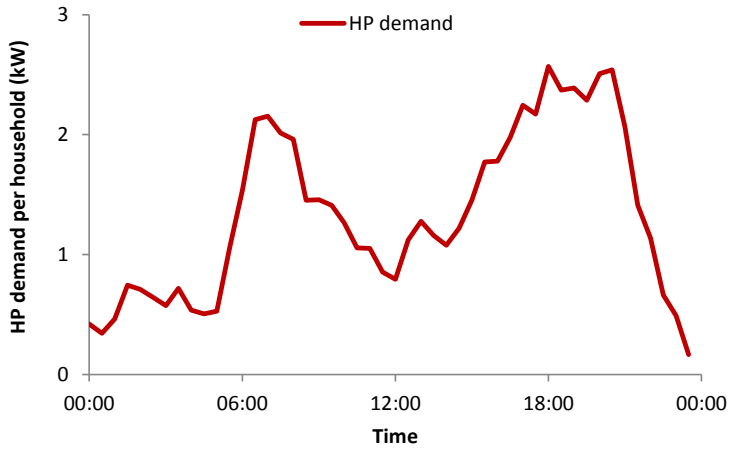

Figure 6-2 Peak (cold winter) day HP demand profile used in the analysis

We further assumed that flexible HP operation would be possible if they were fitted together with heat storage. Based on the findings of [104]and [108], we assumed that for the heat storage size in the order of 10% of peak day heating energy demand, the peak HP demand can be reduced by 35% through using the storage and shifting HP demand into other times of day.

c. Dynamic ToU tariffs

The impact of dToU tariffs on residential customer load has been investigated in detail in the LCL project using a relatively large sample, and the results of the analysis are provided in LCL Report A3 [109]. The analysis has found that the peak reduction of about 9% was achieved through time-differentiated tariffs, while the most engaged trial participants showed a peak reduction of 20%.

Based on these trial findings, we therefore assume in this study that if in future, consumers are educated to the point that today's high-performers become the 'new normal', up to 20% of participating residential electricity demand may be flexible in order to support the efficient operation of the system and integration of intermittent renewables.

d. Industrial and commercial demand-led DSR

The potential of generation and demand-led I&C DSR resources to deliver services to the system has been investigated in the LCL trials, and the results have been analysed in detail in LCL Report A7 [110]. In this study we focus on the contribution of demand-led I&C DSR, which according to the trial was able to deliver significant reductions of commercial building load for a given periods of time. A number of

participating sites were even prepared to fully switch off their air conditioning load for a limited period of time in order to deliver DSR services. DSR events were further found to be associated with significant demand for payback power and to a smaller extent payback energy, which potentially reduces the contribution of DSR sites to reducing network peaks, as illustrated in companion Report 11-1 [111].

For all of these reasons we take a conservative assumption that the achievable demand reduction for participating I&C customers is 10%.

6.2.2 Carbon Assessment of Low Carbon London Trials

The net carbon effect of each trial area (and in some cases, individual events) was calculated by assessing their impact against Elexon grid mix carbon intensity. Baseline CO2 emissions were calculated prior to each event and the impact of the trial, positive or negative calculated against this. These reports detail the carbon effect of the Low Carbon Trial and underpin the basis for the future scenarios discussed within this chapter.

The LCL trial carbon assessment therefore evaluates the present potential of LCL solutions to contribute to overall carbon reduction from the energy system. The figures from the carbon assessment reported and analysed in the annex provide a valuable log of data for further research and study, since they quantify genuine per-event carbon emission values at today's grid carbon intensity.

In this chapter we take a complementary approach, where we project the impact of LCL solutions into the 2030/2050 time horizon, estimating the carbon impact of these solutions in the context of accelerated rollout of LCTs and rapid expansion of renewable and other zero- or low-carbon electricity generation technologies. In doing so, we provide a perspective on the carbon reduction potential from smart LCL solutions in the future electricity system where decarbonisation is a key strategic objective.

6.3 Scenarios and Modelling Approach

This section describes the modelling methodology applied to assess the carbon impact of LCL solutions in the future GB electricity system. It also describes the 2030 and 2050 system scenarios that the carbon impact is quantified against.

6.3.1 Advanced Stochastic Unit Commitment (ASUC) Model

Because of the expected rapid expansion of intermittent renewable capacity, in particular wind and solar PV, the uncertainty that needs to be managed in the electricity system will increase significantly. The uncertainty of forecasted wind output on a time scale several hours ahead requires that a much larger volume of reserve is provided to the system in order to absorb the unpredictable output fluctuations.

In such circumstances relying on traditional deterministic analytical tools for power systems cannot capture all the phenomena driven by increased uncertainty. For that reason chapter 2 has developed the Advanced Stochastic Unit Commitment (ASUC) model, which allows for explicitly capturing the probabilistic properties of wind output and their impact on electricity system operation. This model is capable of dynamically scheduling spinning and standing reserve in the system to ensure that a given level of security of supply is maintained at minimum cost. Therefore, operating reserve requirements are endogenously optimised within the model. Since the LCTs can also contribute to reserve provision, optimal scheduling of various types of reserve is critical to understand the impact of LCTs on the system operation. In addition, stochastic scheduling also enables to optimally split the capacity of LCTs between energy arbitrage and ancillary service provision under different system conditions.

Furthermore, the ASUC model also considers the required level of frequency response in the system, taking into account the effect of reduced system inertia at high RES penetrations. Given that intermittent renewable generation will replace conventional generation, the aggregated inertia in the system provided by rotating synchronous machines will decrease, requiring more frequency regulation to maintain the frequency within the statutory limits. If the required frequency regulation is provided only by part-loaded plants, this may lead to RES curtailment and lower

operating efficiency of conventional plants, eventually increasing carbon emission. Therefore it is important to take into account of this effect when quantifying the impact of frequency regulation provision from LCTs on the system emission performance. Figure 6- illustrates the inertia-dependent frequency regulation requirement for varying levels of wind penetration in the GB system.

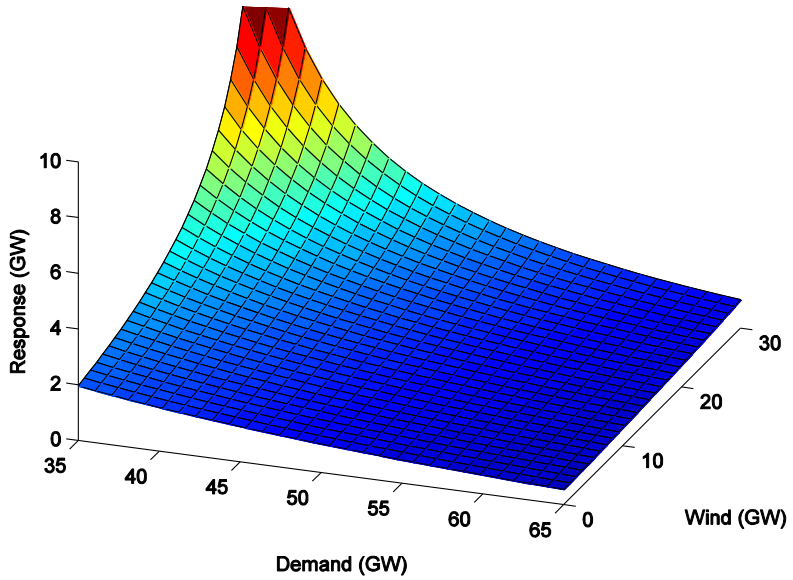

Figure 6-3 Inertia-dependent frequency regulation requirement

6.3.2 Scenarios for Carbon Impact Assessment of Future GB Electricity Systems

In this section we describe the scenarios used to characterise the GB electricity system in 2030 and 2050 in order to provide a background to evaluate the carbon impact of LCL technologies.

a. Key sources of information

In this study, we use two scenarios from the report on synergies and conflicts in the use of DSR prepared by Poyry [112], Green World and Slow Growth, including the associated generation capacities and demand profiles. The two scenarios are designed to deliver carbon emissions in the order of 100 g/kWh and 200 g/kWh, respectively. Generation background to the two scenarios corresponds to National Grid's Gone Green and Slow Progression scenarios, respectively. Demand information also includes the assumptions on electrification of transport and heating demand, as specified in the following sections.

The 2050 scenario used in the study is based on a High Renewable scenario from DECC Carbon Plan [113], with fluctuations of hourly demand constructed as in [106].

b. Scenarios for expected evolution of electricity generation and demand

The assumed generation capacity in the GB system in 2030 and 2050 is presented in Figure 6-.

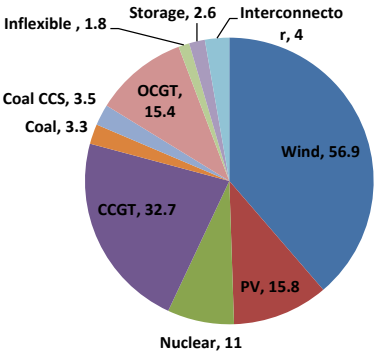

(a) 2030 Green World (GW)

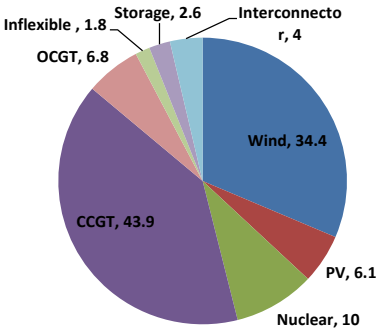

(b) 2030 Slow Progression (SP)

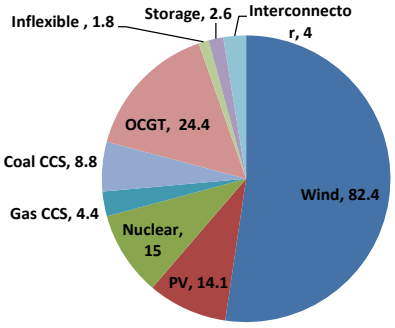

(C) 2050 High Renewable (HR)

Figure 6-4 Generation capacity mix for the GB system in 2030 and 2050

Generation capacity in 2030 Green World (GW) scenario is about 140 GW, of which 72.8 GW is RES generation (56.9 GW of wind and 15.8 GW of solar PV). Total installed capacity in 2030 Slow Progression (SP) scenario is around 104 GW, of which 41.7 GW is RES generation (34.4 GW of wind and 6.1 GW of solar PV). For 2050 High Renewable (HR) scenario, there are 226 GW installed generation, 42% of which is contributed by RES capacity. The penetration of RES with respect to meeting annual electricity demand is 31%, 47% and 54% in 2030 SP, 2030 GW and 2050 HR, respectively.

The demand assumptions are shown in Table 6-1 . The base demand (excluding EV and HP demand) is the same for 2030 GW scenario and 2030 SP scenario, with annual consumption 344 TWh and peak demand 59.1 GW. While the EVs and HPs demand is much higher in GW scenario. The base demand increases moderately in 2050 HR

scenario, however, the EVs and HPs demand increases more than twice compared with that in the GW scenario.

Table 6-1 Demand Information for the GB system in 2030 and 2050

	Annual Demand	Annual EV demand	Annual HP demand
2030 Green World (GW)	**344 TWh**	**18 TWh**	**53 TWh**
2030 Slow Progression (SP)	**344 TWh**	**6.6 TWh**	**24.9 TWh**
2050 High Renewable (HR)	**374 TWh**	**42.7 TWh**	**110 TWh**

c. Uptake scenarios for smart low-carbon technologies

EV and HP uptake in 2030 GW and SP scenarios is assumed in line with those used in [112], which correspond to DECC 4th (2013) Carbon Budget Scenarios 4 and 3, respectively.

Uptake of residential dToU and I&C DSR is varied as follows:

- dToU: 25%, 50% and 75%
- I&C DSR: 25%, 50% and 100%

The flexibility of all smart LCTs was assumed as discussed in Section 6.2.1

6.4 Quantitative Assessment of Carbon Impact of Smart Distribution Networks

In this section the methodology described in Section 6.3.1 is applied to quantify the carbon impact of smart and non-smart LCTs (including EVs, HPs, dToU and I&C DSR) in 2030 and 2050 GB systems. The frequency response capability of EVs and HPs is analysed, as well as the different penetration levels of dToU and I&C DSR. In addition, this section investigates the carbon implications of fully smart cases where the full potential of smart LCTs is used to support system balancing.

6.4.1 Approach to Quantifying the Carbon Impact of Smart LCTs

The carbon impact of smart LCTs is assessed by comparing the annual system emission with and without smart LCTs. The analysed cases are summarised in Table 6-2. EVs and HPs technologies are assessed by using the given demand profiles with and without flexible operation. In addition, studies regarding their response regulation capability are also carried out. Impacts of dToU and I&C DSR with different penetration levels are analysed. For the fully smart case, all the above LCTs are set at the maximum flexibility level, while the fully smart balancing & frequency case assumes DSR can contribute to frequency response and provide inertia.

Table 6-2 Description of Case Studies

		Assumptions
1	**Non-smart**	**No smartness/flexibility from LCTs**
2	**Smart EV**	**EVs are flexible with low frequency response capability**
3	**Smart EV / FR**	**EVs are flexible with high frequency response capability**
4	**Smart HP**	**HPs are flexible without response capability**
5	**Smart HP / FR**	**HPs are flexible with high response capability**
6	**dToU**	**Flexible domestic demand with varying penetrations (25/50/75%)**
7	**I&C DSR**	**Flexible I&C demand with varying penetrations (25/50/100%)**
8	**Fully smart: balancing**	**Maximum flexibility from all DSR for balancing (combined effect of all smart options in case studies 2, 4, 6, and 7, the latter two at the highest penetrations)**
9	**Fully smart: balancing & frequency**	**Maximum flexibility from all DSR for balancing and provision of response and system inertia (combined effect of all smart options in case studies 3, 5, 6, and 7, the latter two at the highest penetrations)**

The results are presented through three different metrics. Firstly, average system emission rate is defined as the ratio of total system carbon emission over the total system demand. The second metric is the incremental carbon emission, which is the ratio of incremental carbon emission caused by EVs/HPs over the corresponding electricity demand. The third metric is carbon emission reduction per unit of energy of "smart" demand, which is calculated as the ratio of total system emission reduction caused by smart LCTs over the corresponding LCTs demand.

6.4.2 Carbon Benefits of Smart Management of LCTs

a. Average System Emissions

Carbon emissions from today's electricity system, also reflected in the LCL trial carbon assessment are around 450 g/kWh. With the expansion of low-carbon technologies, the grid emissions are expected to become massively reduced. Scenarios analysed in this chapter reflect the decarbonisation of the electricity system, and the objective of studies presented is to estimate to which extent LCTs can support an even more ambitious decarbonisation of electricity supply.

In the first step, the annual operation of the system is simulated without any contribution from the LCTs. As shown in the Non-smart case in (Figure 6- - Figure 6-) , the average emission rate for the 2030 GW scenario is 115 g/kWh, while due to lower penetration of RES and Nuclear, the emission rate in 2030 SP scenario is around 150 g/kWh. The combination of high penetration of RES, Nuclear and CCS plants in the 2050 HR scenario leads to a highly decarbonised electricity system with the average emission rate at around 48 g/kWh.

After establishing the baseline system carbon performance, we proceed to quantify the carbon impact of each smart technology on the overall system emissions. The

results for the 2030 GW scenario are presented in Figure 6-. The average system emission rate is reduced by 5 and 8 g/kWh due to smart EVs and smart HPs, respectively, and this is further reduced by 4 and 5 g/kWh if smart they can contribute to frequency regulation. Although smart EVs are in general more flexible than smart HPs, the reduction caused by HPs is higher due to higher volume of HP demand in the system. The average system emission rate is also reduced as the uptake of dToU and I&C DSR increases: up to 5 and 6 g/kWh, respectively. In the fully smart balancing case, the combination of all smart technologies leads to a reduction in specific emissions of more than 17 g/kWh. The highest reduction however is achieved in the case where DSR also provides maximum amount of frequency response and inertia; emissions in this case are about 33 g/kWh lower than in the non-smart case, which is almost double the reduction of the fully smart balancing case.

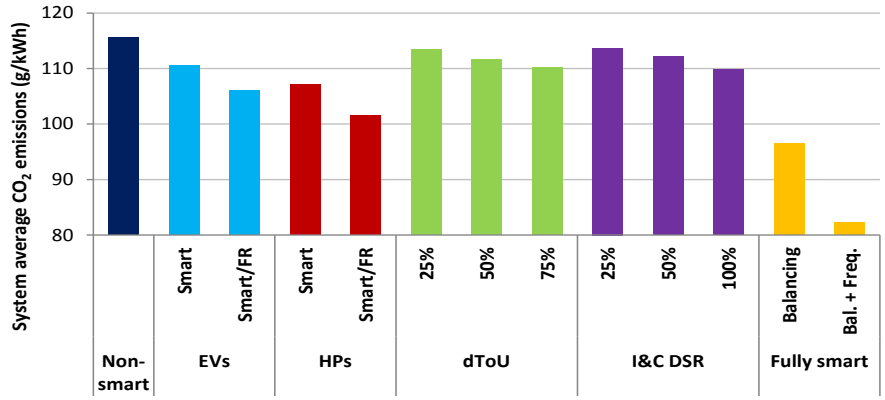

Figure 6-5 Impact of smart technologies on average system carbon emission (2030 GW)

As shown in Figure 6-, similar trends are observed in the 2030 SP scenario. However, due to a lower penetration of RES, the carbon impact of smart LCTs is less significant, as only 8 g/kWh emission reduction is observed in the fully smart balancing case, and 10 g/kWh in the fully smart balancing with frequency control. In addition to lower RES penetration, it is also important to point out that the penetrations of EVs and HPs are also lower when compared with the GW scenario. Therefore, the carbon benefits of smart EVs and HPs reduce the most among the smart LCTs when compared to the GW scenario.

Flexible electrified heating seems to have among the highest decarbonisation potentials, but from our Low Carbon London trials it appears to have the lowest flexibility unless heat storage is built in from the outset. The mass of Electric Vehicles

in future, dToU and I&C DSR are relatively similar in the scale of their impact. However, the scale of the supply chain challenge is very different in each case: to achieve 25% of I&C DSR is likely to be simpler than achieving shift from all electric vehicles, or shift from 25% of residential customers. The latter are only likely to happen with incentives or directives, whereas progress may be made towards the former within existing supply chains.

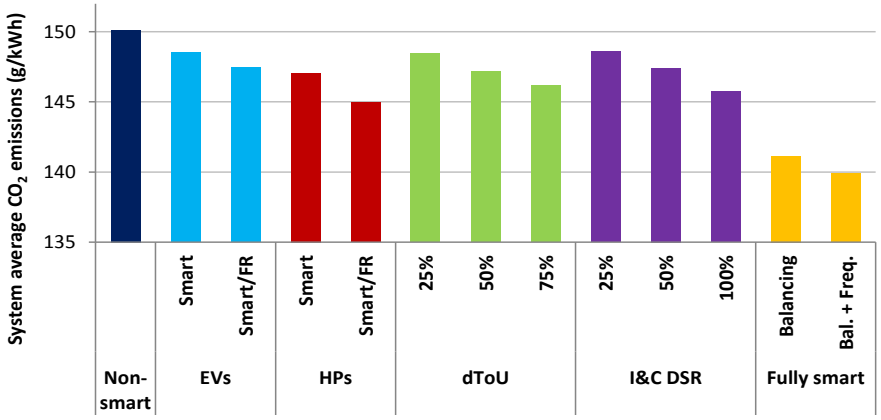

Figure 6-6 Impact of smart technologies on average system carbon emission (2030 SP)

The carbon impact of smart technologies in the 2050 HR scenario is illustrated in Figure 6-. Although the electricity sector in this scenario will have already been largely decarbonised by 2050, smart LCTs could effectively further reduce the average emission rate by up to 15 g/kWh in fully smart cases (no great difference is observed between the balancing case and the one with combined balancing and frequency control). Because of a higher penetration of EVs and HPs than in the other two scenarios, the average emission rate could be reduced from 48 g/kWh in the non-smart case to 38 g/kWh and 36 g/kWh by smart EVs and HPs, respectively. However, the provision of frequency regulation from smart EVs and HPs shows a very small carbon impact due to the fact that the frequency regulation in the non-smart case is provided by low-emitting CCS plants, so the displacement of those, although economically beneficial, does not yield significant improvements in carbon performance.

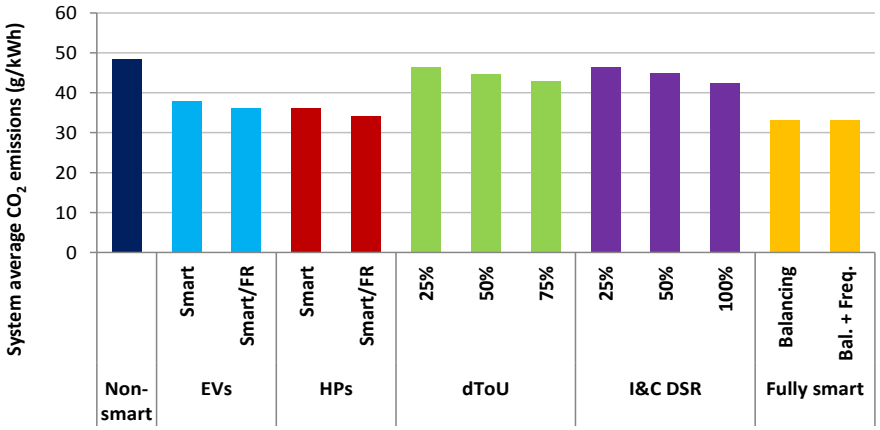

Figure 6-7 Impact of smart technologies on average system carbon emissions (2050 HR)

A summary of average system emissions for the three scenarios and for the non-smart and fully smart (i.e. the most optimistic) cases is provided in Table 6-3. As mentioned before, all of these scenarios assume a significant drop in grid emissions from today's value of around 450 g/kWh.

Table 6-3 Summary of Average System Emissions across Different Scenarios

(in gCO2/kWh)	*Non-smart*	*Fully smart*	*Reduction*
2030 GW	**115.5**	**82.2**	**–28.9%**
2030 SP	**150.1**	**139.9**	**–6.8%**
2050 HR	**48.3**	**34.0**	**–29.7%**

b. Carbon Intensity of Supplying Electrified Transport and Heat Demand

As the transport and heating sector become progressively electrified, additional electricity demand will need to be supplied by the power system, potentially increasing the carbon emissions from the electricity system. Figure 6- shows the weighted average carbon intensity of the electricity consumed by EVs and HPs. The intensities of EV and HP demand have been found for non-smart, smart and smart/FR cases, by quantifying grid emissions in each hour during the year and averaging them over the volume of EV or HP demand while using hourly EV or HP demand levels as weighting factors. For each of the cases included in Figure 6- we also present the average system emissions as vertical error bars.

We observe that in general the carbon intensity in the non-smart cases is higher than the intensity in smart operation cases. We further note that the carbon intensity of HP demand is consistently higher than average emission rate of the whole system, regardless of the scenario and the level of smartness. This follows from the fact that HPs operate during winter when demand is generally higher and more expensive and

more carbon-intensive generation technologies are used (such as e.g. CCGT and OCGT units). That is why even when HPs follow smart operation strategies and consequently reduce total system emissions; their average emission rate is still above the overall system average. Carbon intensity of EV demand in the non-smart cases is around or slightly above the average system emissions, but when smart EV charging strategies are implemented, the emissions associated with EV demand decline rapidly, also causing a decrease in the total system emissions.

In particular, under the 2030 GW scenario the carbon emission rate of EV demand is reduced from 116 to 105 g/kWh by smart charging, and further reduced to around 99 g/kWh in the case with frequency regulation from EVs. Due to lower relative flexibility associated with smart HP operation, as well as its seasonal character, the decrease in the carbon emission rate driven by smart HP operation, when expressed per kWh of HP demand, is slower than for smart EVs, but is still able to reduce the emission rate by 14 g/kWh in the case with frequency response provision.

In the 2030 SP scenario, shown in Figure 6- (b), similar trends for carbon emission rates of EV and HP demand are observed as in the GW scenario. However, due to the lower penetration of RES and nuclear capacity, the ability of smart EVs and HPs to reduce the carbon emission is not as pronounced as in the GW scenario. In other words, the emission rate, which already starts from a comparably higher level than in the GW scenario (over 150 g/kWh), reduces by only 9 i.e. 5 g/kWh for EV and HP demand, respectively, when fully smart operation is accompanied by FR provision.

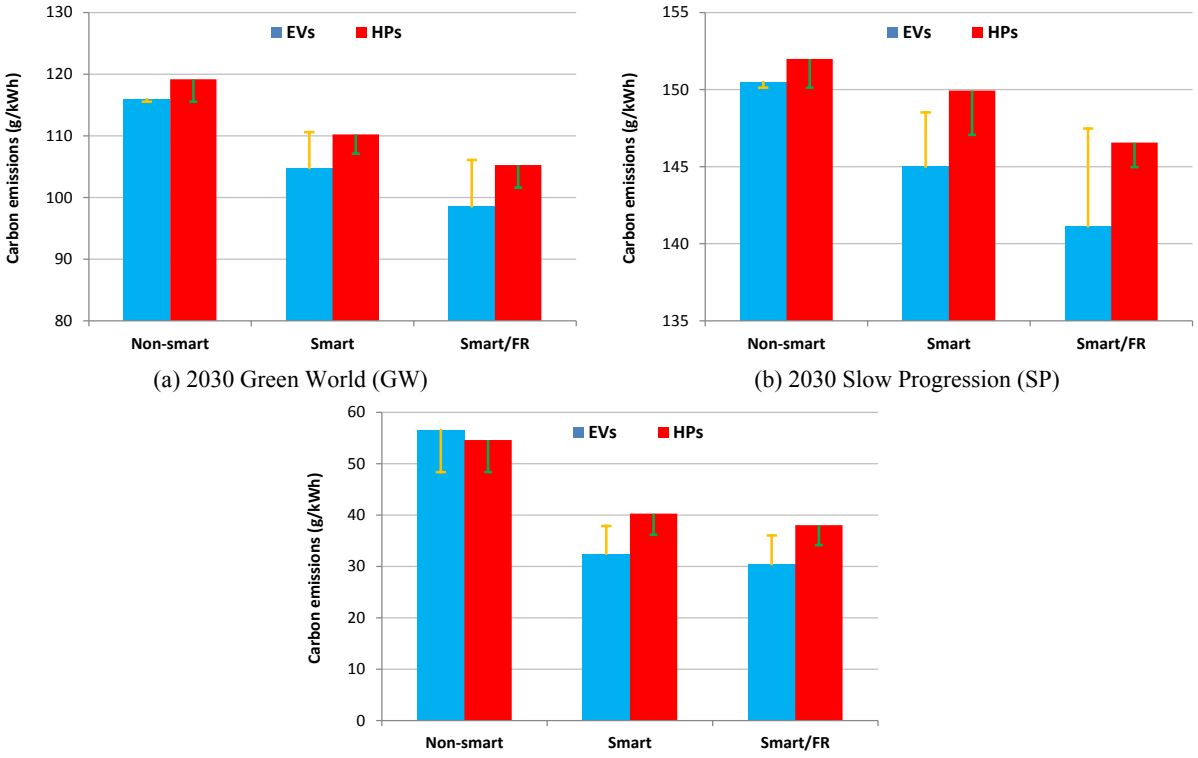

(a) 2030 Green World (GW)

(b) 2030 Slow Progression (SP)

(C) 2050 High Renewable (HR)

Figure 6-8 Carbon emission intensity of supplying EV and HP demand for different levels of smart

Finally, the results presented in Figure 6- (c) demonstrate the carbon emission rate of EV and HP demand in the 2050 HR scenario. In the non-smart case, the average emission rate of the whole system is rather low (48 g/kWh, as shown in Figure 6-), although the carbon emission rate associated with EV and HP demand is slightly higher (57 i.e. 55 g/kWh, respectively). Smart operation strategies reduce the carbon intensity of EVs and HPs to 30 g/kWh for EVs and 38 g/kWh for HPs; both of these figures represent a significant relative reduction from the non-smart cases. We again observe that smart EV charging is more effective in reducing system carbon emissions than smart HP operation – as already discussed, which is primarily driven by the seasonality of HP demand.

c. Avoided Emissions per Unit of Smart Demand

This section estimates the carbon savings driven by the deployment of smart LCTs expressed as annual carbon reduction per unit of "smart" demand. As shown in Figure 6- to Figure 6-4 , all the smart technologies lead to a significant carbon emission reduction per unit demand. These carbon savings in many cases exceed the average system emissions, which means that in some cases the carbon impact of smart

technologies is even better than carbon-neutral, i.e. they are able to create a net offset in carbon emissions per unit of smart demand.

In general, smart EVs show the most prominent reduction per unit demand, up to 220 g/kWh in the 2030 GW scenario, and 150 g/kWh in the 2030 SP and 2050 HR scenarios. dToU and I&C DSR show the second and third largest carbon emission reduction effect among the studied LCTs. However, the results suggest as the increase of penetration level, the avoided emission per unit demand reduces. Due to limited flexibility, smart HPs generate the lowest carbon emission reduction per unit demand, but still could reduce the emissions by around 50-100 g/kWh under different scenarios.

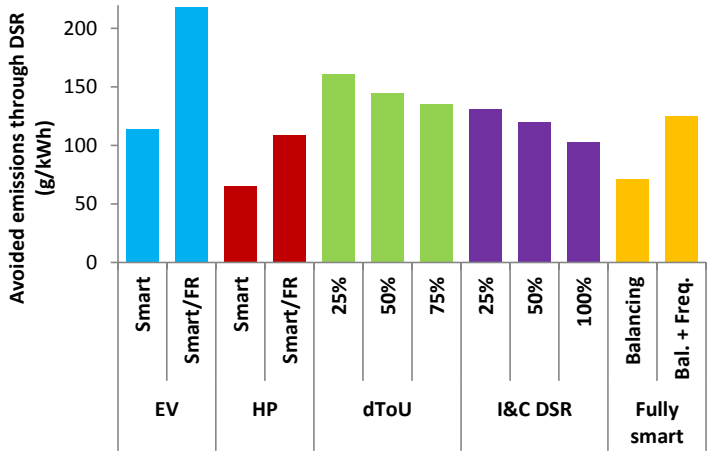

Figure 6-9 Carbon emission reduction per unit of "smart" demand (2030 GW)

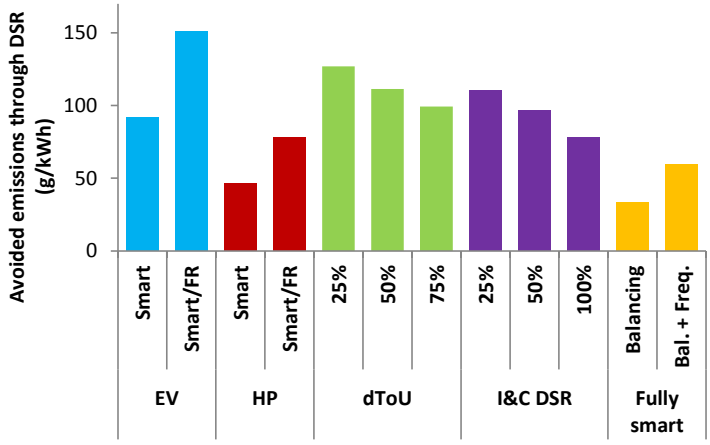

Figure 6-3 Carbon emission reduction per unit of "smart" demand (2030 SP)

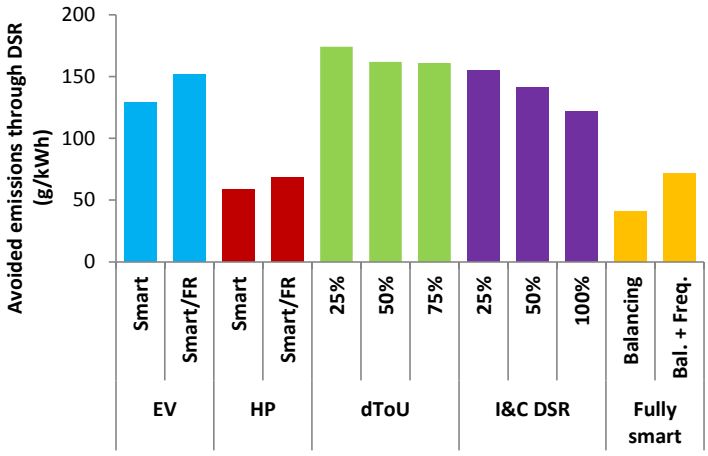

Figure 6-4 Carbon emission reduction per unit of "smart" demand (2050 HR)

In the fully smart case, because of the saturation effect, the carbon emission reduction per unit of "smart" demand reaches the lowest value at around 60 g/kWh in the 2030 GW scenario, 40 g/kWh in the 2030 SP scenario and 45 g/kWh in the 2050 HR scenario. These values however almost double when fully smart balancing is combined with frequency response provision.

6.4.3 Summary of Findings

A large number of numerical studies have been run to quantify the carbon benefit of different LCTs over three representative scenarios in the 2030 to 2050 horizon. Table 6-4 provides a summary of the carbon benefit per unit demand for different LCTs across proposed scenarios, while Figure 6-5 compares the average system emission rates for non-smart case and fully smart with balancing only and with combined provision of balancing and frequency regulation.

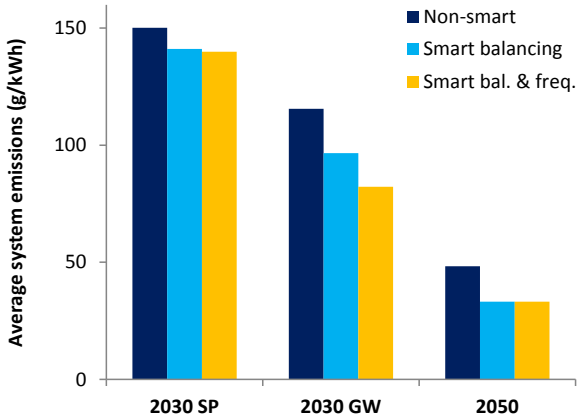

Figure 6-5 System emissions benefits across different years and scenarios

Table 6-4 Summary of Carbon Benefit per Unit Demand of Different LCTs

(in gCO_2/kWh)	*2030 GW*	*2030 SP*	*2050 HR*
EV	92-151	114-218	129-152
HP	46-78	65-109	58-68
dToU	99-127	135-161	161-174
I&C DSR	78-110	103-131	122-155

The results of our studies on carbon impact of smart LCTs suggest the following:

1. Carbon benefits of different DSR technologies expressed per unit of smart demand are primarily driven by the flexibility to shift demand and provide frequency regulation.
2. Carbon benefits of all LCTs increase if they provide frequency response in addition to smart balancing.
3. Carbon benefits are generally more pronounced with higher intermittent RES penetration, but can be limited if the non-renewable generation capacity on the system is mostly zero-carbon (as in the 2050 HR scenario).
4. Integration of electrified transport and heating demand is significantly less carbon intensive if smart operation strategies are adopted.
5. Irrespective of the carbon scenario, or exactly which sources of DSR are adopted, there seems to be potential to reduce average system carbon emissions by an additional 5 g/kWh.

6.5 Impact of Smart LCTs on Renewable Integration Cost

In this section we investigate the impact of smart LCTs (EVs, HPs, dToU and I&C DSR) on the cost of RES integration in the 2030 and 2050 GB systems. We apply the ASUC model described in Section 6.3.1 to quantify the cost reductions associated with lower back-up capacity requirements, reduced system balancing cost and reduced CAPEX due to avoided investment in low-carbon capacity to reach the CO2 target.

6.5.1 Challenges of RES Integration

The UK has a very significant wind power resource that is expected to contribute significantly to the decarbonisation of the electricity system, with almost 12 GW of wind generation already in operation as of November 2014. A key feature of wind as well as solar PV generation is the variability of the primary energy source, which is often referred to as intermittency. Similarly, there has recently been a rapid increase in the number of solar PV installations.

The intermittent nature of wind and solar PV generation creates a number of challenges for system operators, regulators, transmission planners and industry participants. In order to deal with unpredictability and variability of RES, levels of operating reserves and frequency response reserves scheduled by system operators need to increase to ensure that demand and the generation are always balanced. Moreover, any additional generation capacity required to provide "wind or solar firming" for system security reasons can be considered as an additional cost associated with intermittent RES generation.

These system integration impacts need to be assessed in order for the overall system cost of intermittent RES to be quantified. As indicated in Figure 6-6 , the total Whole-System Cost (WSC) of intermittent RES consists of their Levelised Cost of Electricity (LCOE) and the system integration cost of RES. The latter is defined as the total of additional infrastructure and/or operating costs to the system as a result of integrating renewable power generation.

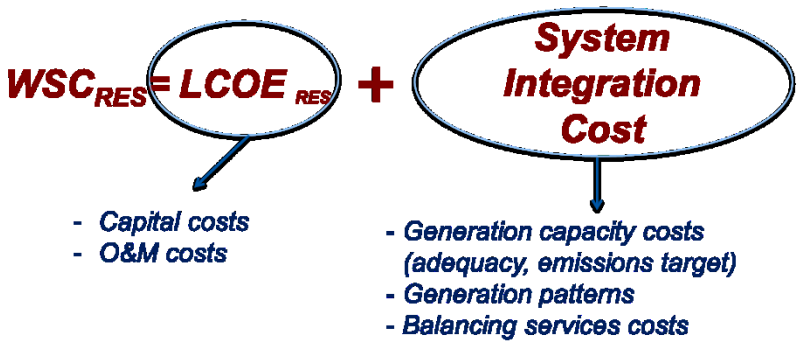

Figure 6-6 Whole-system cost of intermittent RES

LCOE considers the capital cost and O&M cost of RES technologies over their project life while the system integration cost of RES includes the system capacity costs associated with capacity needed for security, balancing costs and the impact of the RES output patterns. Other components of system integration cost, not considered in this study may include transmission and distribution network costs, as well as the cost of network losses; these components would reflect any requirement to reinforce transmission and distribution networks in order to accommodate wind and PV generation. In this study we focus on the capability of smart LCTs to reduce the system integration cost of wind and solar PV generation.

As the system integration cost of RES due to increased requirements for back-up capacity, provision of reserves is significant, it is important to implement new operating approaches that can minimise the integration costs. In this context, we will quantify the benefits of LCT resources trialled in LCL for reducing the system integration cost of wind and solar PV. The benefits will be assessed in the three categories discussed above:

1. *Reduced backup capacity cost*. LCTs have the capability of shifting demand i.e. modifying the effective (net) demand profile seen by conventional generators. If the smart LCTs are operated so that they reduce the net peak demand, this will also reduce the requirement for generation capacity margin in the system while maintaining security of supply. In other words, smart LCTs may improve the capacity value of wind and PV. Reduction in backup capacity cost due to improved capacity value is quantified according to [114].
2. *Reduced balancing operating cost*. This component of the RES integration cost reflects the increased need to provide reserve and response in the system with high RES penetration, as well as the occasional necessity to curtail wind or PV output in order to balance the system (e.g. at times of low demand and high wind or solar output). Smart LCTs have the potential to absorb some of this output that would otherwise be curtailed, while at the same time provide reserve and response services that would otherwise have to be provided by conventional generators at a considerable cost.
3. *Reduced investment cost associated with balancing*. In the context of a specific CO2 target, reducing the curtailment of wind and PV output by deploying smart LCTs also means that less additional zero- or low-carbon generation capacity will need to be built in order to meet the carbon target. We quantify this component of RES integration cost savings by assuming reduced wind output required less CCS capacity to be built.

6.5.2 Case Studies

The studies are based on the 2030 and 2050 GB system scenarios described in Section 6.3.2. The simulations are firstly carried out to characterise the annual operation of the system as well as necessary wind and PV curtailment without any

contribution from DSR (i.e. the non-smart case). After establishing the baseline RES balancing cost, benefits of each DSR technology for RES integration are assessed by comparing the key characteristics of smart and non-smart cases: operating cost, backup capacity requirement and wind curtailment. We do not express the baseline integration cost (without LCTs active in the system) given that the focus of the study is on the contribution of smart LCTs trialled in LCL.

In all studies we treat wind and solar PV collectively as intermittent renewable generation, although in the model these two were disaggregated as illustrated at the end of this section.

Figure 6-7 presents the value of smart LCTs for reducing RES integration cost in the 2030 GW scenario. The same case studies are analysed as in Section 6.4, and the benefits are expressed as annual integration cost savings (with the three components defined in the previous section) divided by the volume of absorbed annual RES output. We note that the greatest integration cost savings are achieved with smart HP operation, mostly because of the large volume of flexible HP demand assumed in this scenario. Total integration cost savings per individual technology vary between about £1 and £5/MWh. If all smart LCTs simultaneously provide balancing to the system, the savings increase to £8/MWh, while if they are additionally capable of providing frequency response, this increases further to £11/MWh. It is also possible to observe that the three components of RES integration benefits arise in broadly similar proportions.

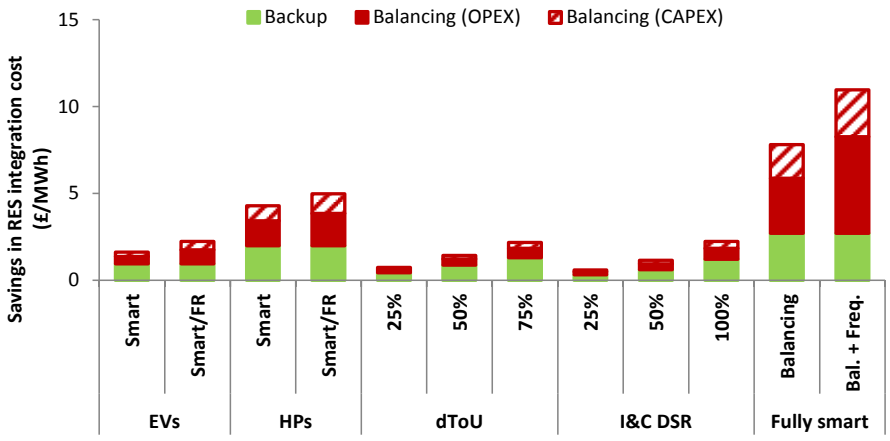

Figure 6-7 Reduced RES integration cost from deployment of smart LCTs (2030 GW)

Results for the same set of case studies but for the 2030 SP scenario are presented in Figure 6-8 . We observe similar trends as in the 2030 GW scenario, although the benefits tend to be lower. Best-case benefits, when all smart LCTs coexist in the system, vary between £6.4 and £7.6/MWh. We also note that the contributions of dToU and I&C DSR slightly increase, given that the volume of residential and commercial demand is the same, while the volume of RES output is lower than in 2030 GW.

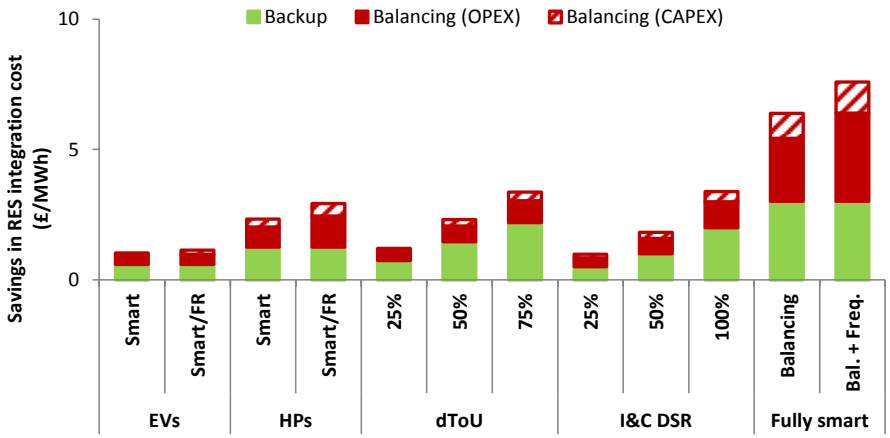

Figure 6-8 Reduced RES integration cost from deployment of smart LCTs (2030 SP)

Finally, in Figure 6-9 we show the RES integration cost savings with smart LCTs in the 2050 HR scenario. The backup component for smart EVs and HPs increases significantly due to the large assumed deployment of these technologies in the 2050 HR scenario. Fully smart cases bring savings of about £10-11/MWh, similar as in the 2030 GW scenario. The balancing CAPEX component in this scenario exceeds those seen in the other two scenarios, as the deployed volume of wind and solar PV, and consequently also of their curtailment, is the greatest. Total integration cost savings for individual technologies varied between £3.8 and £6.5/MWh for EVs and HPs, and between £0.6 and £2.0/MWh for dToU and I&C DSR (savings from these two DSR categories are much lower because the scenario assumes a drastic improvement in energy efficiency and large reduction in residential and commercial electricity demand).

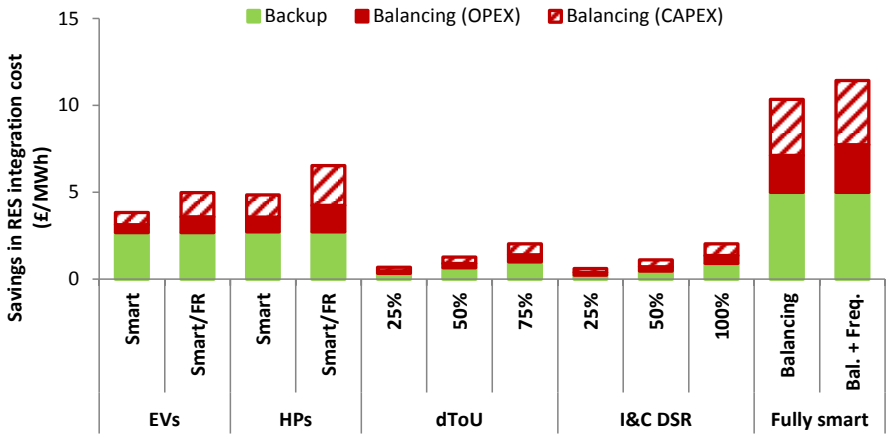

Figure 6-9 Reduced RES integration cost from deployment of smart LCTs (2050 HR)

We finally illustrate that if integration benefits are allocated separately to wind and solar generation, the scale and the composition of benefits might vary considerably between these two technologies. To that end, Figure 6-10shows that while smart LCTs reduce wind curtailment, as well as aggregate RES curtailment that is dominated by wind due to its size, smart utilisation of LCTs may also lead to higher PV curtailment as part of the overall cost-optimal solution (note that the total curtailment still reduces). This suggests the existence of certain trade-offs, where the flexibility of LCTs is used to absorb wind output even at the expense of slightly increased PV curtailment, as it results in a more cost-efficient solution.

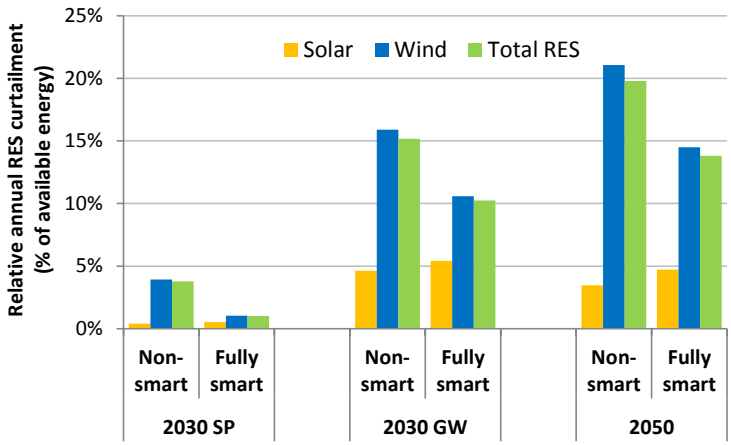

Figure 6-10 Wind and solar PV curtailment in non-smart and fully smart cases

On the example of the 2030 GW scenario, Figure 6-11 further shows how different components of system integration benefits generated by smart LCT operation may arise in markedly different proportions if these benefits are allocated to wind and solar

capacity according to the integration cost driven by these two technologies. Wind capacity dominates the overall RES mix, therefore the integration benefits for wind and total intermittent RES portfolio differ very little. On the other hand, the benefits for PV integration consist almost exclusively of backup cost savings, with the balancing OPEX and CAPEX components almost negligible. As illustrated in the previous figure, this occurs because smart LCT operation is not utilised to reduce PV curtailment, but on the contrary rather allows the PV curtailment to increase in order to use more attractive opportunities to save wind curtailment. Increase in PV curtailment is more than offset by balancing cost savings associated with more efficient system operation, which results in positive although small levels of saving in balancing OPEX and CAPEX categories.

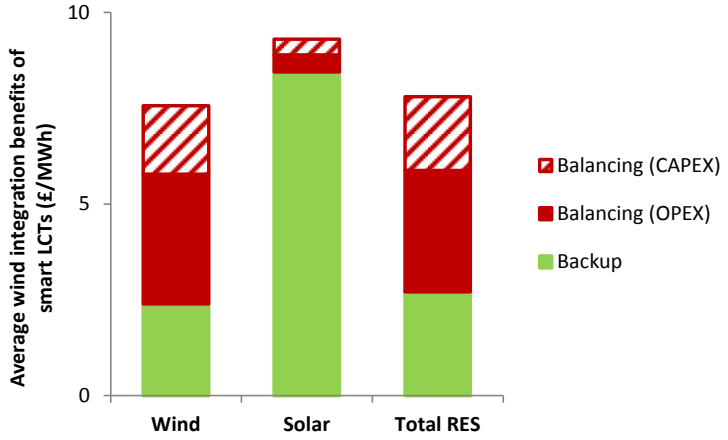

Figure 6-11 Wind and solar PV curtailment in non-smart and fully smart cases

6.5.3 Average and Marginal Value of Smart Technologies

When finding the value of smart LCTs, we distributed their benefits in terms of reduced integration cost across the entire output of intermittent RES generators in a given scenario. It is obvious that if an additional unit of RES capacity is added onto a system that already has significant RES capacity, the additional integration cost of the added capacity is likely to be higher than the average integration cost of the entire RES portfolio. This is because as more wind and PV are added to the system it becomes progressively more difficult to absorb their output without having to resort to generation curtailment. For the same reason, adding the first few megawatts of RES generation to an electricity system usually results in low integration cost given that the

system's inherent flexibility enables it to absorb wind and PV output fluctuations relatively easily.

Therefore, in addition to average RES integration benefits such as those described in Section 6.5.2, we also quantify in this study the marginal benefits of smart LCTs, i.e. the reduction of RES integration cost if a small quantity of RES is added to the capacity already existing in each scenario. We first summarise the average benefits for all three scenarios in Figure 6-, showing the integration benefits for the two fully smart cases (with and without frequency response provision).

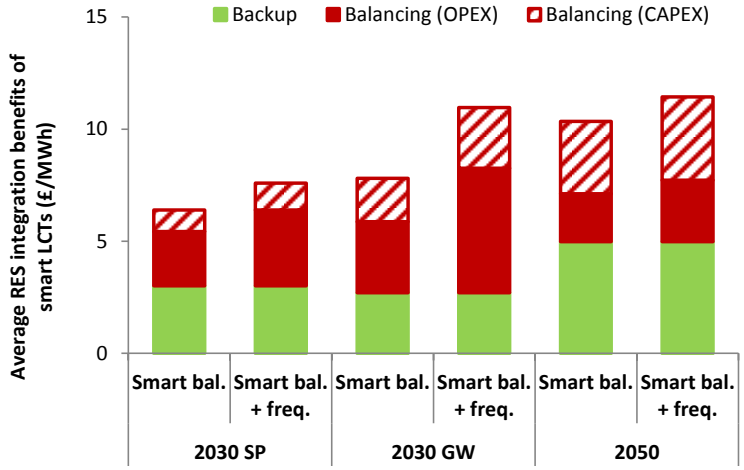

Figure 6-19 Average RES integration benefits from deployment of smart LCTs

In contrast to average benefits, we show in Figure 6-12 the marginal benefits of smart LCT operation when a small quantity of RES capacity is added to the system in 2030 SP, 2030 GW and 2050 HR scenarios. An immediate observation is that the marginal benefits exceed comparable average benefits by a factor of 2 to 3. This suggests that the value of smart LCTs for integrating additional RES capacity in a system that already contains a large share of intermittent renewables is significant. A further conclusion is that decarbonising the electricity system by integrating large amounts of wind and PV capacity can be much more cost-efficient if coupled with smart DSR technologies.

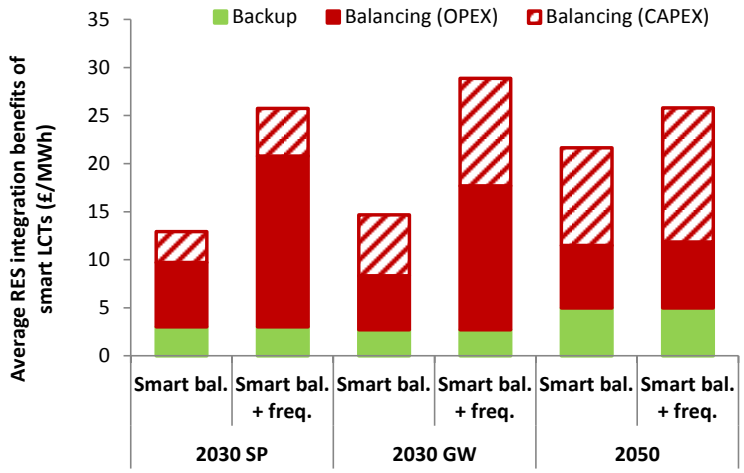

Figure 6-12 Marginal RES integration benefits from deployment of smart LCTs

In the two 2030 scenarios the marginal benefit doubles when frequency response is provided by LCTs in addition to balancing, whereas in the 2050 HR scenario the difference between the two fully smart cases is much smaller. We further note that the dominant component of marginal benefit in the 2030 SP scenario is balancing cost (OPEX); in the 2030 GW scenario balancing OPEX savings are commensurate with balancing-driven CAPEX savings. In the 2050 HR scenario the large volume of RES curtailment makes the balancing CAPEX benefits the dominant component.

6.5.4 Key Findings on Renewable Integration Benefits of Smart Technologies

This section investigated the benefits of LCTs monitored within LCL trials in supporting more efficient integration of intermittent renewable technologies across the three analysed scenarios. From our numerical studies it is possible to draw the following conclusions:

1. DSR technologies have a significant potential to support RES integration by reducing: balancing cost, required back-up generation capacity and cost of replacing curtailed RES output with alternative low-carbon technology to achieve the same emission target.
2. Penetration of individual DSR technologies i.e. the uptake of e.g. EVs, HPs etc. is an important factor in the value of DSR for RES integration.
3. DSR are capable to support cost-efficient decarbonisation of future electricity system by reducing RES integration cost.

4. Average RES integration benefits when all smart LCTs coexist in the system vary between £6.4 and £11.4/MWh of absorbed RES output across the three scenarios.
5. Marginal RES integration benefit found in our studies is 2-3 times higher than the average benefit, suggesting an increasingly important role for DSR in expanding RES capacity beyond the already high penetrations foreseen in the future.

6.6 Findings and Conclusions

In this chapter we have presented the results of a large number of case studies carried out in order to quantify the benefits of LCL solutions i.e. smart DSR technologies on the carbon performance and cost of RES integration in the future GB electricity system. All studies were informed by LCL trials.

We find that LCTs are able to deliver measurable carbon reductions primarily by enabling the future, largely decarbonised electricity system to operate more efficiently. Carbon benefits of different DSR technologies, when expressed per unit of smart demand appear to be a function of the assumed flexibility to shift demand and provide frequency regulation. Provision of frequency response in addition to smart balancing significantly increases the carbon benefits of all LCTs, and the greatest overall system-level reduction is observed in cases where all smart DSR technologies operate simultaneously in the system. Irrespective of the carbon scenario, or exactly which sources of DSR are adopted, there seems to be potential to reduce average system carbon emissions by an additional 5 g/kWh.

Carbon benefits of LCTs are generally more pronounced in systems i.e. scenarios with higher intermittent RES penetration, although there are limits to this trend where the non-renewable generation capacity on the system is also low- or zero-carbon (as in the 2050 HR scenario). Finally, we find that the integration of electrified transport and heating demand is significantly less carbon intensive if smart operation strategies are adopted, making a more positive impact on the overall carbon performance of the economy.

It is worth noting that the primary effort of government and regulators will remain on maintaining a trajectory towards a decarbonised generation fleet and the

electrification of heat and transport, but the flexibility of LCTs provides a measurable incremental benefit.

In the second set of case studies we have established that DSR technologies have a significant potential to support cost-efficient RES integration by reducing:

- RES balancing cost
- Cost of required back-up generation capacity
- Cost of replacing curtailed RES output with an alternative low-carbon technology to achieve the same emission target

In that context our studies show that smart DSR technologies are capable of supporting cost-efficient decarbonisation of future electricity system by reducing RES integration cost. Our studies indicate that the penetration of individual DSR technologies i.e. the uptake of e.g. EVs, HPs etc. is an important factor in the value of DSR for wind integration, as it determines the volume of flexible system services that can be provided by DSR technologies.

Average RES integration benefits when all smart LCTs coexist in the system vary between £6.4 and £11.4/MWh of absorbed RES output across the three scenarios. Marginal RES integration benefit found in our studies is 2-3 times higher than the average benefit, suggesting an important role for DSR in supporting the expansion of RES capacity even beyond the high shares foreseen in future scenarios.

7. Value of Flexibility from Thermal Plants in the Future Low Carbon Power System

7.1 Introduction

The operating reserve requirements and need for flexibility at high penetration of intermittent RES increase significantly above those in the conventional systems. Additional operating reserve is delivered through increased amount of plant operating part-loaded, i.e. less efficiently, and/or through plant with higher costs, leading to an increase in real time system balancing costs. The need for additional reserves and lack of flexibility also decrease the ability of the system to absorb intermittent renewable generation, particularly when high outputs of renewable generation coincide with low demand.

Alternative balancing technologies have been proposed and investigated to help mitigate these challenges [106]. Energy storage will play an important role in the future low carbon power system by saving excess wind and delivering ancillary services [1] [7]. Demand side response has been widely investigated to facility the integration of renewable energy [115] [116] [117]. Interconnection provides the benefits of exporting the renewable energy and sharing ancillary services, which are critical for relatively small power systems, e.g. Ireland [118]. Increasing flexibility of thermal plants is another option to support high penetration of the intermittent RES. The electrification of transport and heating sector and the retirement of aging plants in Europe require investment to build new power plants. At the same time, it is possible to directly invest in retrofitting the existing plant to increase its flexibility. There also exists arguments regarding whether the flexibility of plants should be taken into account when design the capacity mechanism. Therefore, it is crucial to investigate the role and the value of flexible plants in the future low-carbon power system to guide the investment and market design.

Some works have been done to understand the flexibility of thermal plants. Denholm et al [119] demonstrate that high penetration of base-load plants could cause significant renewable energy curtailment. A flexibility index is developed and applied in a system consisted of thermal power plants in [120]. The results suggest that the

need for flexible plants increases as the penetration of RES increases. The above mentioned two literatures focus on the understanding the demand on flexible plants in order to reach high penetration of renewables, while the economic value of flexible plants are assessed in other works. Juan et al [121] propose a Unit Construction and Commitment model, which simultaneously optimises the investment and operation of power system. The results show that the investment would shift from low-cost but inflexible plants to high-cost but flexible plant as the increase of wind penetration level. This chapter also investigates the profitability of flexible plant and suggests that the more frequently the commitment decision updates, the less profit the flexible plants obtain. Rautkivi et al [122] analyses the value of Smart Power Generation in the future system of UK and California with the conclusion that the flexible plants could potentially reduce the balancing cost up to 19%.

However, these above studies are all based on traditional scheduling methods. Recent development of stochastic optimisation in the electricity sector [44] [4] could fundamentally change the way to operate the system, which in turn impacts the value and the need for the enhanced flexibility from conventional plants. Moreover, the increasing requirements of frequency regulation due to the reducing system inertia have not yet been considered when assessing the value of enhanced flexibility. The multi-stage stochastic scheduling framework developed in Chapter 2 is applied to quantify the operational value of enhanced flexibility. This study focuses on the assessment of enhanced flexibility provided by gas-based generation, in particular considering lower Minimum Stable Generation (MSG), higher frequency response capability, higher ramp rate, shorter commitment time and idle state capability. A wide range of sensitivity studies are carried out to understand the value of enhanced flexibility across two representative systems. The impacts of various scheduling strategies, risk attitudes, frequency regulation requirements and carbon taxes are also analysed.

The rest of this chapter is organised as following: Section 7.2 introduces the flexibility features and system assumptions, Section 7.3 presents the main results and Section 7.4 concludes this chapter.

7.2 Flexibility Features and System Assumptions

Main characteristics of flexibility from thermal plants are defined in Table 7-1. MSG determines the maximum boundaries in which the plants can change their output. For instance, plant with the capability to change its output from 20% to 100% contributes more into the system flexibility than the plant with the capability to change its output from 50% to 100%. The maximum response capability defines the maximum proportion of the plant capacity which can contribute to the frequency response service. Higher ramp rate means the plant can adjust its output faster to compensate the changes in the system. Commitment time describes how long thermal plants take from offline status to online status. Shorter commitment time means less uncertainty to face when making start up decision. Idle state is the capability to keep the plant online but without energy production.

Table 7-1 Definition of Flexibility Features

	Base case	*Enhanced Flexibility*
Minimum Stable Generation (MSG)	**50%**	**20%**
Max Response Capability (Response)	**17%**	**40%**
Ramp Rate	**32%/10mins**	**50%/10mins**
Commitment Time (CT)	**4 hours**	**2 hours**
Idle State (Idle)	**No**	**With**

The value of enhanced flexibility is analysed in two systems, which mean to represent flexible and inflexible generation mix. The detailed information is shown in Table 7-2. Peak demand in the system is 50 GW with annual energy consumption 293TWh. 80% of hydro plants are assumed to be equipped with 10h reservoir, while 20% are run-of-river. Nuclear plants are assumed to operate at full-load all the time. Fuel price and carbon cost are chosen to match the predictions in years 2020-2030 of the International Energy Agency for the 450 scenario [69]. Unless otherwise specified, the forecast error of wind generation is assumed to be 10% of installed capacity in 4-hour ahead and moreover, 5GW of CCGTs are assumed to be equipped with enhanced flexibility.

Table 7-2 Generation Mix of Flexible System and Inflexible System

	Nuclear	*CCS*	*GAS*	*COAL*	*OCGT*	*Hydro*
Flexible System (GW)	**0**	**7.2**	**16.8**	**12**	**7.2**	**16.8**
Inflexible System (GW)	**33.6**	**5.7**	**6.3**	**2.4**	**2.7**	**9**

Table 7-3 Main Economic Assumptions

	CO2	COAL	GAS	Nuclear
Price	74.2€/T	3.23€/GJ	8.85€/GJ	0.256€/GJ

The stochastic scheduling tool is first applied to the base-case systems without any improved flexibility features. The results are presented in Figure 7-1. The flexible system shows high operation cost while relatively low wind curtailment. On the other hand, the nuclear-dominated inflexible system shows low operation cost while large amount of wind is curtailed. Moreover, the emission rate in the flexible system reduces from 310 g/kWh to 90 g/kWh when the wind penetration level increases from 0 to 60%; while the emission rate in the flexible system keeps at around 45 g/kWh regardless of wind penetration levels. Choosing the two base case systems with distinguished performances would help in understanding the key drivers of the value of enhanced flexibility.

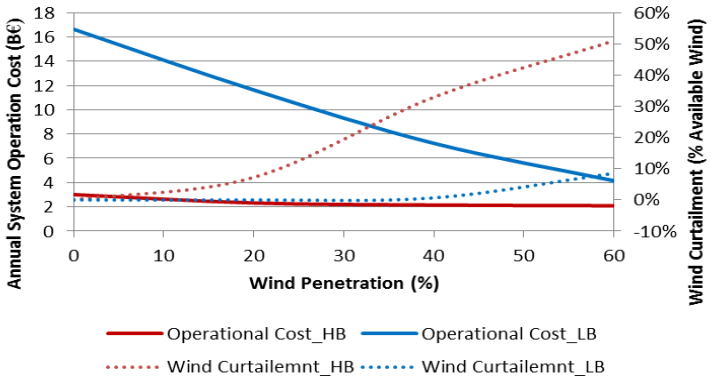

(a) Operation cost and wind curtailment

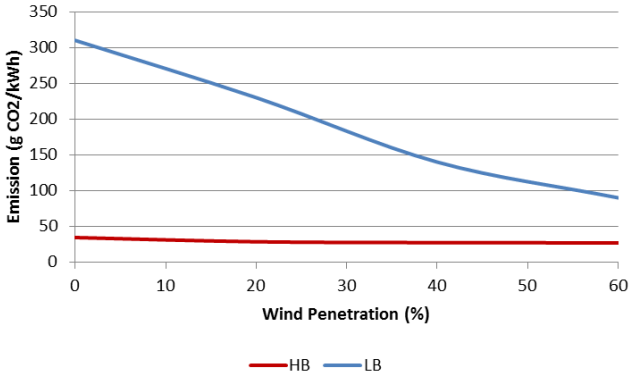

(b) Emission rate

Figure 7-1 Performance of base case systems.

7.3 Value of Enhanced Flexibility from Thermal Plants

The value of the enhancement on each flexibility parameter in the flexible system is shown in Figure 7-2. In general, we observe that the value of enhanced flexibility

increases with higher penetration of wind. Because high wind penetration increases the need for reserve provision, enhanced flexibility becomes more desirable. However the value of high response capability is low in this system. As there is a significant amount of flexible hydro plants providing low-cost frequency response, there is no need in this system for the plants with enhanced response capability. The simulation results (Figure 7-2 (b)) also suggest that the presence of enhanced flexibility from thermal plants significantly reduces wind curtailment in the case of 60% wind penetration.

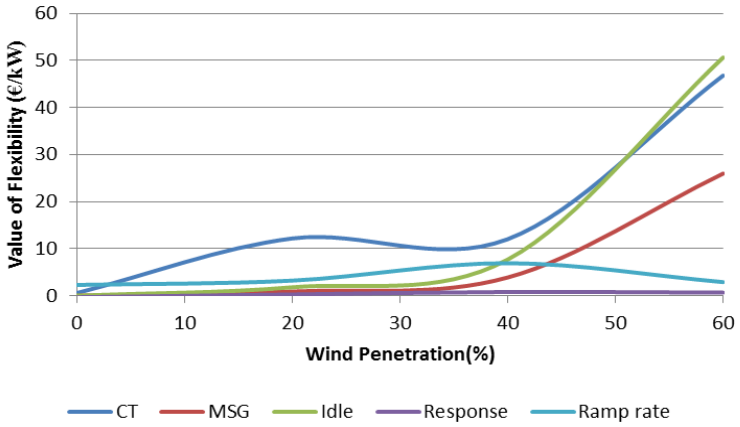

(a) Economic value of enhanced flexibility

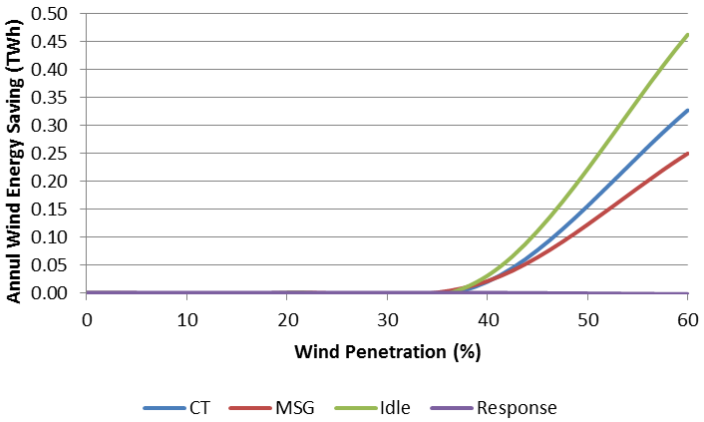

(b) Annual wind energy saving from enhanced flexibility

Figure 7-2 Benefits of enhanced flexibility in the flexible system.

The benefit of enhanced flexibility in the inflexible system is presented in Figure 7-3. Lower MSG and higher response capability show constant high value regardless of wind penetration level, while the value of idle state, shorter commitment time and ramp rate is very low. Due to lack of frequency regulation capabilities for base-load

plants (i.e. nuclear), gas plants are scheduled to run only to provide fast response, which causes curtailment of wind power and/or de-load of nuclear generation. Therefore, high response capability and low MSG are extremely valuable. However, Figure 7-3 (b) suggests that these two enhanced flexibilities cause additional wind curtailment due to the shift of frequency response provision from OCGT to flexible CCGT, which leads to more energy production to provide the same amount of frequency response. Although the wind curtailment increases, the overall system emission rate (Figure 7-3 (c)) significantly reduces with the enhanced flexibility. In this system, the value of reserve related service (through commitment time, idle state and ramp rate) is low as de-loaded nuclear plants and curtailed wind generation can provide sufficient low-cost operating reserve.

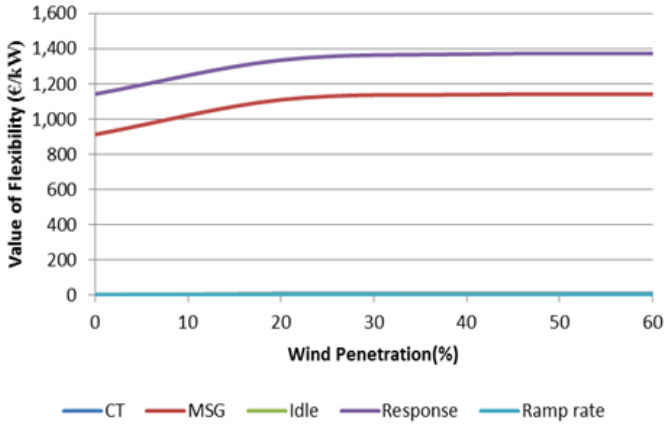

(a) Economic value of enhanced flexibility

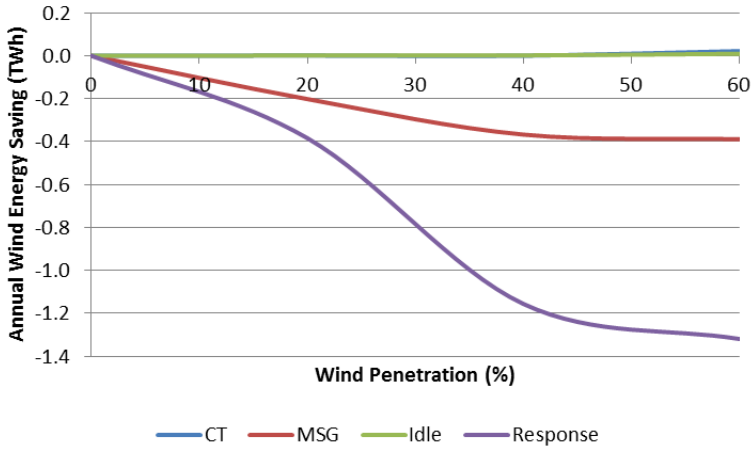

(b) Annual wind energy saving from enhanced flexibility

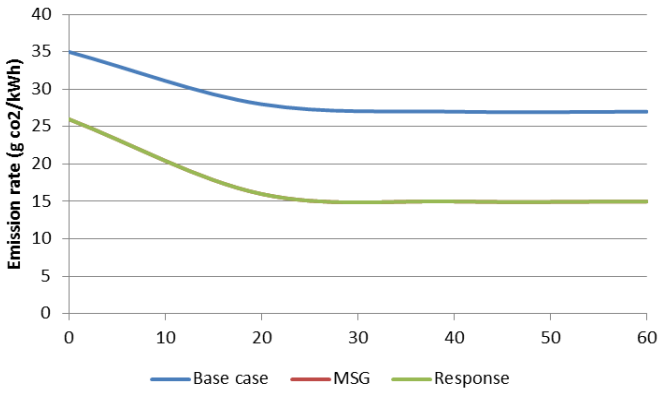

(c) System emission rate

Figure 7-3 Benefits of enhanced flexibility in the inflexible system.

7.3.1 How Many Flexible Plants Are Required?

In order to understand how many flexible plants are required in the system, value of enhanced flexibility is calculated with different penetration levels of flexible plants. Figure 7-4 provides the value of improving selected flexibility features of CCGTs with different penetration in the flexible system. In this specific example, the operation cost reduction reduces significantly when more than ~6% of the total plant capacity is equipped with the improved flexibility features.

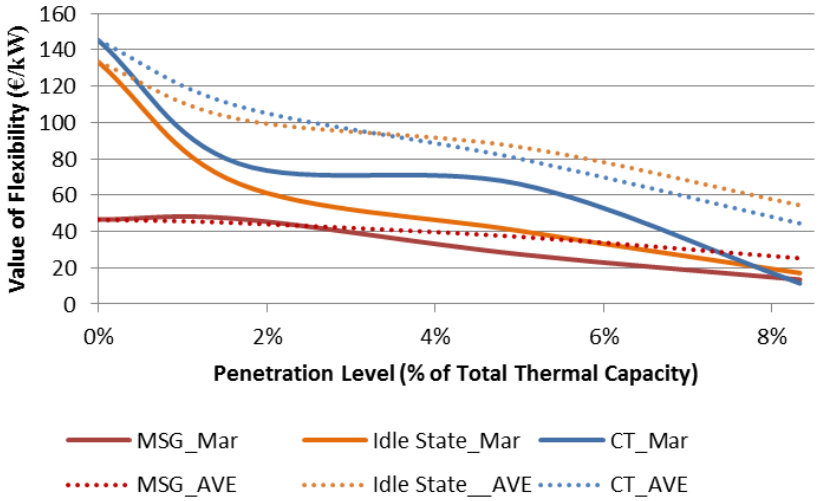

Figure 7-4 Value of enhanced flexibility in the flexible system with different penetration level of flexible plants.

The results in the inflexible system are shown in Figure 7-5. Although the high response capability is extremely valuable in the inflexible system, the marginal value declines rapidly with increase of penetration level and reaches zero after ~5% of the

total plant capacity. Since the volume of frequency response market is small, assumed to cover the largest power plant (1.8GW), once there are enough flexible generators providing low-cost frequency response, the marginal value becomes zero.

For policy makers this means that it might be that more cost-effective enabling market structures can be achieved by providing incentives to put in place a limited number of flexible power plants, compared to capacity payments to all power plants

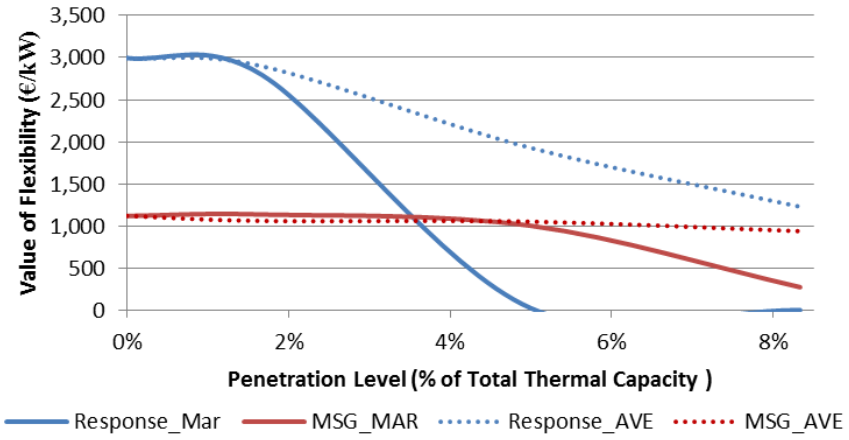

Figure 7-5 Value of enhanced flexibility in the inflexible system with different penetration level of flexible plants.

7.3.2 How Flexible the Plants Need to be?

Another important aspect need to be investigated is how flexible the plants need to be. The more flexible the plant becomes, the more cost there would be. Therefore, it is necessary to balance the cost to improve the flexibility and the benefit from the enhanced flexibility. The improvements of some specific flexibility features are varied and the associated value is quantified. This study focuses on the high-valued flexibility features in the inflexible system. For both the lower MSG and higher primary frequency capability, simulation results (Figure 7-6 and Figure 7-7) suggest that the value increase almost linearly in the range of interest. However, increase of MSG from 50% to 40% would not make CCGT competitive with other technologies in providing frequency response, which therefore shows no value of this improvement. Given the annualised investment cost associated with different level of enhanced flexibility, the presented results could be used as a reference to determine the optimal flexibility levels of the thermal plants.

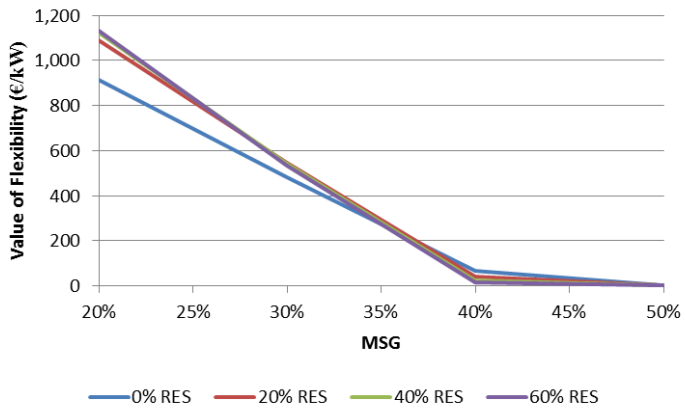

Figure 7-6 Value of enhanced flexibility with different levels of MSG in the inflexible system.

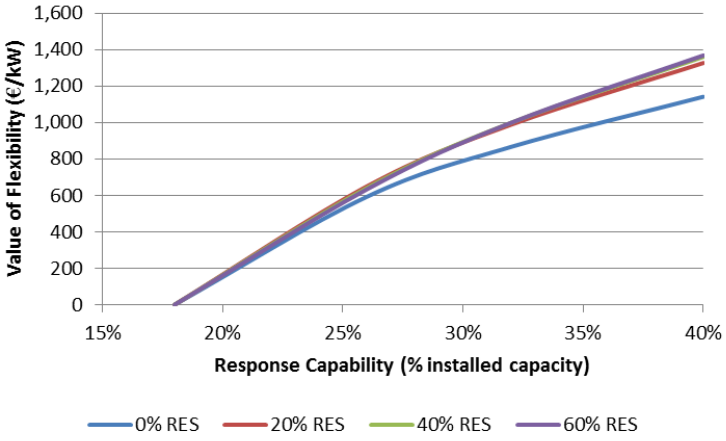

Figure 7-7 Value of enhanced flexibility with different levels of response capability in the inflexible system.

7.3.3 Solar versus Wind Integration

Wind and solar Photovoltaic (PV) are very different in terms of time distribution:

1. Solar produces mainly 8-12 hours a day, depending on seasonal and specific weather conditions.
2. Wind power typically produces with no interruptions over a much longer period of time, but low wind periods can last for several days.

From this point of view, PV production is easier to predict, particularly for hourly variations. However, for large shares of penetration, solar is generally more difficult to integrate, compared to wind. This is illustrated with an example in Figure 7-8, where the penetration is scaled-up to 50% of the overall energy produced, in the case of wind only (left), and of a mix of 40% PV and 60% wind (right). Load demand and wind and PV production data (before being scaled-up) are taken from the German

TSO area of Amprion. As clearly shown, PV exceeds the load demand almost every day, while wind production is most of the time below the load demand. As clearly shown, even if base load (represented as a blue bar) is reduced to zero, solar production would still exceed the load demand, thus no flexibility or variation of fleet composition would be able to eliminate solar curtailment (energy storage, exports, and demand-side-management are not in the scope of this analysis).

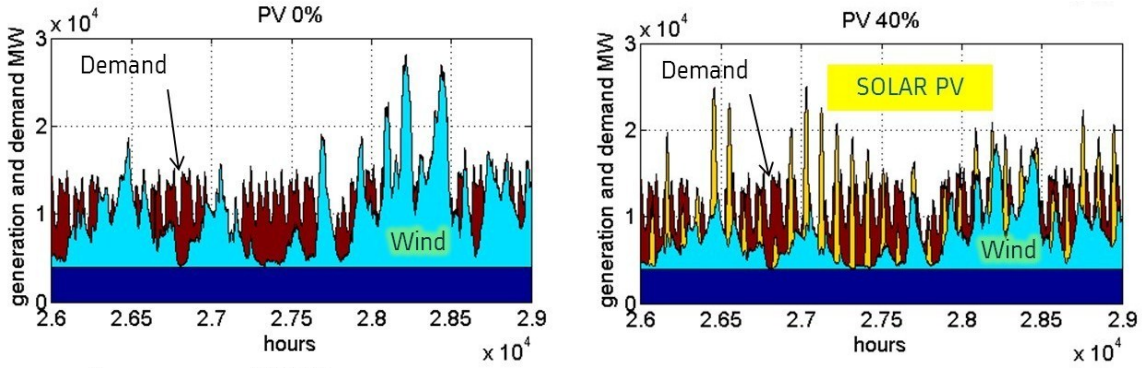

Figure 7-8 Example of 50% RES penetration, of which 40% PV and 60% Wind (right) and wind only (left)

The different nature of solar and wind has a major impact on thermal power plants operation if PV or wind is the dominating RES. In particular, thermal plants cycles are expected to be more severe in the case of PV. This is shown in Figure 7-9, where annual start-ups for different RES penetrations are displayed, in the case of flexible system. The increased number of start/stops in the case of PV is due to the fact that solar energy appears and disappears daily, whereas wind has cycles of intermittency more widely distributed. One should also note that start/stops do not increase monotony with wind penetration. For some CCGT, the number of starts/stops decreases when wind penetration is higher than 20-30%. This can be explained by an increased parking time of such power plants. This is clearly not the case for PV, as power plants have to provide power to the grid when after sunset, no matter the capacity of PV installed. However, the enhanced flexibility in the system with PV as dominating RES shows the similar value as that in the system with wind as dominating RES.

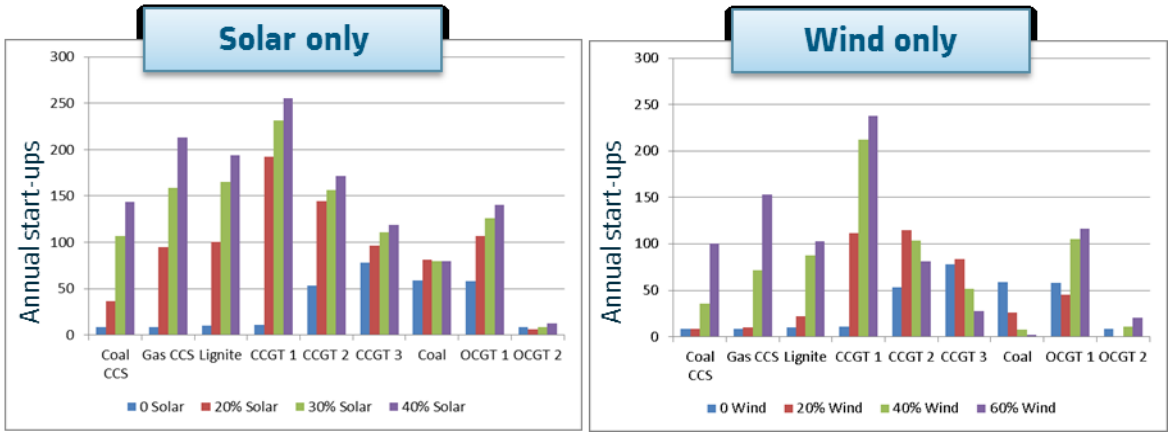

Figure 7-9 Example of annual start-ups in the case of solar only (left) and wind only (right), for different level of RES penetration

7.3.4 Impact of Scheduling Methods on the Value of Enhanced Flexibility

The value of flexibility is primarily driven by the need for various ancillary services induced by the integration of wind power. Different scheduling methods would require different ancillary services, e.g. allocation between standing and spinning reserves. Recent works [45] [3] show that stochastic scheduling method results in lower operation cost and lower renewable curtailment than traditional deterministic method, especially with high penetration of RES. Although deterministic scheduling is still the dominating method in present power systems, stochastic scheduling is likely to be implemented more widely as increasing penetration of intermittent RES. The different scheduling methods show significant impact on the value of storage in [1]. Therefore, this section investigates the impact of different scheduling methods and time resolutions on the value of enhanced flexibility from thermal plants.

The deterministic and stochastic scheduling methods are used to quantify the values of enhanced flexibility in the systems with 60% of wind penetration. The deterministic method here refers to the case that reserve and frequency response requirements are calculated dynamically but only based on a single scenario as current operation practice.

As shown in Figure 7-10, MSG and Idle-state shows almost twice of the value in deterministic scheduling case while the value of commitment time is reduced significantly. The reason can be explained by the fact that the deterministic scheduling method tends to rely more on spinning reserve, which would increase the values of

spinning reserve related flexibility features (e.g. MSG and idle-state) and decrease the value of standing reserve related flexibility features (e.g. commitment time). The results in Figure 7-11 suggest that modelling of 10-min operation in stochastic framework increases the need of operating reserve to compensate intra-hour variability and uncertainty of wind generation, leading to an increased value of the enhanced flexibility. In general, the need and the value of enhanced flexibility show significant differences by using different scheduling methods in the flexible system.

On the contrary, the value of enhanced flexibility in the inflexible system is not highly affected either by scheduling methods (Figure 7-12) or by time resolutions (Figure 7-13). The reason is that the value of flexibility in inflexible system is primarily driven by the need of fast frequency response, which is not highly related to the scheduling methods or time resolutions. However, MSG and high response capability shows lower value in the deterministic scheduling (as shown in Figure 7-12) because that the deterministic scheduling tends to keep more generators online, which reduces the challenge of providing fast frequency response.

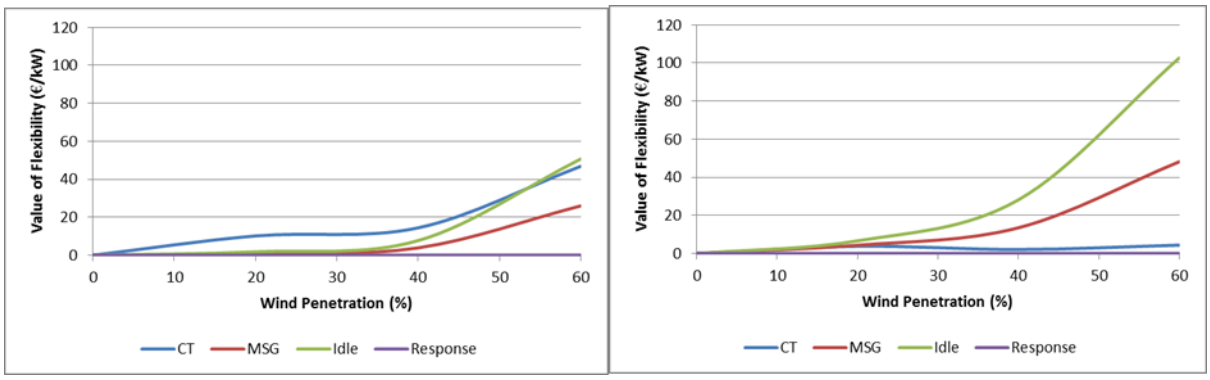

Figure 7-10 Value of flexibility in flexible system: Stochastic (left) VS Deterministic (right)

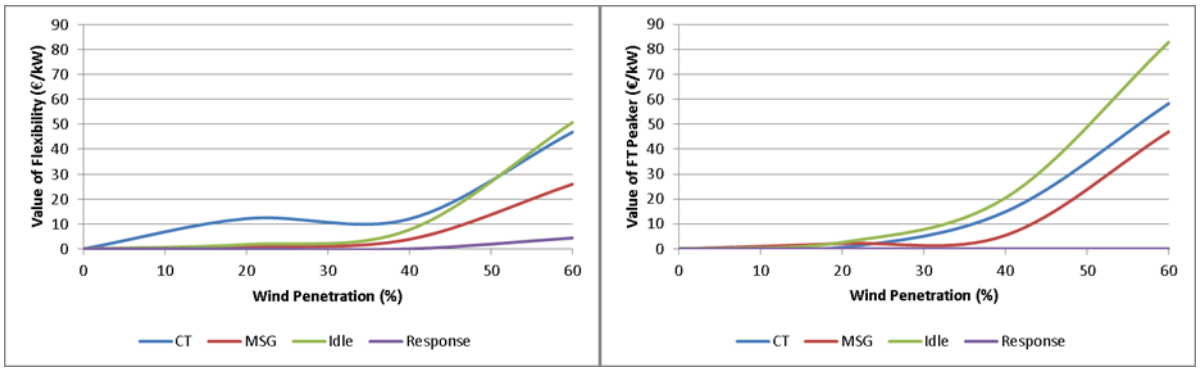

Figure 7-11 Value of flexibility in flexible system: Hourly (left) VS 10 mins (right)

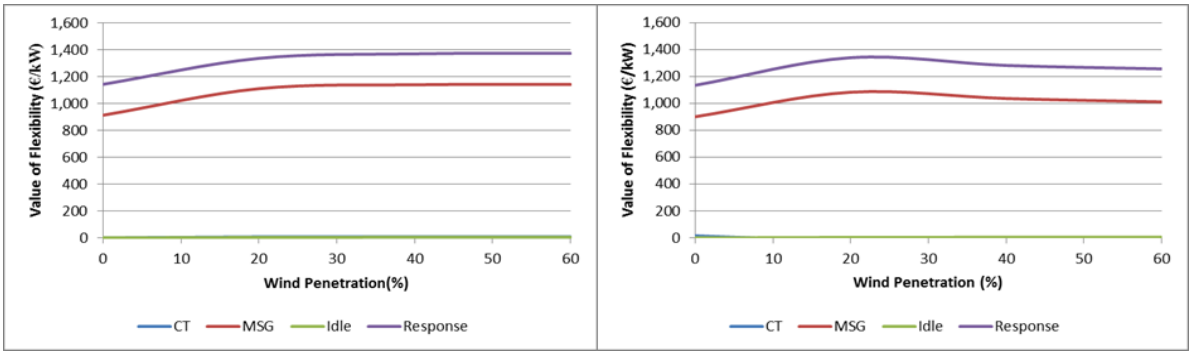

Figure 7-12 Value of flexibility in inflexible system: Stochastic (left) VS Deterministic (right)

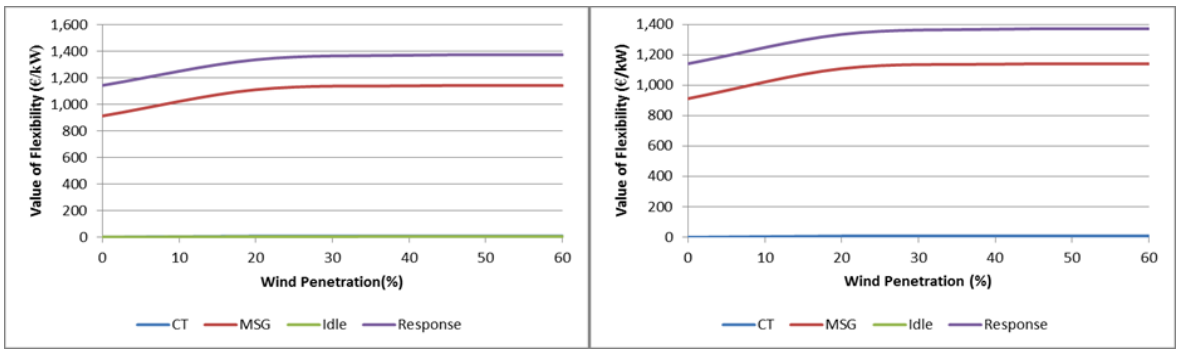

Figure 7-13 Value of flexibility in inflexible system: Hourly (left) VS 10 mins (right)

7.3.5 Impact of Risk Attitude on the Value of Enhanced Flexibility

In the stochastic framework, risk preference of system operator affects the operation of the system, especially the amount and the type of scheduled reserve services. Therefore, it is important to understand the impact of risk preference on the value of flexibility. As shown in Figure 7-14 , risk aversion would increases the value of Idle-state and MSG, while reduces the value of CT. The reason is that the risk aversion causes over-schedule of spinning reserve, which increases the spinning reserve related flexibility (Idle-state and MSG) while decreases the standing reserve related flexibility (CT)

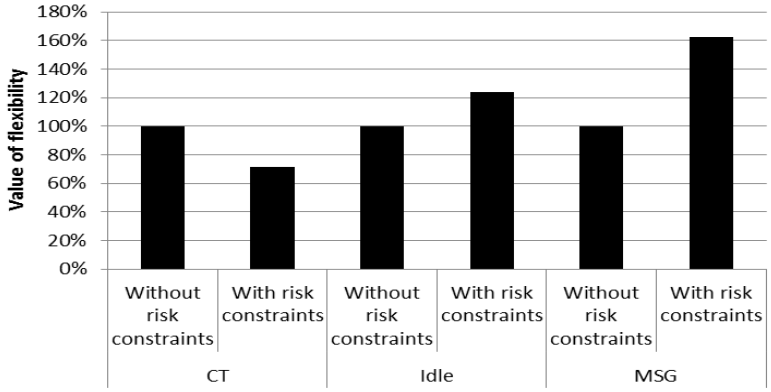

Figure 7-14 Value of flexibility: Risk Neutral VS Risk Aversion

7.3.6 Impact of Inertia-dependent Response Requirements on the Value of Enhanced Flexibility

Another issue associated with integration of renewables is the reduction of system inertia, which in turn increases the fast frequency response requirements. The impact of this issue on the value of enhanced flexibility is investigated in this section. The value of all the flexibility features (Figure 7-15) in the flexible system gets significant increase when inertia-dependent response requirement is taken into account. Out of expectation, the reserve related flexibility features gets significant increase although the inertia-dependent response requirement is only expected to increase the demand for frequency response. This is related to the fact that the requirements of frequency regulation depend on the system inertia, which will in turn be driven by the amount of synchronised conventional plant and the system demand. Different realisations of wind production could significantly change the schedule of conventional plants, resulting in different levels of system inertia. Shorter commitment time and idle state could be used to reduce the cost associated with this uncertainty, leading to an increased value of those enhanced flexibility features.

Considering inertia-dependent response requirement would increase the value of frequency response related flexibility (low MSG and high response capability) in the inflexible system due to increased frequency response requirements (Figure 7-16). The value of high response capability increases by almost 3 times, while the value of MSG increases by around 1.5 times. However, the value of other enhanced flexibility features remains to be very low.

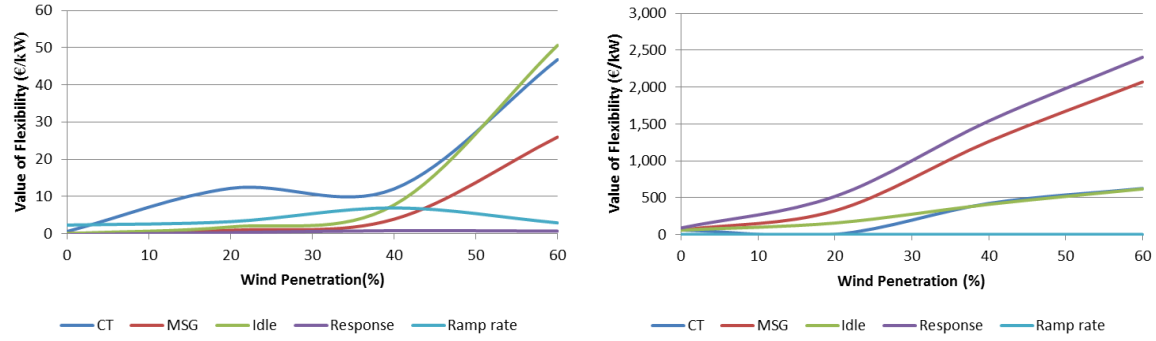

Figure 7-15 Value of flexibility in the flexible system: Constant Response Requirement (left) VS Inertia Dependent Response Requirement (right)

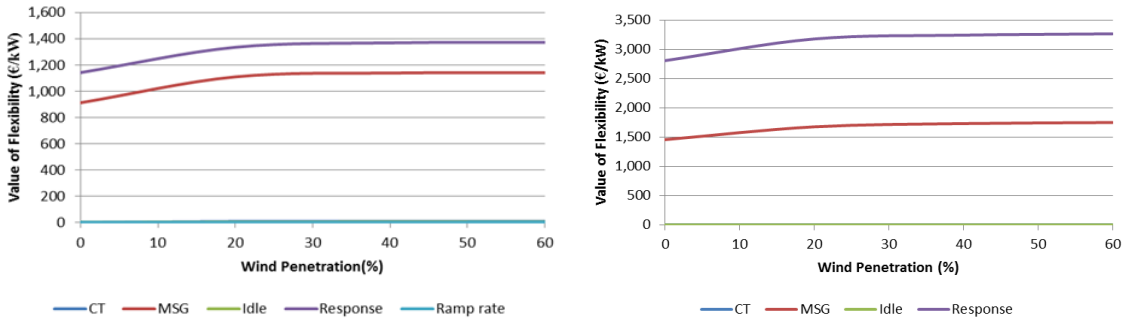

Figure 7-16 Value of flexibility in the inflexible system: Constant Response Requirement (left) VS Inertia Dependent Response Requirement (right)

7.3.7 Impact of Carbon Tax on the Value of Enhanced Flexibility

Recently, various renewable energy support schemes have been proposed and implemented all over the world. Carbon tax is one of the most widely implemented schemes. Although nuclear and coal plants serve as base load due to their low operation cost, while CCGTs are used to support peaking demand in present power systems, the introduction of carbon tax could change this situation due to the high emission rate of coal plant. Therefore, different carbon taxes are introduced in this section to investigate their impact on the value of enhanced flexibility. Two different carbon prices are considered, 73€/tonne (2030 prediction) and 20€/tonne, respectively.

In the flexible system with 60% wind penetration, with the increase of carbon price, the value of enhanced flexibility from CCGT increases (Figure 7-17), while the value of enhanced flexibility from coal plants decreases (Figure 7-18). This is because high carbon price make the operation of coal plants much more expensive than CCGT and causes that fewer coal plants are scheduled to produce, even after being equipped with enhanced flexibility. There is a clear trend that as the increase of carbon price, the value of enhanced flexibility shifts from coal plants to CCGT.

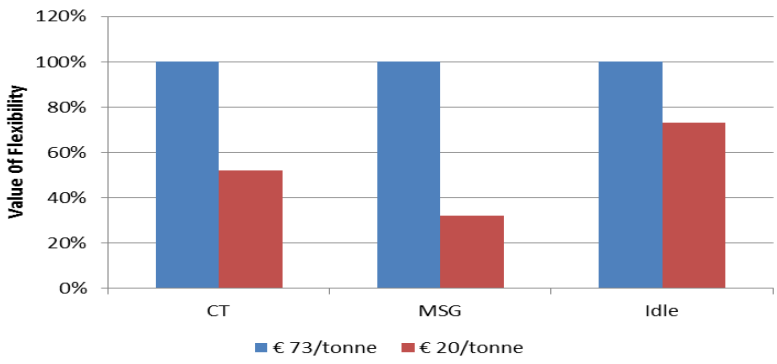

Figure 7-17 Impact of carbon tax on the value of flexibility of CCGTs in the flexible system

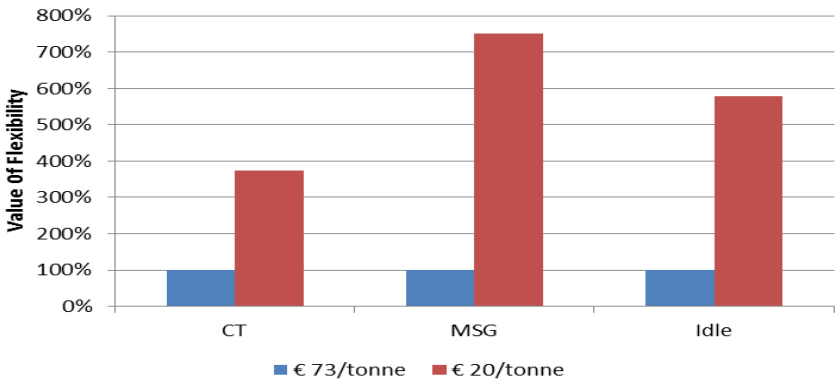

Figure 7-18 Impact of carbon tax on the value of flexibility of Coal plants in the flexible system.

Since value of flexible CCGT in the inflexible system is from replacing OCGT in providing frequency response and the emission rate of OCGT is much higher than CCGT, the higher carbon price increases the value of enhanced response capability and MSG from CCGTs (Figure 7-19).

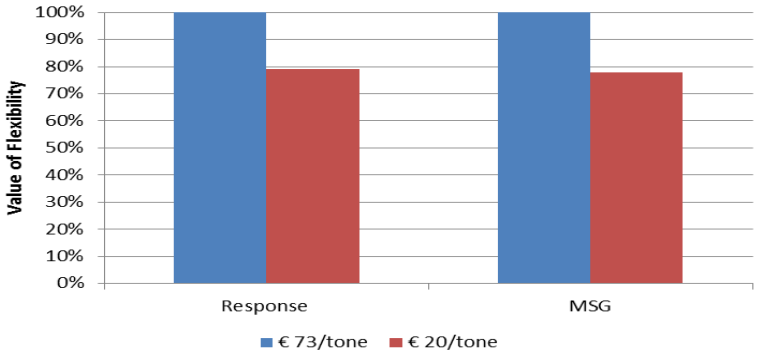

Figure 7-19 Impact of carbon tax on the value of flexibility of CCGTs in the inflexible system.

7.3.8 Market Regard on Flexibility

The value of the flexibility features analysed in the present study is rarely accrued to the plants generating such a value. A typical example is reported in Figure 7-20 for the case of 1 GW CCGT plants with improved MSG from 50% to 20%. The difference between the energy produced by the CCGT before and after the improvement is reported on the right hand side. After the MSG is improved, the related CCGT will be operated more time at reduced load, thus it will produce less energy (in the figure the reduction at 40% wind penetration is about ~500 GWh, equivalent to ~5% abs reduction of the capacity factor). In a market where revenues are mainly driven by the energy sold, this clearly represents a disadvantage for the flexible CCGT itself. Currently there are different fora, working groups and initiatives

with the main aim of suggesting possible ways of modifying current market regulations. It should be noticed that a capacity market based on capacity only would not provide any reward to flexibility, thus it would not produce any of the benefits shown in this chapter.

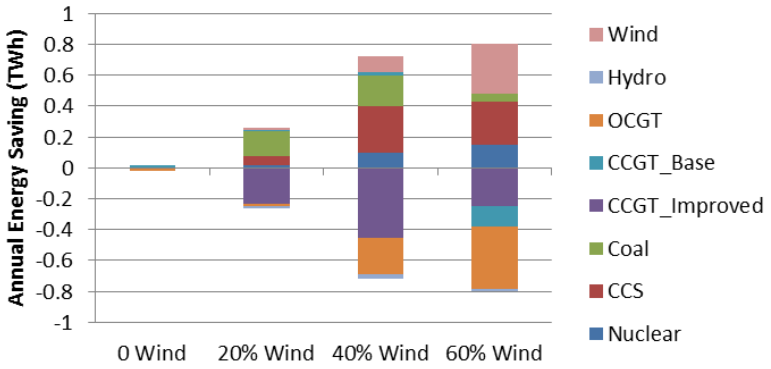

Figure 7-20 Differences in annual energy

7.4 Conclusion and Future Work

This chapter investigates the value of enhanced flexibility from thermal plants in the future low carbon systems. It has been shown that the value of enhanced flexibility increases with the penetration of wind energy; however, different systems require different types of flexibility features. In the coal and gas dominated system, the value of reserve related flexibility features (short commitment time, idle state and so no) is higher, while in the nuclear dominated system, frequency response related flexibility features (high response capability and low MSG) are more desirable. The analysis also suggests that the different system scheduling methods could significantly change the value of enhanced flexibility features. In the flexible system, traditional deterministic schedule would increase the value of lower MSG and Idle state, while decrease the value of shorter commitment time. Another study suggest that risk aversion would increases the value of Idle-state and lower MSG, while reduces the value of shorter commitment time. The reason is that the risk aversion causes over-schedule of spinning reserve, leading to an increase of the value of the spinning reserve related flexibility features and decreases the standing reserve related flexibility features. The value of enhanced flexibility gets significant increase when inertia-dependent response requirement is taken into account. High carbon price shifts the value of enhanced flexibility from coal-fired plants to gas plants.

8. Conclusion and Future Works

This thesis proposes novel analytical models for assessing the role and the value of various flexibility resources in the future low-carbon systems with high penetration of RES. This chapter highlights the key contributions of this thesis and outlines the most promising avenues for further research.

8.1 Stochastic Unit Commitment with Inertia-dependent Frequency Regulation

A novel mixed integer linear programming (MILP) formulation has been developed for stochastic unit commitment (*chapter 2*). The model optimises system operation by simultaneously scheduling energy production, standing/spinning reserves and inertia-dependent frequency regulation in light of uncertainties associated with wind production and generation outages. Post-fault dynamic frequency requirements (rate of change of frequency, frequency nadir and quasi-steady-state frequency) are formulated as MILP constraints by using a simplified model of system dynamics. Moreover the proposed methodology permits to recognise the impact of wind uncertainty on system inertia. The analysis suggests that the increased rating of the largest plant and the growing penetration of wind energy will make constraints associated with transient frequency evolution significantly more relevant. Moreover, we demonstrate the change in frequency response requirement from being determined by quasi-steady-state frequency limit, to being driven by nadir frequency limit.

Case studies are carried out in the 2030 GB system to demonstrate the importance of incorporating inertia-dependent frequency regulation in the stochastic scheduling. The proposed model enables the impact that different settings of frequency response delivery time, RoCoF limit and load damping rate would have on the system operation cost and on the wind curtailment to be assessed. The results obtained regarding the RoCoF and delivery time can provide economic evidence to support appropriate reforms of the grid code. Furthermore, we demonstrate the value of recognising different inertia capabilities of generators in the scheduling process, which may facilitate the future development of inertia-related market. The advantages of the proposed model in understanding the value of flexibility are also discussed.

8.2 The Role and the Value of Various Flexibility Resources in the Future Low-carbon Systems

8.2.1 Energy Storage

This thesis presents the analysis for ES with the application in the energy and ancillary services markets (*chapter 3*). Stochastic system and storage scheduling model is proposed and implemented.

A large set of studies has been carried out to understand the value of ES and the key drivers that affect the value across different scenarios. The results suggest that in the energy and ancillary services markets, the value of ES is mainly driven by the temporal arbitrage opportunities created by volatility in either or both day-ahead and real-time (balancing) energy prices. On top of energy and balancing services, ES can also provide additional ancillary services e.g. FR. The value of ES is shown to be site-specific in case when distribution network is constrained. The effect of network constraints will become increasingly significant in the future system and ES will facilitate cost-effective integration of low-carbon generation and demand connected to the constrained distribution networks.

Due to relatively high costs associated with current ES technologies, reviewed technologies do not appear to be cost-effective in the present power system. However, with the expected reduction of the costs and significantly increased value in the future system, some technologies such as (Li-ion, Vanadium flow, NaS, ZEBRA, Advance lead acid) may become attractive.

8.2.2 Frequency Regulation Support from Wind Plants

A novel methodology is proposed and applied to assess the role and the value of frequency regulation support from wind plants (*chapter 4*). The model incorporates the frequency regulation support from WPs into generation scheduling, therefore enabling the benefits of alternative frequency regulation control strategies to be quantified. Studies are carried out in the future GB power system with different wind penetration levels and frequency regulation requirements. The results suggest the SI could effectively reduce the system operation cost in the system, especially with high penetration of wind generation. In addition, marginal operation cost saving of SI provision from WPs is investigated, which could be used to support cost-benefit

analysis for determining the amount of WPs to be equipped with SI capability. The relaxation of RoCoF limit significantly reduces the demand on the SI provision from WPs. The impact of uncertainty in the capacity of WPs being online on the operation cost saving is shown to be significant only in the system with low penetration of WPs with SI capability. Moreover, the effects of recovery period are system specified. There is moderate impact of recovery period in the system with tight RoCoF limits. While in the system with relaxed RoCoF limit, very aggressive design of SI capability could even increase the operation cost. In fact, there exists an optimal time constant of SI that would achieve the maximum operation cost saving. This optimal time constant depends on the installed capacity of WPs, the magnitude of recovery effect and the frequency regulation requirement. The results also suggest that there would be significant benefits in reducing the recovery effect of SI provision. The tuneable controller of SI leads to higher benefits than fixed controller of SI if the recovery effect is severe.

The analysis carried out also demonstrates that there would be no value for WPs tin providing PFR in the system with the present RoCoF limit. But when the relaxed RoCoF is applied, PFR provision could achieve similar cost saving as SI provision. Combined provision of SI and PFR shows marginal extra benefits over SI only. However, the additional PFR due to severe recovery effect could significantly increase the demand on the combined provision.

8.2.3 Demand Side Response

This thesis proposes a novel demand side response model (DSRM) for TCLs (*chapter 5*). The DSRM explicitly models and controls the recovery period after frequency regulation provision and thus optimally allocates multiple frequency services to balance the benefit of the demand side frequency support and the cost of supplying extra power with reserve generators during the devices' recovery phase. The proposed method is integrated within the multi-stage stochastic unit commitment. The case study attests the value of the proposed DSRM compared with an alternative approach for demand response schemes. In particular, the large cost savings obtained are due to the flexible response provision and especially due to the inclusion of the recovery phase, suppressed in other frameworks. In fact, the inclusion of a fast energy

recovery allows for large secondary response provision. Hence, the results suggest the need for a simultaneous provision of primary and secondary response. The relation between the additional reserve required and the secondary response from TCLs is given by the function L_3 that depends only on Δt_3 if Δt_1 and Δt_2 are fixed. Moreover we verified that there exits the optimal setting for Δt_3, which maximise the value of DSR. Finally we discussed the impact that rolling planning has on the TCLs quality of the service.

Moreover, this thesis analyses and quantifies the implications of electric vehicle (EV) deployment, heat pumps (HPs), industrial and commercial (I&C) and dynamic time-of-use (dToU) tariffs for the carbon emissions and renewable integration cost of the broader UK electricity system (*chapter 6*). The results of the analysis suggest that LCTs are able to deliver measurable carbon reductions primarily by enabling the future, largely decarbonised electricity system to operate more efficiently. Carbon benefits of different DSR technologies are found to be in the range of 50-200 g/kWh of flexible demand, and are a function of the assumed flexibility to shift demand to times of lower carbon grid intensity and provide frequency regulation. Carbon benefits of LCTs are generally more pronounced in scenarios with higher penetration of intermittent RES, although there are limits to this trend where the non-renewable generation capacity on the system is also low-carbon. Finally, we find that the integration of electrified transport and heating demand would be significantly less carbon intensive if smart operation strategies are adopted, making a very positive impact on the overall carbon performance of the economy.

The second set of studies focused on the potential of DSR technologies to support cost-efficient integration of RWS. System integration benefits of DSR are assessed in the sense of reducing the overall system cost of intermittent RES. The total Whole-System Cost (WSC) of intermittent RES is defined as the sum of their Levelised Cost of Electricity (LCOE) and the system integration cost. Case studies demonstrate that smart DSR technologies are capable of supporting cost-efficient decarbonisation of future electricity system by reducing renewable integration cost. Penetration of individual DSR technologies i.e. the uptake of e.g. EVs, HPs etc. is a critical factor for

the value of DSR for wind integration, as it determines the volume of flexible system services that can be provided by DSR technologies.

8.2.4 Enhanced Flexibility from Conventional Plants

The advanced SUC proposed in chapter 2 is applied to investigate the value of enhanced flexibility from conventional plants in the future low carbon system (*chapter 7*). It has been shown that value of enhanced flexibility increases with penetration of wind energy; however, different systems require different types of flexibility features. In the coal and gas dominated system, the value of reserve related flexibility features (Short commitment time, Idle state and so no) is higher, while in the nuclear dominated system, frequency response related flexibility features (High response capability and low MSG) are more desirable. The analysis also suggests that different system scheduling methods could significantly change the value of enhanced flexibility features. In the low base system, traditional deterministic schedule would increase the value of MSG and Idle state, while decrease the value of CT. Risk aversion would increases the value of Idle-state and MSG, while reduces the value of CT. High carbon price swifts the value of flexibility from Coal-fired plants to gas plants.

8.3 Future Work

Based on the findings of this thesis, several important research areas are identified that deserve attention in future work:

1. **Modelling of the multi-bus systems:** the operation of real power systems is constrained by limits of the transmission system, both in terms of capacities and reliabilities. This is of particular relevance to wind integrated systems, because the wind resource is typically far from the load centres, and it may not be optimal or feasible to build enough transmission capacity to guarantee the system's ability to transport all the available generation. Moreover, there are growing concerns regarding the sharing of flexibility across transmission network. The ability to simulate a multi-bus system, therefore, would greatly improve the usefulness of the proposed model in real life wind integration studies, whether the study was focussed on realistic modelling of transmission-

constrained dispatch or on optimisation of the transmission network itself. The scenario tree would need to be extended to include a multi-dimensional wind uncertainty. The correlations between forecast errors in different regions could be assumed to be +1 or −1, and therefore the wind output would have only one degree of uncertainty, as with the single-bus model. However, in general this is not a realistic assumption. Thus, a multi-dimensional integration is needed in order to establish the expected operating costs at each time horizon. A simple extension of the scenario tree construction methodology of chapter 2 would be cumbersome even for very simple systems.

2. **Modelling of the uncertainty and energy recovery associated with frequency regulation capability of wind plants**: this thesis only considers the uncertainty associated with online capacity of WPs when determining the aggregated SI capability. In fact, as discussed in [63], a more detailed model could be developed by taking into account of probability distribution of wind speeds and wind ramps. Moreover, two simplified relationships between additional PFR at steady state and the time constant of SI are assumed in this thesis. Further research is needed to model more accurately the relationship between SI contribution and additional PFR in the steady-state and incorporate this in the system scheduling.
3. **Modelling of the uncertainty associated with demand side response**: there is significant uncertainty associated with the deliverability of flexibility from DSR [123], which is not directly addressed in this thesis. The uncertainty regarding the price elasticity of demand is incorporated into robust UC in [124] and SUC in [125]. However, more research is required in order to fully understand how to properly integrate the uncertainty with the deliverability of the flexibility provision from DSR into SUC and how the benefit of flexibility provided by DSR could be affected by this uncertainty especially when the system operators all over the world are generally risk averse.
4. **Market reward of flexibility**: As studied in this thesis, it is becoming clear that the flexibility resources are beneficial for the operation of the future low-carbon power system with high penetration of RES. However, it is still unclear how

this benefit can be captured by the providers of the flexibility under present market framework. The inertia provision from wind plants shows the significant benefits in terms of operation cost reduction and RES curtailment saving. However, for most of the existing electricity markets, these do not exist inertia market. Similar to the inertia market as proposed in [85], a framework for rewarding the provision of frequency regulation by WPs should be developed. Similarly, the value of enhanced flexibility features from conventional plants analysed in the chapter 7 is rarely accrued to the plants generating such a value. As an example, after the MSG is reduced, the related CCGT will be operated more time at reduced load, thus it will produce less energy. In the present market where revenues are mainly driven by the energy sold, this clearly represents a disadvantage for the flexible CCGT itself. Currently there are different fora, working groups and initiatives with the main aim of suggesting possible ways of modifying current market regulations. It should be noticed that a capacity market based on capacity only would not provide any reward to flexibility. It is a promising area to develop a market arrangement which could appropriately reward and incentivise the flexibility provided by various resources.

Reference

[1] G. Strbac, M. Aunedi, D. Pudjianto, P. Djapic, F. Teng, A. Sturt, D. Jackravut, R. Sansom, V. Yufit and N. Brandon, "Strategic Assessment of the Role and Value of Energy Storage Systems in the UK Low Carbon Energy Future," Carbon Trust, London, 2012.

[2] A. Sturt, "Stochastic Scheduling of Wind-Intergrated Power Systems, PhD thesis," Imperial College London, 2011.

[3] A.Tuohy, P. Meibom, E. Denny and M. O'Malley, "Unit Commitment for System With Significant Wind Penetration," *IEEE Trans. Power Syst.,* vol. 24, no. 2, pp. 592-601, 2009.

[4] A. Papavasiliou, S. S. Oren and R. P. O'Neill, "Reserve Requirements for Wind Power Integration: A Scenario-Based Stochastic Programming Framework," *IEEE Trans. Power Syst.,* vol. 26, no. 4, pp. 2197 - 2011, 2011.

[5] H. Chavez, R. Baldick and S.Sharma, "Governor Rate-Constrained OPF for Primary Frequency Control Adequacy," *IEEE trans. Power Syst.,* vol. 29, no. 3, pp. 1473-1480, 2014.

[6] Y. Lee and R. Baldick, " A Frequency-Constrained Stochastic Economic Dispatch Model," *IEEE Trans. Power Syst.,* vol. 28, no. 3, pp. 2301-2312, 2013.

[7] A. Tuohy and M. O'Malley, "Pumped storage in systems with very high wind penetration," *Energy Policy,* vol. 39, p. 1965–1974, 2011.

[8] R. Sioshansi, P. Denholm, T. Jenkin and J. Weiss, "Estimating the value of electricity storage in PJM: Arbitrage and some welfare effects," *Energy Economics,* vol. 31, p. 269–277, 2009.

[9] R. H. Byrne and C. A. Silva-Monroy, "Estimating the Maximum Potential Revenue for Grid Connected Electricity Storage: Arbitrage and Regulation," SAND2012-3863, Sandia National Laboratories, 2012.

[10] R. Doherty, A. Mullane, G. L. Nolan, D. J. Burke, A. Bryson and M. O'Malley, "An Assessment of the Impact of Wind Generation on System Frequency Contro," *IEEE trans. Power Syst.,* vol. 25, no. 1, pp. 452 - 460, 2010.

[11] L. Ruttledge, N. W.Miller, J. O'Sullivan and D. Flynn, "frequency response of power systems with variable speed wind turbines," *IEEE Transactions on Sustainable Energy,* vol. 3, no. 4, pp. 683 - 691, 2012.

[12] I. D. Margaris, S. A. Papathanassiou, N. D. Hatziargyriou, A. D. Hansen and P. Sørensen, "Frequency Control in Autonomous Power Systems With High Wind Power Penetration," *IEEE Trans. Sustain. Energy.,* vol. 3, no. 2, pp. 189 - 199, 2012.

[13] L. Wu and D. Infield, "Power system frequency management challenges – a new approach to assessing the potential of wind capacity to aid system frequency stability," *IET Renewable Power Generation,* pp. 733-739, 2014.

[14] E.Karangelos and F. Bouffard, "Towards Full Integration of Demand-Side Resources in Joint Forward Energy/Reserve Electricity Markets," *IEEE Trans. Power Syst.,* vol. 27, no. 1, pp. 280-289, Feb. 2012.

[15] F. Teng, V. Trovato and G. Strbac, "Stochastic Scheduling with Inertia-dependent Frequency Response Requirements," *IEEE Trans. Power Syst.,* Submitted.

[16] F. Teng, D. Pudjianto, G. Strbac, N. Brandon, A. Thomson and J. Miles, "Potential Value of Energy Storage in the UK Electricity System," *Proceedings of the ICE - Energy,* accepted.

[17] F. Teng and G. Strbac, "Assessment of the Role and Value of Frequency Response Support from Wind Plants," *IEEE Trans on Energy Conversion,* Submitted.

[18] V. Trovato, F. Teng and G. Strbac, "Stochastic Scheduling with Flexible Demand Response from Thermostatic Loads," *IEEE Trans. Smart Grids,* Submitted.

[19] M. Aunedi, F. Teng and G. Strbac, "Carbon impact of smart distribution networks," Report D6 for the "Low Carbon London" LCNF project: Imperial College London, 2014.

[20] F. Teng, D. Pudjianto, G. Strbac, F. Ferretti and R. Bove, "Assessment of the Value of Plant Flexibility," in *Renewable Power Generation Conference (RPG 2014), 3rd*, Naples, 2014.

[21] R. Bove, F. Ferretti, P. Paelinck, G. Strbac and F. Teng, "Installed Base and Flexibility: New Realities for the European Power Sector," in *PowerGen Europe*, 2013.

[22] EirGrid and SONI, "Facilitation of Renewables," 2010. [Online]. Available:

http://www.eirgrid.com/renewables/facilitationofrenewables/.

[23] E. M. Garrigle, J. Deane and P. Leahy, “How much wind energy will be curtailed on the 2020 Irish power system?,” *Renewable Energy,* no. 55, pp. 544 - 553, 2013.

[24] A. J.Conejo, m. Carrion and J. M.Morales, Decision Making Under Uncertainty in Electricity Markets, New York: Springer, 2010.

[25] P.Meibom, R.Barth, B.Hasche, H.Brand, C.Weber and M.O'Malley, “Stochastic Optimization Model to Study the Operational Impacts of High Wind Penetrations in Ireland,” *IEEE Trans. Power Syst.,* vol. 26, no. 3, pp. 1367-1379, 2011.

[26] J. Wang, J. Wang, C. Liu and J. P. Ruiz, “Stochastic unit commitment with sub-hourly dispatch constraints,” *Applied Energy,* vol. 105, pp. 418 - 422, 2013.

[27] E. A. Bakirtzis, P. N. Biskas, D. P. Labridis and A. G. Bakirtzis, “Multiple Time Resolution Unit Commitment for Short-Term Operations Scheduling Under High Renewable Penetration,” *IEEE Trans. Power Syst.,* vol. 29, no. 1, pp. 149 - 159, 2014.

[28] E. Ela and M. O’Malley, “Studying the Variability and Uncertainty Impacts of Variable Generation at Multiple Timescales,” *IEEE Trans. Power Syst.,* vol. 27, no. 3, pp. 1324 - 1333, 2012.

[29] J.F. Restrepo and F. Galiana, “Unit commitment with primary frequency regulation constraints,” *IEEE Trans. Power Syst.,* vol. 20, no. 4, pp. 1588-1596, 2005.

[30] R. Doherty, G. Lalor, and M. O’Malley, “Frequency control in competitive electricity market dispatch,” *IEEE Trans. Power Syst.,* vol. 20, no. 3, pp. 1588-1596, 2005.

[31] H.Ahmadi and H.Ghasemi, “Security-Constrained Unit Commitment With Linearized System Frequency Limit Constraints,” *IEEE Trans. Power Syst.,* vol. 29, no. 4, pp. 1536 - 1545, July 2014.

[32] National Grid, “Security and Quality of Supply Standards,” [Online]. Available: http://www2.nationalgrid.com/UK/Industry-information/Electricity-codes/System-Security-and-Quality-of-Supply-Standards/.

[33] A. Sturt and G. Strbac, “Time-series modelling of power output for large-scale wind fleets,” *Wind Energy,* vol. 14, no. 8, pp. 953-966, 2011.

[34] A. Sturt and G. Strbac, “A time series model for the aggregate Great Britain wind output circa 2030,” *IET Renewable Power Generation,* 2013.

[35] R. Billiton and R. Allan, Reliability evaluation of power system, Plenum, Ed., New York, 1996.

[36] A. Sturt and G. Strbac, “Value of stochastic reserve policies in low-carbon power systems,” *Institution of Mechanical Engineers, Part O: Journal of Risk and Reliability,* pp. 51-64, 2012.

[37] F. Bouffard and F. Galiana, “Stochastic security for operations planning with significant wind power generation,” *IEEE Trans. Power Syst.,* vol. 23, pp. 306-316, 2008.

[38] A. Papavasiliou, S. S. Oren and R. P. O’Neill, “Reserve Requirements for Wind Power Integration: A Scenario-Based Stochastic Programming Framework,” *IEEE TRANSACTIONS ON POWER SYSTEMS,* vol. 26, no. 4, pp. 2197 - 2011, 2011.

[39] J. Morales, A. Conejo and and J. P´erez-Ruiz, “Economic valuation of reserves in power systems with high penetration of wind power,” *IEEE Transactions on Power Systems,* vol. 24, no. 2, p. 900–910, 2009.

[40] J. Dupa˘cov´a, N. Gr¨owe-Kuska and W. R¨omisch, “Scenario reduction in stochastic programming,” *Mathematical Programming,* vol. 95, no. 3, p. 493–512, 2002.

[41] t. P. Meibon el, “WILMAR: Wind Power Integration in Liberalised Electricity Makerts,” [Online]. Avalible: http://www.wilmar.risoe.dk, 2006.

[42] A.Tuohy, P. Meibom, E. Denny and M. O'Malley, “Unit Commitment for System With Significant Wind Penetration,” *Power Systems, IEEE Transctions on,* vol. 24, no. 2, pp. 592-601, 2009.

[43] P. Ruiz, C. Philbrick and P. Sauer, “Uncertainty Management in the Unit Commitment Problem,” *IEEE Transactions on Power Systems,* vol. 24, no. 2, pp. 642 - 651, 2009.

[44] P. Meibom, R. Barth, B. Hasche, H. Brand, C. Weber and M. O’Malley, “Stochastic optimization model to study the operational impacts of high wind penetrations in Ireland,” *IEEE Transactions on Power Systems,* vol. 26, no. 3, p. 1367–1379, 2011.

[45] A. Sturt and G. Strbac, “Efficient stochastic scheduling for simulation of wind-integrated power systems,” *IEEE Trans. Power Syst.,* vol. 27, no. 3, pp. 323-334, 2012.

[46] A. Street, F. Oliveira and J. M. Arroyo, “Contingency-Constrained Unit Commitment With n - K Security Criterion: A Robust Optimization Approach,” *IEEE TRANSACTIONS ON POWER SYSTEMS,* vol. 26, no. 3, pp. 1581 - 1590, 2011.

[47] C. Zhao, J. Wang, J.-P. Watson and J.-P. Watson, "Multi-Stage Robust Unit Commitment Considering Wind and Demand Response Uncertainties," *IEEE TRANSACTIONS ON POWER SYSTEMS,* vol. 28, no. 3, pp. 2708 - 2717, 2013.

[48] D. Bertsimas, E. Litvinov, X. A. Sun, J. Zhao and T. Zheng, "Adaptive Robust Optimization for the Security Constrained Unit Commitment Problem," *IEEE TRANSACTIONS ON POWER SYSTEMS,* vol. 28, no. 1, pp. 52 - 63, 2013.

[49] C. Zhao and Y. Guan, "Unified Stochastic and Robust Unit Commitment," *IEEE TRANSACTIONS ON POWER SYSTEMS,* vol. 28, no. 3, pp. 3353 -3361, 2013.

[50] Q. Wang, Y. Guan and J. Wang, "A chance-constrained two-stage stochastic programfor unit commitment with uncertain wind power output," *IEEE Transaction on Power Systems,* vol. 27 , no. 1, pp. 206 - 212, 2012.

[51] H. Wu, M. Shahidehpour, Z. Li and W. Tian, "Chance-Constrained Day-Ahead Scheduling in Stochastic Power System Operation," *IEEE TRANSACTIONS ON POWER SYSTEMS,* vol. 29, no. 4, pp. 1583 - 1591, 2014.

[52] R. Rockafellar and S. Uryasev, "Optimization of conditional value-at-risk," *J.Risk,* vol. 2, pp. 21 - 42, 2000.

[53] W. Qianfan, J-P. Watson and Y. Guan, "Two-Stage Robust Optimization for Contingency Constrained Unit Commitment," *IEEE Trans. Power Syst.,* vol. 28, no. 3, pp. 2366-2375, 2013.

[54] Energy Networks Association and National Grid, "Frequency Changes during Large Disturbances and their Impact on the Total System," 2013.

[55] J. O'Sullivan, A. Rogers, D. Flynn, P. Smith and M. O'Malley, "Studying the Maximum Instantaneous Non-Synchronous Generation in an Island System—Frequency Stability Challenges in Ireland," *IEEE Trans. Power Syst.,* vol. 29, no. 6, pp. 2943 - 2951, 2014.

[56] P. Kundur, Power system staility and control, London: McGraw-Hill, 1994.

[57] Hao Huang; Fangxing Li, "Sensitivity analysis of load-damping characteristic in power system frequency regulation," *IEEE Trans. Power Syst.,* vol. 28, no. 2, pp. 1324-1335, 2013.

[58] M. Aunedi, P.-A. Kountouriotis, J. E. O. Calderon, D. Angeli and G. Strbac, "Economic and Environmental Benefits of Dynamic Demand in Providing Frequency Regulation," *IEEE Trans. Smart Grids,* vol. 4, no. 4, pp. 2036 - 2048, Dec 2013.

[59] FICO, "FICO Xpress optimization suite," [Online]. Available: http://optimization.fico.com.

[60] National Grid frequency fesponse working group, "Frequency Response report," 2013.

[61] E.Ela at al., "Market designs for the primary frequency response ancillary service— Part I: Motivation and design Part," *IEEE Trans. Power Syst.,* vol. 29, no. 1, pp. 421-431, 2014.

[62] F. Teng, M. Aunedi and G. Strbac, "Value of Demand Side Participation in Frequency Regulation," in *23rd International Conference on Electricity Distribution*, 2015.

[63] W. Lei and D. Infield, "Towards an assessment of power system frequency support from wind plant—modeling aggregate inertial response," *IEEE Trans. Power Syst.,* vol. 28, pp. 2283-2291, 2013.

[64] R. Doherty, A. Mullane, G. (. Nolan, D. J. Burke, A. Bryson and M. O'Malley, "An assessment of the impact of wind generation on system frequency control," *IEEE Trans. Power Syst.,* vol. 25, no. 1, pp. 452-460, 2010.

[65] Energy Research Partnership, "The future role for energy storage in the UK," 2011.

[66] M. Black and G. Strbac, "Value of bulk energy storage for managing wind power fluctuations," *IEEE Trans. Energy Convers,* vol. 22, pp. 197-205, 2007.

[67] stoRE, "Facilitating energy storage to allow high penetration of intermittent," stoRE, 2013.

[68] Elexon, "http://www.elexon.co.uk/," [Online].

[69] IEA, "World Energy Outlook 2013," IEA, 2013.

[70] A. Sturt and G. Strbac, "Efficient stochastic scheduling for simulation of wind-integrated power systems," *IEEE Trans. Power Syst.,* vol. 27, no. 3, pp. 323-334, 2012.

[71] S. Wong and J. D. Fuller, "Pricing Energy and Reserves Using Stochastic Optimization in an Alternative Electricity Market," *IEEE Trans. Power Syst.,* vol. 22, no. 2, pp. 631 - 638, 2007.

[72] E. Karangelos and F. Bouffard, "Towards Full Integration of Demand-Side Resources in Joint Forward Energy/Reserve Electricity Markets," *IEEE TRANSACTIONS ON POWER SYSTEMS,* vol. 27, no. 1, pp. 280-289, 2012.

[73] S. Gill, E. Barbour, I. Wilson and D. Infield, “Maximising revenue for non-firm distributed wind generation with energy storage in an active management scheme,” *IET Renewable Power Generation,* vol. 7, no. 5, pp. 421-430, 2013.

[74] A. A. Akhil, G. Huff, A. B. Currier, B. C. Kaun, D. M. Rastler, S. B. Chen, A. L. Cotter, D. T. Bradshaw and W. D. Gauntlett, “Energy Storage Handbook in collaboration with NRECA,” SANDIA, 2013.

[75] M. Kintner-Meyer, P. Balducci, W. Colella, M. Elizondo, C. Jin, T. Nguyen, V. Viswanathan and Y. Zhang, “National Assessment of enegy storage fir grid balancing and artitrage Phase 1,WECC,” PNNL, 2012.

[76] H. L. Ferreiraa, R. Gardeb, G. Fullic, W. Klinga and J. P. Lopesd, “Characterisation of electrical energy storage technologies,” *Energy,* vol. 53, pp. 288-298, 2013.

[77] A. Chatzivasileiadi and I. K. Eleni Ampatzi, “Characteristics of electrical energy storage technologies and their applications in buildings,” *Renewable and Sustainable Energy Reviews,* vol. 25, pp. 814-830, 2013.

[78] J. Ekanayake and N. Jenkins, “Comparison of the Response of Doubly Fed and Fixed-Speed Induction Generator Wind Turbines to Changes in Network Frequency,” *IEEE Trans. Energy Convers.,* vol. 19, no. 4, pp. 700 - 802, 2004.

[79] O. Anaya-Lara, F. Hughes, N. Jenkins and G. Strbac, “Contribution of DFIG-based wind farms to power system short-term frequency regulation,” *IEE Proceedings Generation, Transmission and Distribution,* vol. 153, pp. 164 - 170, 2006.

[80] E. Muljadi, V. Gevorgian, M. Singh and S. Santoso, “Understanding inertial and frequency response of wind power plants,” in *PEMWA*, 2012.

[81] N. R. Ullah, T. Thiringer and D. Karlsson, “Temporary Primary Frequency Control Support by Variable Speed Wind Turbines— Potential and Applications,” *IEEE Trans. Power Syst.,* vol. 23, no. 2, pp. 601 - 612, 2008.

[82] Z. Miao, L. Fan, D. Osborn and S. Yuvarajan, “Wind Farms With HVDC Delivery in Inertial Response and Primary Frequency Control,” *IEEE Trans. Energy Convers.,* vol. 25, no. 4, pp. 1171 - 1178, 2010.

[83] S. I. Nanou, G. N. Patsakis and S. A. Papathanassiou, “Assessment of communication-independent grid code compatibility solutions for VSC–HVDC connected offshore wind farms,” *Electric Power Systems Research,* vol. 121, p. 38 – 51, 2015.

[84] V. Gevorgian, Y. Zhang and E. Ela, “Investigating the Impacts of Wind Generation Participation in Interconnection Frequency Response,” *IEEE Trans. Sustain. Energy,* p. Accepted, 2014.

[85] E. Ela, V. Gevorgian, P. Fleming, Y. Zhang, M. Singh, E. Muljadi, A. Scholbrook, J. Aho, A. Buckspan, L. Pao, V. Singhvi, A. Tuohy, P. Pourbeik, D. Brooks and N. Bhatt, “Active Power Controls from Wind Power: Bridging the Gaps,” NREL Technical Report TP-5D00-60574, 2014.

[86] E. Sáiz-Marín, J. García-González, J. Barquín and E. Lobato, “Economic Assessment of the Participation of Wind Generation in the Secondary Regulation Market,” *IEEE Trans. Power Syst,* vol. 27, no. 2, pp. 866-874, 2012.

[87] J. Brisebois and N. Aubut, “Wind farm inertia emulation to fulfill Hydro-Québec's specific need,” in *IEEE Power and Energy Society General Meeting* , 2011.

[88] Y.Tan and D.Kirschen, “Co-optimization of Energy and Reserve in Electricity Markets with Demand-side Participation in Reserve Services,” in *PSCE*, Atlanta, 2006.

[89] J.Wang N.Redondo and F.Galiana, “Demand-side reserve offers in joint energy/reserve electricity markets,” *IEEE Trans. Power Syst.,* vol. 18, no. 4, pp. 1300-1306, Nov. 2003.

[90] M.Aunedi et al., “Economic and Environmental Benefits of Dynamic Demand in Providing Frequency Regulation,” *IEEE Tans. Smart Grid,* vol. 4, no. 4, pp. 2036-2048, 2013.

[91] J.L. Mathieu, S.Koch and D.S.Callaway, “State estimation and control of electric loads to manage real-time energy imbalance,” *IEEE Trans. on Power Syst.,* vol. 28, no. 1, pp. 430-440, Nov 2013.

[92] R.Moreno, R.Moreira and G. Strbac, “A MILP model for optimising multi-service portfolios of distributed energy storage,” *Applied Energy - Elsevier,* 2014.

[93] D.Callaway and S. Hiskens, “Achieving Controllability of Electric Loads,” *Proceedings of the IEEE,* vol. 39, no. 1, pp. 184-199, 2011.

[94] V.Trovato, S.Tindemans and G.Strbac, “Security constrained economic dispatch with flexible thermostatically controlled loads,” in *ISGT Europe* , Istanbul, 2014.

[95] F.Teng, V.Trovato and G.Strbac, “Stochastic scheduling with inertia-dependent frequency regulation,” *submitted.*

[96] S.Tindemans, V.Trovato and G.Strbac, “Decentralised control of thermostatic loads for flexible demand response,” *IEEE Trans. on Control Syst. Technol,* no. 99, 2015.

[97] V.Trovato, S.Tindemans and G.Strbac, “The leaky storage model for optimal multi-service allocation of thermostatic loads,” *Submitted.*

[98] PJM, “Energy & Ancillary Services Market Operations,” 2015. [Online]. Available: www.pjm.com/~/media/documents/manuals/m11.ashx.

[99] C.Jianming et al., “Scheduling direct load control to minimize system operation cost,” *IEEE Trans. Power Syst.,* vol. 10, no. 4, Nov. 1995.

[100] I.Erinmez, D.Bickers, G.Wood and W.Hung, “NG experience with frequency control in response by generators England and Wales - provision of frequency,” in *IEEE PES Winter Meeting*, New York, 1999.

[101] V.Trovato, S.Tindemans and G.Strbac, “Controlling the synchronization and payback associated with the provision of frequency services by dynamic demand,” in *22nd CIRED Conference*, Sotckholm, 2013.

[102] M. Aunedi, M. Woolf, M. Bilton and G. Strbac, “Impact and opportunities for wide-scale electric vehicle deployment, Report B1 for the “Low Carbon London”,” LCNF project: Imperial College London, 2014.

[103] M. Bilton, N. E. Chike, M. Woolf, P. Djapic, M. Wilcox and G. Strbac, “Impact of low voltage – connected low carbon technologies on network utilisation, Report B4 for the “Low Carbon London”,” LCNF project: Imperial College London, 2014.

[104] G. Strbac, C. K. Gan, M. Aunedi, V. Stanojevic, P. Djapic, J. Dejvises, P. Mancarella, A. Hawkes, D. Pudjianto, S. L. Vine, J. Polak, D. Openshaw, S. Burns, P. West, D. Brogden, A. Creighton and A. Claxton, “Benefits of Advanced Smart Metering for Demand Response-Based Control of Distribution Networks,” report for the Energy Networks Association,, April 2010.

[105] C. Trust, “Micro-CHP Accelerator Final Report,” March 2011.

[106] G. Strbac, M. Aunedi, D. Pudjianto, P. Djapic, S. Gammons and R. Druce, “Understanding the Balancing Challenge,” Report for the UK Department of Energy and Climate Change, 2012.

[107] G. Strbac, D. Pudjianto, P. Djapic and M. Aunedi, “Infrastructure in a low-carbon energy system to 2030: Transmission and distribution,” Report for the Committee on Climate Change, April 2014.

[108] M. Aunedi, “Value of flexible demand-side technologies in future low-carbon systems,” PhD thesis, Imperial College London, UK, July 2013.

[109] J. Schofield, R. Carmichael, S. Tindemans, M. Woolf, M. Bilton and G. Strbac, “Residential consumer responsiveness to time-varying pricing, Report A3 for the “Low Carbon London”,” LCNF project: Imperial College London, 2014.

[110] M. Woolf, T. Ustinova, E. Ortega, H. O’Brien, P. Djapic and G. Strbac, “Distributed generation and demand response services for the smart distribution network, Report A7 for the “Low Carbon London”,” LCNF project: Imperial College London, 2014.

[111] P. Djapic, M. Kairudeen, M. Aunedi, J. Dragovic, D. Papadaskalopoulos, I. Konstantelo and G. Strbac, “Operation and design of smart distribution networks, Report 11-1 for the “Low Carbon London”.,” LCNF project: Imperial College London, 2014.

[112] Poyry, “Synergies and conflicts in the use of DSR for national and local issues,” report to UK Power Networks, July 2014.

[113] H. Government, “The Carbon Plan: Delivering our low carbon future,” December 2011.

[114] A. A. Shakoor, “Security and cost evaluation of power generation systems with intermittent energy sources,” PhD thesis, University of Manchester, 2005.

[115] G. Strbac, “Demand side management: benefits and challenges,” *Energy Policy,* vol. 36, no. 2, pp. 4419 - 4426, 2008.

[116] R. Sioshansi, “Modelling the impacts of electricity tariffs on Plug-In hybrid electric vehicle charging, costs and emissions,” *Operatons Research,* vol. 60, no. 2, pp. 1 - 11, 2012.

[117] S. O. A. Papavasiliou, “A stochastic unit commitment model for integrating renewable supply and demand response,” in *IEEE PES General Meeting*, 2012.

[118] Eirgrid, “Interconnection Economic Feasibility Report,” 2009.

[119] P. Denholm and M. Hand, “Grid flexibility and storage required to achieve very high penetration of variable renewable electricity,” *Energy Policy,* vol. 39, no. 3, pp. 1817-1830.

[120] L. Eamonn, D. Flynn and M. O'Malley, “Evaluation of power system flexibility,” *IEEE Trans. Power Systems ,* vol. 27, no. 2, pp. 922 - 931, 2012.

[121] J. Ma, V. Silva, R. Belhomme, D. S. Kirschen and L. F. Ochoa, “Evaluating and Planning Flexibility in Sustainable Power Systems,” *IEEE Trans. Sustain. Energy,* vol. 4, no. 1, pp. 200 - 209, 2012.

[122] M. Rautkivi and M. Kruisdijk, “Future Market Design for Reliable Electricity Systems in Europe,” in *POWERGEN Europe*, 2013.

[123] Y. Mu, J. Wu, J. Ekanayake, N. Jenkins and H. Jia, “Primary Frequency Response From Electric Vehicles in the Great Britain Power System,” *IEEE Trans. Smart Grid,* vol. 4, no. 2, pp. 1142 - 1150, 2013.

[124] G. Liu and K. T. , “Robust unit commitment considering uncertain demand response,” *Electric Power Systems Research,* vol. 119, pp. 126 - 137, 2015.

[125] Q. Wang, J. Wang and Y. Guan, “Stochastic Unit Commitment With Uncertain Demand Response,” *IEEE Trans. Power Syst.,* vol. 28, no. 1, pp. 562 - 563, 2013.

[126] F. Teng and G. Strbac, “Evaluation of Synthetic Inertia Provision from Wind Plants,” in *IEEE PES General Meeting* , 2015.

[127] R. Energy, “Electricity Market Reform - Analysis of policy options,” 2010.